Estimating Hydraulic Properties of the Floridan Aquifer System by Analysis of Earth-Tide, Ocean-Tide, and Barometric Effects, Collier and Hendry Counties, Florida

By Michael L. Merritt

U.S. GEOLOGICAL SURVEY

Water-Resources Investigations Report 03–4267

Prepared in cooperation with the

South Florida Water Management District

Tallahassee, Florida
2004

U.S. DEPARTMENT OF THE INTERIOR
GALE A. NORTON, Secretary

U.S. GEOLOGICAL SURVEY
Charles G. Groat, Director

For additional information
write to:

U.S. Geological Survey
2010 Levy Avenue
Tallahassee, FL 32301

Copies of this report can be purchased from:

U.S. Geological Survey
Branch of Information Services
Box 25286
Denver, CO 80225-0286
888-ASK-USGS

Additional information about water resources in Florida is available on the World Wide Web at **http://fl.water.usgs.gov**

CONTENTS

FIGURES

TABLES

CONVERSION FACTORS AND VERTICAL DATUM

Multiply	By	To obtain
	Length	
inch (in.)	2.54	centimeter
foot (ft)	0.3048	meter
mile (mi)	1.609	kilometer
	Area	
acre	0.4047	hectare
square mile (mi^2)	2.590	square kilometer
	Mass	
pound (lb)	0.4536	kilogram
	Flow Rate	
cubic foot per second (ft^3/s)	0.02832	cubic meter per second
million gallons per day (Mgal/d)	0.04381	cubic meter per second
inch per year (in/yr)	25.4	millimeter per year
	Pressure	
1 millimeter of Hg (mercury)	0.044602	feet of water at 4 degrees Celsius
1 millimeter of Hg (mercury)	1.33322	millibars
1 millimeter of Hg (mercury)	0.019337	pounds per square inch
	Hydraulic Conductivity	
foot per day (ft/d)	0.3048	meter per day
	**Transmissivity*	
foot squared per day (ft^2/d)	0.09290	meter squared per day
	Leakance	
foot per day per foot [(ft/d)/ft]	1.0	meter per day per meter

*The standard unit for transmissivity is cubic foot per day per square foot times foot of aquifer thickness [$(ft^3/d)/ft^2$]ft. In this report, the mathematically reduced form, foot squared per day (ft^2/d), is used for convenience.

Temperature in degrees Fahrenheit (°F) may be converted to degrees Celsius (°C) as follows: °C=(°F-32)/1.8.

Vertical coordinate information is referenced to the National Geodetic Vertical Datum of 1929 (NGVD 29).

Horizontal coordinate information (latitude-longitude) is referenced to the North American Datum of 1927 (NAD27).

Acronyms:

bls	below land surface
CFSW	Clewiston Field Station weather site
NOAA	National Oceanic and Atmospheric Administration
SFWMD	South Florida Water Management District
USGS	U.S. Geological Survey

Estimating Hydraulic Properties of the Floridan Aquifer System by Analysis of Earth-Tide, Ocean-Tide, and Barometric Effects, Collier and Hendry Counties, Florida

By Michael L. Merritt

ABSTRACT

Aquifers are subjected to mechanical stresses from natural, non-anthropogenic, processes such as pressure loading or mechanical forcing of the aquifer by ocean tides, earth tides, and pressure fluctuations in the atmosphere. The resulting head fluctuations are evident even in deep confined aquifers. The present study was conducted for the purpose of reviewing the research that has been done on the use of these phenomena for estimating the values of aquifer properties, and determining which of the analytical techniques might be useful for estimating hydraulic properties in the dissolved-carbonate hydrologic environment of southern Florida. Fifteen techniques are discussed in this report, of which four were applied.

An analytical solution for head oscillations in a well near enough to the ocean to be influenced by ocean tides was applied to data from monitor zones in a well near Naples, Florida. The solution assumes a completely non-leaky confining unit of infinite extent. Resulting values of transmissivity are in general agreement with the results of aquifer performance tests performed by the South Florida Water Management District. There seems to be an inconsistency between results of the amplitude ratio analysis and independent estimates of loading efficiency. A more general analytical solution that takes leakage through the confining layer into account yielded estimates that were lower than those obtained using the non-leaky method, and closer to the South Florida Water Management District estimates. A numerical model with a cross-sectional grid design was applied to explore additional aspects of the problem.

A relation between specific storage and the head oscillation observed in a well provided estimates of specific storage that were considered reasonable. Porosity estimates based on the specific storage estimates were consistent with values obtained from measurements on core samples. Methods are described for determining aquifer diffusivity by comparing the time-varying drawdown in an open well with periodic pressure-head oscillations in the aquifer, but the applicability of such methods might be limited in studies of the Floridan aquifer system.

INTRODUCTION

Since its inception, an important part of the science of ground-water hydrology has involved the estimation of values for aquifer properties, volume-averaged theoretical variables that quantify in a general way the water-transmitting and water-storage properties of subsurface formations. Estimates are usually based on measured data describing the change in the pressure field in a body of subsurface water caused by the application of mechanical stresses that alter the rate of water movement and release of water from storage within the rock matrix. One such stress is the forcing of water into and out the formation by

pumping from a well, or by injection of water into a well at a known rate. Doing this in conjunction with a planned program to collect pressure data (an aquifer test) is the most common method used for determining aquifer property values. Hydrologists have devised a variety of analytical methods to analyze the relation between the pumping or injection rate and changes in the pressure field.

Aquifers are also subjected to mechanical stresses from natural, non-anthropogenic, processes. These include pressure loading or mechanical forcing of the aquifer by ocean tides, earth tides, and pressure fluctuations in the atmosphere. Where an aquifer is overlain by an ocean, the tidal oscillations in the ocean are associated with a pressure loading or unloading of the formations underlying the ocean. One effect is that heads (pressure heads or water levels) in wells near the ocean will rise and fall. The same motion of the sun and moon that causes ocean tides also causes dilatation of subsurface formations (expansion and contraction of the rock matrix). These effects are referred to as earth tides. As the rock matrix expands and contracts, the pressure in water contained within the rock pores falls and rises, which affects the heads measured in wells. Atmospheric pressure fluctuations also cause a pressure loading or unloading of subsurface formations that is manifest in fluctuations of heads in wells. The effects are evident even in deep confined aquifers that maintain a substantial head difference from surface formations across tight confining layers.

Hydrologists early in the 20th century realized that ocean tides and atmospheric-pressure fluctuations caused corresponding fluctuations in heads in wells and began to pursue the goal of using these natural processes to deduce information about aquifer properties. Papers by Jacob (1940) and Ferris (1951) were among the first to describe the use of tidally influenced heads to estimate aquifer properties. The research has continued to the present day (2003), and recent papers represent new contributions to existing technology.

The present study: (1) reviews the research on the use of tidally influenced and other naturally forced head fluctuations for estimating aquifer properties, (2) determines which of these methods are useful in the hydrologic environment of southern Florida, and (3) applies selected algorithms to a data set of heads from wells in Collier and Hendry Counties. The study was conducted by the U.S. Geological Survey (USGS) in cooperation with the South Florida Water Management District, who also supplied the data set.

Using water-level fluctuations caused by natural processes for the cited purposes could represent a significant cost savings over the substantial costs associated with well drilling, instrumentation, and manpower required by more conventional aquifer testing. Even where aquifer testing is done, use of water-level fluctuations caused by natural processes can help to validate the results of the aquifer testing. If the data are collected during a period of monitoring prior to aquifer testing, they can be used to aid in the design of the tests. The methods described in this report appear to have potential usefulness for hydrologists in southern Florida and elsewhere.

Purpose and Scope

The purpose of this report is to document results of the review of research into the use of tidally influenced and other naturally forced head data to estimate values of aquifer properties. The report serves as a digest of the results of research previously documented in the technical literature, and presents results of the application of selected methods to head data obtained from wells located in Collier and Hendry Counties.

The review of research groups the various methods into four main categories according to the specific objectives of the research. The application of selected methods is preceded in the report by a presentation and explanation of the field data used in the analysis, and includes a description of the data analysis and other calculations that are made to yield numerical estimates based on the field data. Where research methods are not applied, a brief description is included, with appropriate references, as a guide to readers who may wish to investigate the alternative or more advanced methods.

Acknowledgments

The author expresses appreciation to Emily Richardson, South Florida Water Management District, for supporting the study, and to Michael J. Bennett, South Florida Water Management District, for providing data. The author is grateful to Paul Hsieh, National Research Program, USGS, Menlo Park, California, for providing analytical software, review, and consultative assistance, and to Edwin P. Weeks, National Research Program, USGS, Lakewood, Colorado, for report review and helpful suggestions.

DESCRIPTION OF THE STUDY AREA

The study area is best characterized as that part of southwestern Florida that includes the location of test wells providing data for the study and the locations of additional sites where atmospheric and ocean tide data were acquired (fig. 1). This region lies generally between 81 and 82 degrees of longitude and between 26 and 27 degrees of latitude and includes all or most of Lee, Hendry, and Collier Counties. The topography is flat, and wetlands are present throughout much of Hendry and Collier Counties. The Big Cypress National Preserve extends into the southern part of the study area (fig. 1). Two Native American

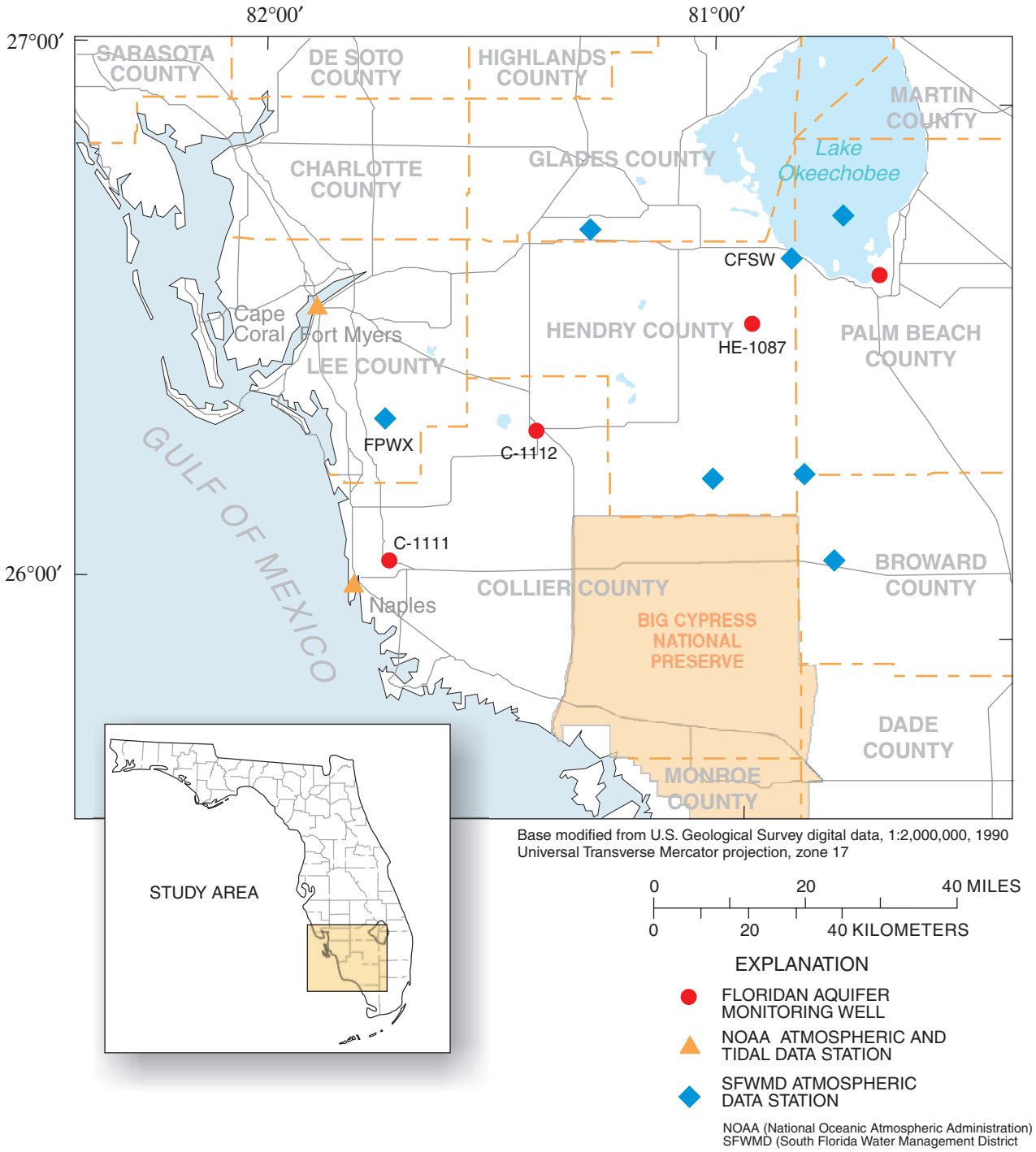

Figure 1. Location of study area and selected sites, southwestern Florida.

Reservations are located in southern Hendry and western Broward Counties. Most of Hendry County and eastern Lee County is rural, but the central and western part of Lee County is heavily urbanized (cities of Fort Myers and Cape Coral).

Like most of the State, the region is subtropical with hot, wet summers and cool, dry winters. Only rarely does the air temperature go below freezing. Winters in the region are marked by the frequent passage of air masses of high and low pressure (warm and cold fronts). Winter air pressure extremes of 997 to 1,034 millibars (mb) were measured by the National Oceanic and Atmospheric Administration (NOAA) at Naples (fig. 1) during the 1998-2000 calendar years. Summers have less atmospheric-pressure variation (non-cyclonic summer extremes of 1,006 to 1,021 mb were measured at Naples in 1998-2000), but the occasional passage of tropical disturbances in late summer and fall can bring about markedly low atmospheric pressure. A pressure of 991.7 mb was measured at Naples during the passage of Tropical Storm Mitch on November 5, 1998, and a pressure of 998.5 mb was measured during the passage of Hurricane Irene on October 15, 1999.

Hydrogeology of the Study Area

Southern Florida is underlain by rocks of Cenozoic age to a depth of about 5,000 feet (ft) (Meyer, 1989, p. 5). The rocks are principally carbonates (limestone and dolostone), with minor amounts of evaporites (gypsum and anhydrite) in the lower part and clastics (sand and clay) in the upper part. The movement of ground water from the inland areas to the ocean and the reverse (the inland movement of seawater in the saline-water zone postulated by Meyer) occurs primarily through the carbonate rocks (Meyer, 1989, p. 5). The brief description of lithology and stratigraphy that follows is a summary of the more extensive discussion included in Reese (2000).

The Floridan aquifer system in southwestern Florida includes (from oldest to youngest) the upper part of the Cedar Keys formation of Paleocene age, the Oldsmar Formation of early Eocene age, the Avon Park Formation of middle Eocene age, the Ocala Limestone of late Eocene age, and the Suwannee Limestone of early Oligocene age (fig.2). Overlying the Suwannee Limestone is the Hawthorn Group of Miocene and late Oligocene age, which (as defined by Scott (1988)) is divided into the Peace River Formation in the upper part and the Arcadia Formation in the lower part. The Hawthorn Group is largely composed of clastics and acts as an effective confining bed for aquifers in underlying formations. Reese (2000) prepared 10 hydrogeologic sections through southwestern Florida that show the stratigraphy in detail at many control points, including the test/monitor wells that provided tidally influenced head data for this study. The predominant rock types found in each formation are described (fig. 2) by Reese (2000).

The Floridan aquifer system is one of three principal aquifer systems in southwestern Florida. The other two are the surficial and intermediate aquifer systems. In southwestern Florida, the surficial aquifer system includes the water-table aquifer and the lower Tamiami aquifer (fig. 2). The intermediate aquifer system lies within the Hawthorn Group and includes, in descending order, the sandstone aquifer and the mid-Hawthorn aquifer. The sandstone aquifer is present in Lee County and in western Hendry and Collier Counties (Reese, 2000). The mid-Hawthorn aquifer is absent in most of Hendry County.

The Upper Floridan aquifer includes the lower part of the Hawthorn Group, the Suwannee Limestone, the Ocala Limestone, and the upper part of the Avon Park Formation. Reese (2000) refers to production zones, where present, in the lower part of the Hawthorn Group as the lower Hawthorn producing zone. Generally, the Upper Floridan aquifer in southwestern Florida consists of several thin water-bearing zones of relatively high permeability interlayered with thick zones of much lower permeability. The Upper Floridan water-bearing zones usually are composed of limestone or limestone with interbedded dolomite, and are characterized by secondary porosity, and are not differentiated into named aquifers by Reese (2000).

The Lower Floridan aquifer includes the dolomite-evaporite unit described by Reese (2000) that may be within the lower part of the Avon Park Formation or the upper part of the Oldsmar Formation, and extends down into the Cedar Keys Formation. Reese (2000) regards the Avon Park and Oldsmar Formations as being quite difficult to differentiate. The Lower Floridan aquifer also is characterized by thin water-bearing zones of high permeability interlayered with thick zones of low permeability. The zones of high permeability commonly are composed of sucrostic dolomite that collapses when drilled into. Some of the collapsed dolomitic zones used for waste injection have remarkably high permeability.

Series		Geologic Unit		Approximate thickness (feet)	Lithology	Hydrogeologic unit		Approximate thickness (feet)
Holocene to Pliocene		Undifferentiated		0 - 70	Quartz sand, silt, clay, and shell	Surficial aquifer system	Water-table aquifer	20 - 100
		Tamiami Formation		0 - 175	Silt, sandy clay, micritic limestone, sandy, shelly limestone, calcereous sandstone, and quartz sand		Confining beds	0 - 60
							Lower Tamiami aquifer	25 - 160
Miocene		Hawthorn Group	Peace River Formation	50 - 400	Interbedded sand, silt, gravel, clay, carbonate, and phosphatic sand	Intermediate aquifer system	Confining unit	20 - 100
							Sandstone aquifer	0 - 100
							Confining unit	10 - 250
			Arcadia Formation	400 - 550	Sandy limestone, shell beds, dolomite, phosphatic sand and carbonate, sand, silt, and clay		Mid-Hawthorn aquifer	0 - 130
							Confining unit	100 - 400
Early Oligocene		Suwannee Limestone		0 - 600	Fossiliferous, calcarenitic limestone	FLORIDAN AQUIFER SYSTEM	Lower Hawthorn producing zone	0 - 300
Eocene	Late	Ocala Limestone		0 - 400	Chalky to fossiliferous calcarenitic limestone		Upper Floridan aquifer	700 - 1,200
	Middle	Avon Park Formation		900 - 1,200	Fine-grained, micritic to fossiliferous limestone, dolomitic limestone, dense dolomite, and gypsum		Middle confining unit	500 - 800
				?				
	Early	Oldsmar Formation		800 - 1,400			Lower Floridan aquifer (Boulder zone)	1,400 - 1,800 (400)
Paleocene		Cedar Keys Formation		500 - 700	Dolomite and dolomitic limestone			
				1,200?	Massive anhydrite beds		Sub-Floridan confining unit	1,200?

Figure 2. Generalized geology and hydrogeology of southwestern Florida (from Reese, 2000).

The conceptualization of the Floridan aquifer system as upper and lower aquifers separated by a middle confining unit is a somewhat inadequate generalization. Thin, water-bearing zones can be found anywhere within the carbonate sequence extending downward from the lower part of the Hawthorn Group to the Cedar Keys Formation. The concept of a middle confining unit attempts to describe an interval between the one to several limestone water-bearing zones of secondary porosity in the upper part of the sequence and the collapsed dolomitic water-bearing zones in the lower part of the sequence, an interval in which the occurrence of water-bearing zones is less in a vertically spatially averaged sense than in the upper and lower parts of the sequence. It is difficult to select upper and lower elevations for such a confining unit at individual well sites, and also difficult to generalize confining-unit boundaries on a regionally extensive scale.

Water in the upper Floridan producing zones is under artesian pressure and flows from wells open at land surface. The equivalent freshwater head decreases from a high near the center line of the peninsula to sea level at the coasts (Meyer, 1989). The head measured in a well is an inverse function of the density of the water column in the well. Assuming that the water-column density is representative of that of the screened zone, or open hole, of the well, the water density will increase with depth of the open-hole zone because the dissolved solids concentration of the formation water increases with depth. In the Floridan aquifer system in the study area, brackish water (less than 10,000 milligrams per liter (mg/L) of total dissolved solids) overlies and is separated from water of seawater salinity (more than 35,000 mg/L of dissolved solids) by a salinity transition zone that is 100 ft or less in thickness at many sites. The salinity transition zone is deeper than 2,000 ft in the central part of the Florida peninsula and as shallow as 1,000 ft on the mainland near the southwestern coast of Florida. Hydraulic gradients in variable-density ground water are discussed by Hickey (1989). The relation of freshwater and environmental heads is discussed by Lusczynski (1961). Concepts of variable-density flow are presented by Mason and Kipp (1998).

Tidally influenced head data for this study were acquired from monitor zones in three wells extending into the dolomite-evaporite unit of the Lower Floridan aquifer. The locations and various identification numbers assigned to the wells are provided in table 1. These wells were drilled by the South Florida Water Management District (SFWMD) as part of a program to investigate the Floridan aquifer system in southwestern Florida as a possible future source of water for public supply. The depth intervals of the zones and characteristics of the formations from which the data are acquired are given in table 2. Depth intervals extend from 690 ft in the basal Hawthorn unit to 2,350 ft in the dolomite-evaporite unit. The lower heads in the deepest monitor zones in wells C-1111 and C-1112 probably do not imply a hydraulic potential across an intervening confining unit, but probably are consistent with the hydraulic influence of the saline-water density of the lower zones, as explained above.

Table 1. Locations and identification numbers of monitor wells providing data for this study

[Longitude of the ocean coast west of C-1111 is 81° 48' 49"; USGS, U.S. Geological Survey]

Location	Florida Bureau of Geology identification number	USGS local identification number	Latitude (degrees, minutes, seconds)	Longitude (degrees, minutes, seconds)
I-75 Canal near Naples, Florida	W-17405	C-1111	26° 10' 12"	81° 43' 51"
Immokalee Waste Water Treatment Plant, Immokalee, Florida	W-17391	C-1112	26° 24' 48"	81° 25' 24"
L-2 Canal near Clewiston, Florida	W-17093	HE-1087	26° 36' 30"	80° 56' 58"

Table 2. Description of monitor zones providing tidally influenced head data for the study

[C-1111 is 4.9 miles from the west coast of Florida (LSD = 9.87 feet); C-1112 is 28 miles from the west coast of Florida (LSD = 31.45 feet); and HE-1087 is 57 miles from both east and west coasts of Florida (LSD = 17.84 feet). LSD is land surface datum in feet above NGVD 29]

Monitor zone	Depth interval (feet)	Head (feet)	Formation	Water-quality zone
C-1111 (I-75 Canal site)				
MZ-1	690-760	34-35	Basal Hawthorn and upper Suwannee Limestone	brackish-water zone
MZ-2	905-1,050	34-35	Suwannee Limestone	base of brackish-water zone
MZ-3	2,300-2,350	7-10	Dolomite-evaporite unit	saline-water zone
C-1112 (Immokalee site)				
MZ-2	1,060-1,140	53-55	Top of Ocala Limestone	brackish-water zone
MZ-3	1,752-1,880	53-56	Mid to lower Avon Park Formation	brackish-water zone
MZ-4	2,134-2,354	30-37	Dolomite-evaporite unit	saline-water zone
HE-1087 (L-2 Canal site)				
MZ	1,400-1,810	57-59	Avon Park Formation	brackish-water zone

NATURALLY OCCURRING STRESSES ON AQUIFERS

Many of the mechanical stresses applied to the materials (water and rock) that comprise the subsurface have naturally occurring causes rather than the anthropogenic ones familiar to hydrologists (aquifer tests, pumping for water supply, or injection). The subsurface is stressed by forces that change during the movement of the sun and moon relative to the earth, and by changes in loading arising from changes of the weight of the overlying atmosphere (atmospheric pressure). Many of these forces are periodic in nature (tidal), such as those exerted by lunar and solar motions and by periodic variations in atmospheric pressure, but some are aperiodic, such as the change in loading accompanying episodic changes in atmospheric pressure occurring over random periods of days or weeks that are caused by the movement of air masses of higher and lower pressure across the surface of the earth.

The effects of pressure loading from ocean tides and atmospheric-pressure changes are evident in deep confined aquifers that maintain a substantial head difference from surface formations across tight confining layers. Pressure loading effects also are evident from changes in the altitude of the water table related to recharge and draining or drying of surficial aquifers. The downward transmission of pressure usually is considered to be instantaneous (Spane, 2002), transmitted by grain-to-grain contact through the rock matrix (Rojstaczer, 1988), and is not associated with the vertical movement of water, except when related to the movement of the water table or in other special cases that are described near the end of this report. (When the water-table altitude changes, there may also be a concomitant change in the rate of downward leakage through confining layers.) The effects of pressure loading from atmospheric-pressure changes usually are nearly uniform over relatively large regions, so that resulting lateral flows are slight.

Solar and Lunar Stresses

The gravitational influences of the sun and moon cause sea level to rise slightly at some locations on the surface of the earth and to fall at other locations, depending on the geometric relation of each location with the astronomic bodies and the mass of the earth. These sea-level oscillations vary periodically with the changing positions of the sun and moon at a given location and are referred to as ocean tides. The range of sea level tidal oscillation varies across the earth as a function of many factors, such as the configuration of coastlines and local bathymetry. In the study area, the normal range of oscillation generally is from 2 to 4 ft (fig. 3). The sea level tidal oscillation causes an oscillation in the pressure loading on materials of the underlying subsurface, which causes oscillations of pressure or head in wells. The inland part of the

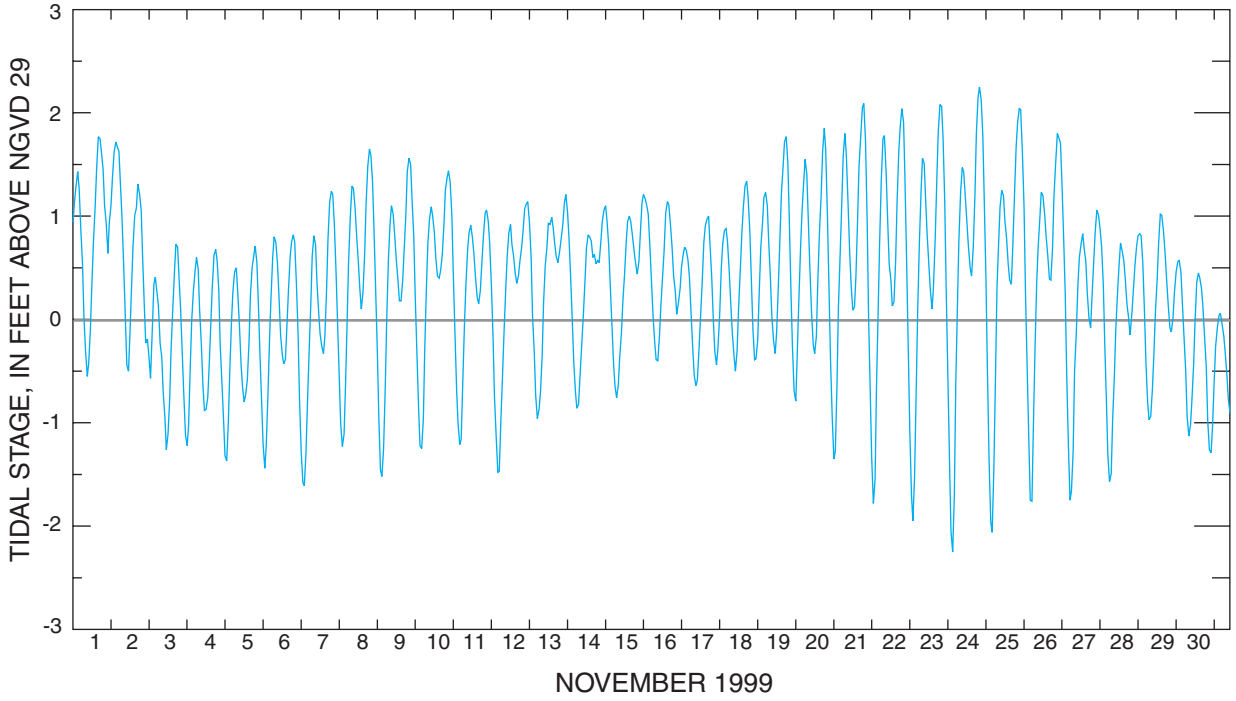

Figure 3. The ocean tide at the National Oceanic Atmospheric Administration site, Naples, Florida, November 1999.

formation, at a distance from the surface loading, responds hydraulically as if an oscillatory pumping/injection sequence were being performed in the subsurface beneath the ocean at the coastline.

Such a case is illustrated in figure 4. The head in MZ-3 in C-1111, east of Naples (the I-75 Canal site test well) and 4.9 miles from the ocean, is a subdued image of the ocean tide measured by NOAA at Naples, although a slight phase shift is apparent in the well data. The approximate range of the tidally induced head oscillations is 0.5 ft. The monitor zone is a saline-water zone at 2,300 ft below land surface (bls) (table 2). Higher brackish-water monitor zones at 690 and 905 ft bls have average heads of 34-35 ft above NGVD 29 (land surface is about 10 ft above NGVD 29), demonstrating that all of the zones are well-confined from the surface where the ocean tides occur.

When pressure loading from the surface occurs, part of the stress is absorbed by the rock matrix, so that only part of the stress is transmitted to the water contained within the formation. Van der Kamp and Gale (1983) define the ratio of the change in pore pressure (Δp_f) to an areally uniform change in pressure loading at land surface (Δp_t) as the "loading efficiency" (γ). Earlier writers (Jacob, 1940; Ferris,1951), considering the case of ocean-tide loading at the surface, referred to the change in pressure head within the formation (Δh_f) to the tidal stage change at the surface (Δh_t) as "tidal efficiency" (T_e). As will be shown later, tidal efficiency and loading efficiency are not the same.

Inland wells respond hydraulically to pressure oscillations at the coastline that have been reduced in amplitude by the factor T_e from the ocean tide oscillations at the surface of the ocean at the coast. If the subsea outcrop of the formation occurs near the coastline, the pressure oscillations in the aquifer at the coastline will just be the ocean-tide oscillations.

Solar and lunar motions also cause stretching and contracting of the subsurface rock matrix, decreasing and increasing the pressure of the water contained within the rock pores. This is evidenced in oscillations in the pressure or head of wells, even in mid-continental locations far from the influence of ocean tides. Such phenomena are termed earth tides. Heads recorded in the monitor zone in well HE-1087, located virtually equidistant (57 miles) from the east and west coasts of Florida, show tidal oscillations having a range of about 0.1 ft (fig. 5), that represent the combined influences of earth tides and periodic atmospheric-pressure fluctuations.

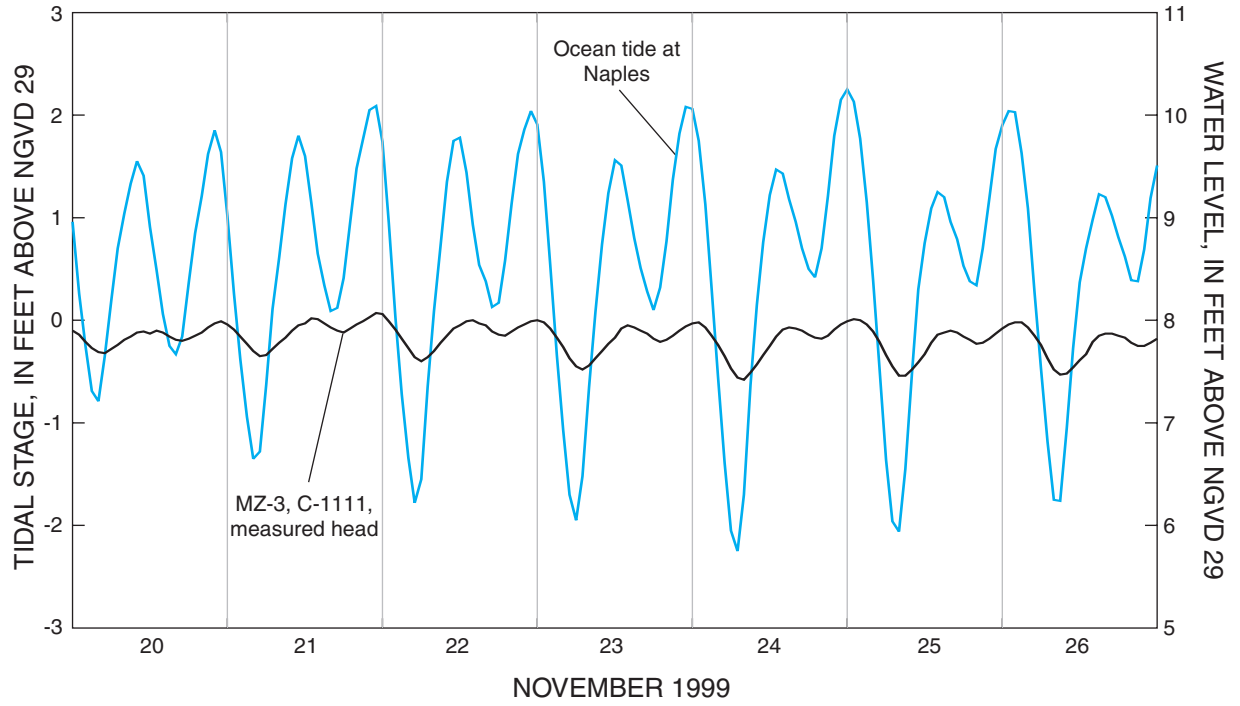

Figure 4. The ocean tide at Naples, Florida, and the measured head in well C-1111, November 20-26, 1999.

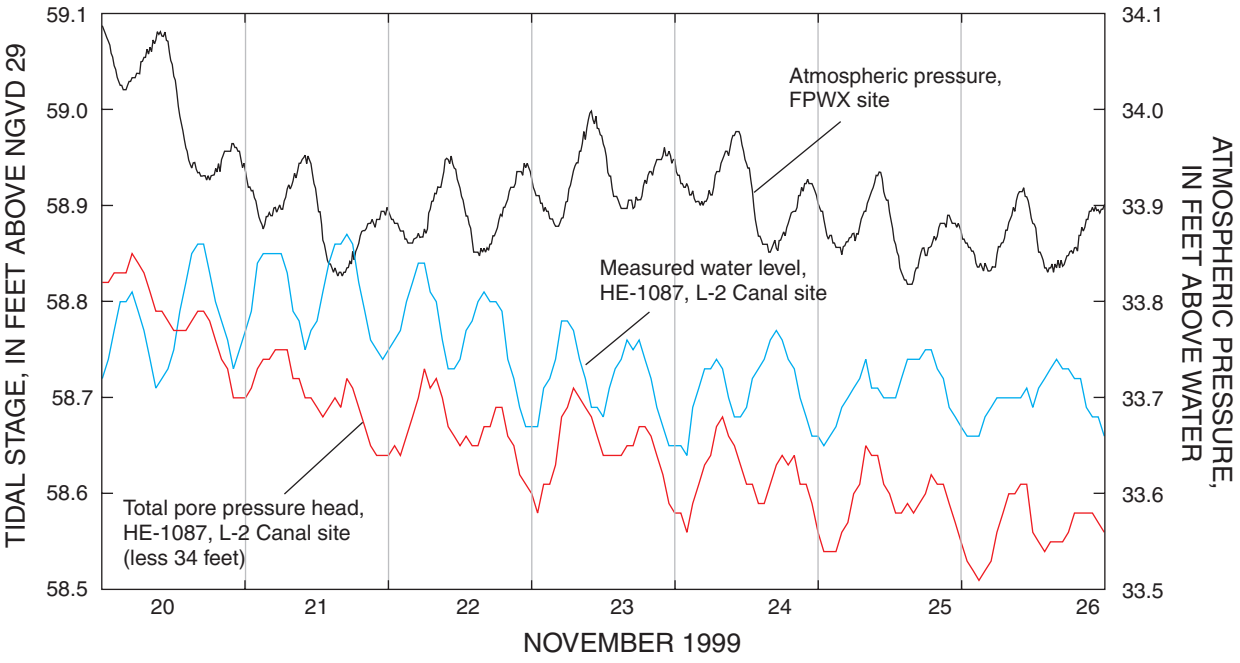

Figure 5. The measured head and total head in well HE-1087, and the atmospheric pressure at station FPWX, November 20-26, 1999.

Gregg (1966) theorized that earth tides are exactly out of phase with the ocean tides. This concept also is stated by Meyer (1974, p. 16). The reasoning was that, when the moon passes over a location on the earth's surface where a confining layer overlies an aquifer beneath the ocean, the bulge in the earth's crust would cause a lateral stretching of the earth's material and an increase in pore space, reducing hydraulic pressure. The same lunar passage causes a rise in the ocean stage, increasing the pressure loading from the surface on the aquifer. Because of the complexity and interrelation of lunar and solar movements and the differences in their effects, this hypothesis probably needs further investigation. No other publications known to the author subsequent to Meyer (1974) have included a study of this subject.

Direct measurements of earth tides are not possible as in the case of ocean tides. However, the theoretical tidal potential, $W_2(\theta,\phi,t)$, where θ is the latitude, ϕ is the longitude, and t is time, can be used to derive the range of the tidal oscillation at points on the earth's surface. $W_2(\theta,\phi,t)$ will be defined in a later section.

Atmospheric Stresses

The other major class of natural stresses acting on subsurface formations are the pressure loading and unloading caused by changes in the weight of the atmosphere. These changes are linked to periodic (diurnal and semidiurnal) changes in atmospheric pressure and to aperiodic, longer-term movements of masses of air of higher and lower pressure across the surface of the earth. The periodic oscillations of head (fig. 5) shown for well HE-1087 in November 1999 are caused by both periodic atmospheric-pressure oscillations and by earth tides.

Also shown in figure 5 is the atmospheric pressure measured at station FPWX (fig. 1). The inverse correlation between the periodic variations of the atmospheric pressure and head measured in the well is evident for this 7-day period, typical of many parts of the period of record. Slight differences in the phases of the corresponding highs and lows are related to the earth tide influence. Where the periodic atmospheric pressure and earth tide oscillations are out of phase, the relation of periodic atmospheric-pressure oscillations to the measured heads is more complex.

A description of the exact causes of the periodic atmospheric-pressure variations is beyond the scope of this report, but the variations probably are related to the heating and cooling, expansion and contraction, and rising and falling of the air mass near land surface. Ritzi and others (1991) discounted the possibility that solar and lunar effects on the atmosphere explain diurnal variation. Chapman and Lindzen (1970) explain the phenomenon of barometric tide in terms of the cyclic heating of atmospheric water vapor and ozone. Most investigators note that daily lows tend to occur in the early morning and early afternoon and that daily highs occur in the late morning and late afternoon. Clark (1967) described atmospheric pressure as "being high at about 10 am and pm and low at about 4 am and pm." An investigation of data for January 1998 and July 1999 made as part of this study indicates that the timing of peaks and lows is quite variable within a 2-3 hour period from day to day, and is often hard to determine precisely because of fluctuations about the peak or low within a 2-hour period containing the peak or low.

The movement of air masses of varying pressure causes fluctuations in heads in wells that are aperiodic and of the same duration (days or weeks) as the presence of an air mass of a given characteristic pressure in the area. There is an inverse correlation between the average atmospheric pressure typical of these time periods and heads measured in wells for the same periods (fig. 6). In the study area, fluctuations in atmospheric pressure caused by movement of air masses, and the consequent inverse fluctuations of heads measured in wells, are more frequent in winter, when episodic "cold fronts" (higher pressure) alternate with "warm fronts" (lower pressure). As previously noted, pronounced low pressure events may occur in late summer or early autumn in conjunction with tropical storms.

Barometric pressure measurements in the study area from four stations operated by SFWMD and from one station operated by NOAA (fig. 1) were evaluated. Data from the various stations were plotted against each other for selected time periods and were found to be in close agreement with, at most, only a slight (1 millimeter of Hg (mercury)) bias.

As previously noted, when pressure loading from the surface occurs, part of the stress is absorbed by the rock matrix so that only part of the stress is transmitted to the water contained within the formation. On the other hand, the surface of the water column in an open well is subjected to the full extent of the atmospheric-pressure change, so that the water level in the well is determined by both the pore

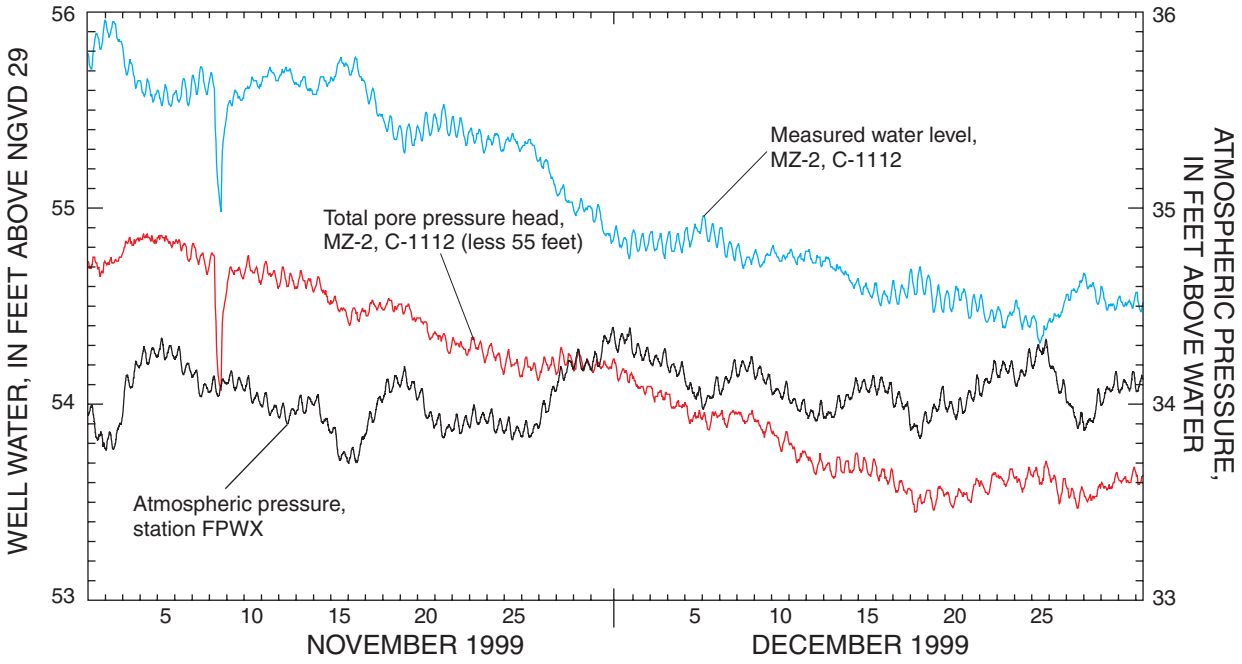

Figure 6. The measured head and total head in well C-1112, and the atmospheric pressure at station FPWX, November and December 1999.

pressure (absolute pressure) change in the aquifer and the atmospheric-pressure change at the water surface. In this report, the ratio of the change in the water level in an open well (Δh_w) to the atmospheric-pressure change at the surface, converted to feet of water (Δh_a), is termed barometric efficiency (B_e). Open wells at inland locations, therefore, show measured head fluctuations that have been reduced in amplitude by the factor B_e from the atmospheric-pressure fluctuations at land surface.

The artesian monitor zones of this study were shut in, and pressure was measured by means of pressure transducers located in the wellhead. If the pressure transducers had also been shut in and not vented to the atmosphere, the measured pressures would have been pore (absolute) pressures. Many pressure sensors are designed to measure pore pressure. However, pressure-head data supplied by the SFWMD for this study were measured using In-Situ Troll 4000 pressure recorders containing pressure transducers that were vented to the atmosphere (M. Bennett, South Florida Water Management District, written commun., December 2000) in a way that prevented the discharge of water under artesian pressure. Because the transducers were vented, the pressure-head measurements are relative to atmospheric-pressure ("gage pressure"), and have the same interpretation as water levels that would be obtained from wells open to the atmosphere.

The instrument readout showed heads in feet of freshwater computed from the measured pressures in pounds per square inch (psi) using a conversion factor of 2.31 ft of water/psi that assumes the water was of freshwater density. Use of a single standard value (2.31) for the head conversion regardless of the salinities of water in the various monitor zones was not considered a source of error, because calculations (to be described later) used small tidal head variations of the order of 0.1-1.0 ft.

The inverse correlation between measured head and atmospheric pressure (figs. 5-6) is a result of the head data being referenced to atmospheric pressure, and is also characteristic of open-well water levels. Pore pressure heads (heads computed from absolute pressure in the aquifer) should increase as atmospheric-pressure loading increases. The increase in the aquifer, however, is damped by an amount represented by the loading efficiency. Considering the case of an open well, because the pressure at the water surface in the well changes by an amount equal to the atmospheric-pressure increase, the net pressure change at the well water surface is an increase in downward pressure, so that the water surface is lowered (lower

head in the well) as the atmospheric and pore pressures increase. In the case of a vented transducer, the damped pore pressure is opposed by the atmospheric-pressure change, resulting in the same inverse correlation.

That this scenario is the case for head data from the SFWMD wells (fig. 1) is demonstrated (figs. 5-6) by plotting the pore pressure head, computed by adding atmospheric pressure, converted to feet of water, to the head measured in the well. The positive correlation between aperiodic changes in atmospheric head and pore pressure head is evident (fig. 6). The periodic changes (fig. 5) have a more complex interpretation, being negatively correlated in the first 2 days shown in the figure and positively correlated in the last 3 days. This is likely the result of the influence of earth tides.

Because heads measured in the wells are referenced to atmospheric pressure, barometric efficiencies computed based on these data have a different significance from loading efficiencies based on true formation pressures. These concepts are clarified in the following section.

Estimates of loading efficiency and relation to tidal and barometric efficiencies

An "amplitude factor" is presented by Jacob (1950) and Ferris (1951) to describe the change of formation pressure caused by an areally distributed change of pressure at land surface. "Amplitude factor" was a new term that replaced the term "tidal efficiency" used by Jacob (1940) in presenting the same factor. The amplitude factor of Jacob and Ferris was defined as:

$$\frac{\alpha}{\alpha + \eta\beta}, \qquad (1)$$

where

α is the vertical compressibility of the skeletal aquifer (psi^{-1}) (inverse pounds per square inch),

β is the compressibility of water (psi^{-1}), and

η is porosity (unitless).

A more rigorous expression for the formation pressure change caused by surface loading that takes the possible compressibility of the solid fraction of the aquifer into account was presented by Van der Kamp and Gale (1983) and referred to as "loading efficiency" (γ):

$$\gamma = \frac{B(1+\nu)}{3(1-\nu) - 2AB(1-2\nu)}, \qquad (2)$$

where

$$A = 1 - \frac{K}{K_s}, \text{ and} \qquad (3)$$

$$B = \left(\frac{1}{K} - \frac{1}{K_s}\right)\left[\left(\frac{1}{K} - \frac{1}{K_s}\right) + \eta\left(\frac{1}{K_f} - \frac{1}{K_s}\right)\right]^{-1}, \qquad (4)$$

where

K is the bulk modulus of elasticity of the formation (the inverse of compressibility),

η is the interconnected porosity of the formation, and

K_f and K_s are the bulk moduli of elasticity of water and of "the solid fraction including the effect of unconnected pores" (Van der Kamp and Gale, 1983).

The Poisson ratio (ν), a constant for most materials, is the ratio of the amount of transverse contractual strain (compression) that occurs when a material is subjected to a longitudinal extensional strain (stretching) to the amount of the longitudinal strain.

Van der Kamp and Gale (1983) state that these equations "constitute a rigorous expression for the undrained response of pore pressure to a change of surface load if horizontal displacements are negligible." These authors showed that if the solids are incompressible ($1/K_s = 0$) and the confined modulus of elasticity is written as:

$$K' = \frac{3K(1-\nu)}{1+\nu}, \qquad (5)$$

then equation 2 reduces to Jacob's amplitude factor, $(\alpha/(\alpha+\eta\beta)$. Because values for ν for most rocks do not deviate appreciably from $\nu = 0.25$ (P. A. Hsieh, U.S. Geological Survey, written commun., 2003), then $K' \cong 1.8\,K$. Van der Kamp and Gale (1983) note that B (equation 4) reduces to a form that also appears analogous to Jacob's amplitude factor when $1/K_s = 0$. They note, however, that "the distinction between B and γ resides in the fact that B represents the ratio of change of pore pressure to change of octahedral normal stress while γ represents the ratio of pore pressure change to change of vertical stress when horizontal deformations

are negligible." Van der Kamp and Gale (1983) also state that "in field applications, the loading efficiency γ is a more useful parameter, since generally only the load (or change of vertical stress) is known." Only values of the confined modulus K' should be used in equation 1 (E. P. Weeks, U.S. Geological Survey, written commun., 2003), since Jacob (1940) assumed α to represent vertical compressibility. Values of bulk modulus (K) should be converted to confined modulus by use of equation 5 before use in equation 1.

In the terminology and notation adopted for use in this report, Van der Kamp's "loading efficiency" (γ) is understood to be, as defined, the true loading efficiency that takes into account compressibility of the solid fraction of the aquifer. Jacob's "amplitude factor" is understood to be an approximation for γ that assumes the solids to be incompressible ($1/K_s = 0$). Both Jacob's factor and a data-based estimate of the pore pressure response to surface loading are termed "loading efficiency" and denoted L_e. If the solid fraction is, in fact, incompressible, $L_e = \gamma$.

The term "tidal efficiency" (T_e) has a more specialized application, representing the pore pressure change at the coast caused by ocean tides. As will be shown, tidal efficiency has a numerical value lower than loading efficiency. Some authors (Gregg, 1966; Erskine, 1991) use the terms "tidal efficiency" or "tidal efficiency factor" in a spatially varying sense, including the exponential decrease with distance from tidewater in the mathematical expression and in estimates based on well data.

The loading efficiency relation of Jacob and Ferris (equation 1) is used to estimate a range of probable values of L_e based on values cited for rock compressibility by various authors. The standard value for the compressibility of water is 3.34×10^{-6} psi^{-1} (inverse pound-force per square inch) at normal atmospheric pressure and 20 degrees Celcius. In the carbonate Upper Floridan aquifer, porosities of the order of 35 percent commonly are measured on cores or estimated from geophysical logging (solid dolomite sections commonly have a lower porosity, possibly no more than 15 percent). Domenico and Schwartz (1997) suggest 1.6×10^{-8} to 3.3×10^{-7} psi^{-1} as a typical range of values for the compressibility of fissured or jointed rock. Using this range of values, and assuming a porosity of 35 percent, the loading efficiency estimate would range from 1.4 to 22 percent.

Robinson and Bell (1971) cite Birch (1966) in stating a range of 1×10^{11} to 3×10^{11} dynes per square centimeter (dynes/cm^2) for the bulk modulus of aquifer matrix material "representative of common sedimentary rocks" and said to be based on analysis of rock samples (Rhoads and Robinson, 1979). Assuming a Poisson ratio (ν) value of 0.25, and using equation 5 to convert to confined modulus, this is equivalent to a range of vertical compressibilities of 0.13×10^{-6} to 0.38×10^{-6} psi^{-1}. The corresponding range of the loading efficiency estimate (L_e) would be 10 to 25 percent. However, results of a field study by Rhoads and Robinson (1979) led to computed estimates of bulk modulus (4.05×10^{10} to 13.87×10^{10} dynes/cm^2, equivalent to a vertical compressibility range of 0.28×10^{-6} to 0.94×10^{-6} psi^{-1}). The corresponding range of L_e would be 19 to 45 percent. Rhoads and Robinson (1979) suggest that their lower estimates of bulk modulus could be the result of larger fractures and solution cavities in the aquifer and not present in rock samples.

The relation between aquifer compressibility (α) and loading efficiency, based on the value for water compressibility (β) cited above, is shown for an aquifer compressibility range of 1×10^{-7} to 1×10^{-4} psi^{-1} and for aquifer porosities of 15, 30, and 45 percent (fig. 7). The graph shows that, in highly compressible formations, pressure changes are nearly equal to the imposed pressure loading, but that relatively incompressible formations absorb most of the pressure loading.

Jacob (1940) also derived a relation for the open-well barometric efficiency:

$$B_e = \frac{\theta\beta}{\alpha + \theta\beta} = 1 - L_e, \qquad (6)$$

and showed, as a consequence, that open-well barometric efficiency (B_e) and loading efficiency (L_e) summed to unity. Citing this work, Van der Kamp and Gale (1983) state that "in analyzing the barometric response of the water level in a well open to the atmosphere, the influence of barometric pressure acting directly on the water surface in the well should be born in mind." Rhoads and Robinson (1979) note that "an increase in atmospheric pressure . . . causes a change in pore pressure in the aquifer, which is equal to the change in atmospheric pressure plus the change in water level in the well."

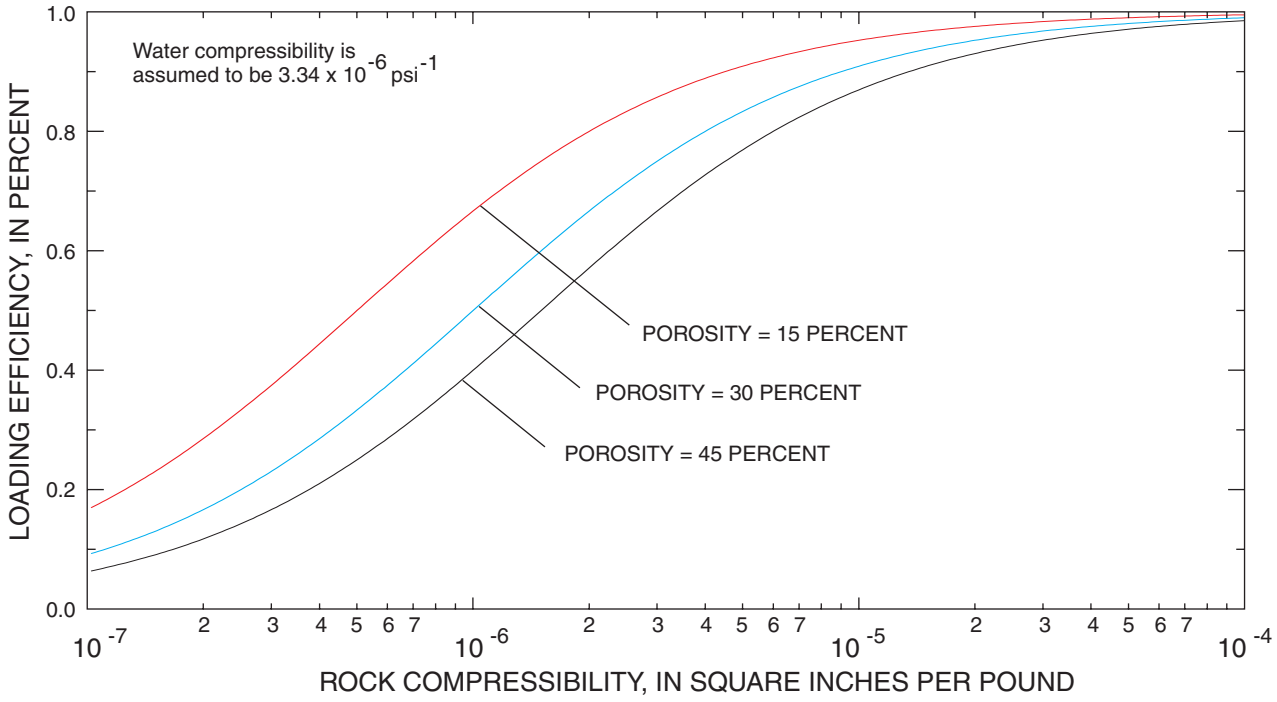

Figure 7. The relation between matrix compressibility and loading efficiency for three values of matrix porosity, based on Jacob's formula for loading efficiency.

Determination of barometric efficiency by Clark's method

It is often useful to know the open-well barometric efficiency of a given set of barometrically affected head data; such knowledge is helpful in obtaining estimates of loading efficiency needed for application of methods used in this study. Clark (1967) devised such a method based on aperiodic, long-term pressure variations arising from the movement of air masses and corresponding measured head changes in the well. This method was investigated as part of this study, and was found to work well with some data sets and to provide inaccurate or meaningless results in others.

In order to summarize the steps of Clark's method, time series of barometric-pressure and head measurements are assumed to have: (1) the same beginning and end times; (2) the same, equally spaced time increment for independent measurements (1 hour in the example below); and (3) no missing values. Barometric-pressure measurements are converted to feet of water. (A factor of 0.044602 converts millimeters of mercury to feet of water, and a factor of 1.33322 converts millimeters of mercury to millibars.) Proceeding incrementally from one time step (t_i) to the next, concurrent sums of barometric-pressure (b_i) and head (h_i) changes are generated according to the following criteria:

$$\Delta b_i = b_i - b_{i-1} , \quad (7)$$

$$\Delta h_i = h_i - h_{i-1} , \quad (8)$$

$$\beta_i = \Delta b_i \cdot \Delta h_i , \quad (9)$$

$$S_b^i = S_b^{i-1} + |\Delta b_i| , \quad (10)$$

$$S_h^i = S_h^{i-1} - |\Delta h_i| \text{ if } \beta_i > 0 , \quad (11)$$

$$S_h^i = S_h^{i-1} + |\Delta h_i| \text{ if } \beta_i < 0 , \text{ and} \quad (12)$$

$$S_h^i = S_h^{i-1} \text{ if } \Delta b_i = 0 \ . \qquad (13)$$

In Clark's description of his method, the sign convention was to consider Δh_i to be positive when head is rising and to consider Δb_i to be positive when barometric pressure is falling. Equations 7-13 implicitly include this convention. The procedure was devised to separate incremental changes in head caused by atmospheric-pressure fluctuations from changes caused by other influences. The time series of S_h^i is plotted as a function of the corresponding time series S_b^i, and a regression line is drawn through the data. (The linear fit function of the S-Plus software was used for this study.) The slope of the regression line is the calculated barometric efficiency B_e.

The Clark method was used with good results for head data measured in two of the three monitor zones in well C-1112, 28 miles from the coast of the Gulf of Mexico north of Naples, and with limited success in the third (figs. 8-10). Head data from MZ-2 (1,060-1,140 ft bls) measured in November and December 1999 and corresponding atmospheric-pressure measurements from station FPWX are shown in figure 6. The Clark method was applied to the entire period of record of heads used in this study (April 1999-November 2000). The linear fit to the plot of the two computed sums (fig. 8) for head data from MZ-2 indicates a barometric efficiency of 63 percent.

After barometric efficiency is estimated, the value is partly verified by using it to remove the atmospheric-pressure effects from the well water-level data. Software developed for this study used barometric-pressure changes and the estimated barometric efficiency (B_e) to correct the head data for the barometric influence. Initial corrections to the data often created a slight bias between the averages of the original and corrected data sets. This bias was found to be inconvenient in making graphical comparisons of the original and corrected head data sets. Therefore, the software was executed a second time with the bias removed by adding a constant correction value (*COR*). The correction procedure is as follows:

$$\delta w_i = -(B_e \cdot \ \Delta b_i) \ , \qquad (14)$$

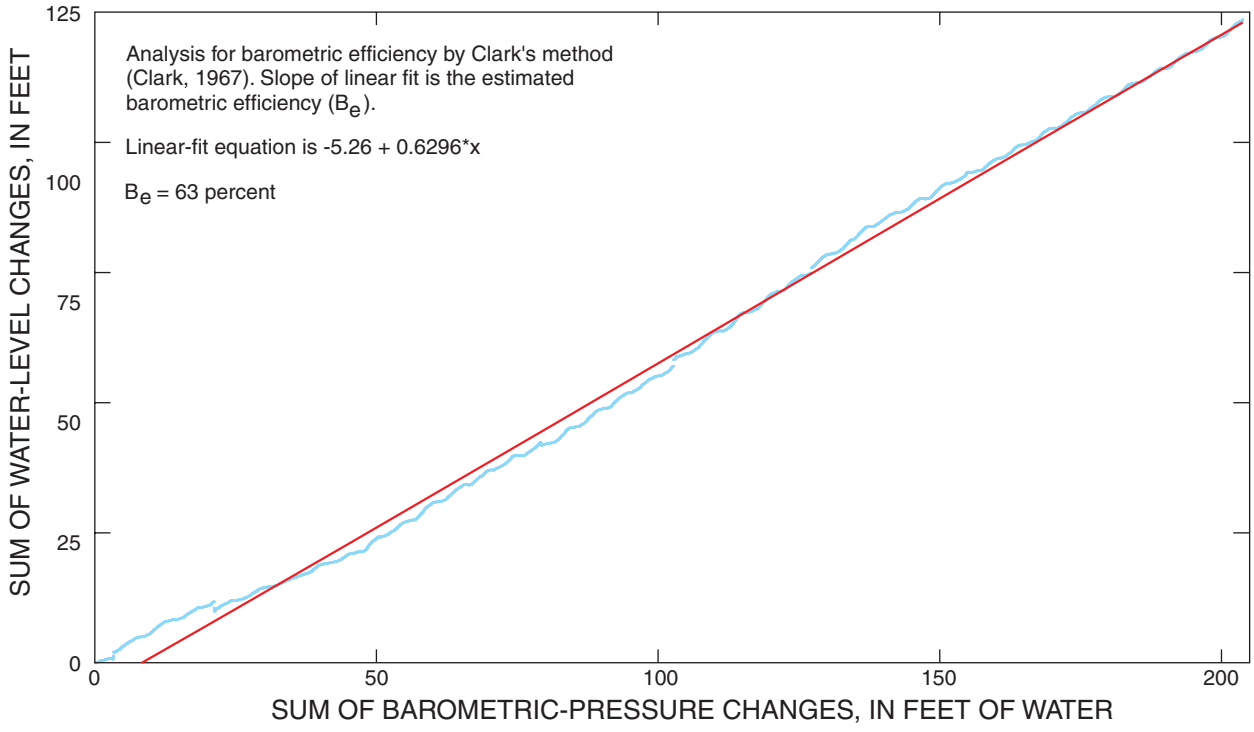

Figure 8. Computation of barometric efficiency based on measured-head data from MZ-2, well C-1112.

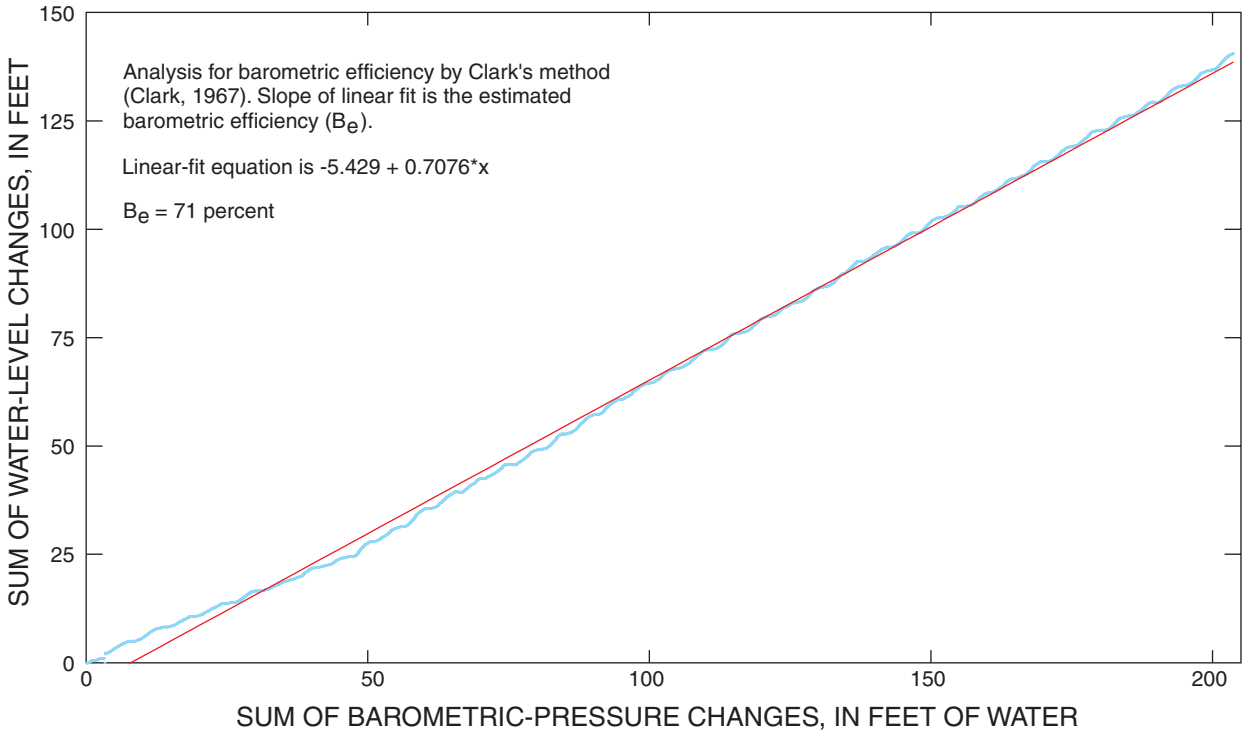

Figure 9. Computation of barometric efficiency based on measured-head data from MZ-3, well C-1112.

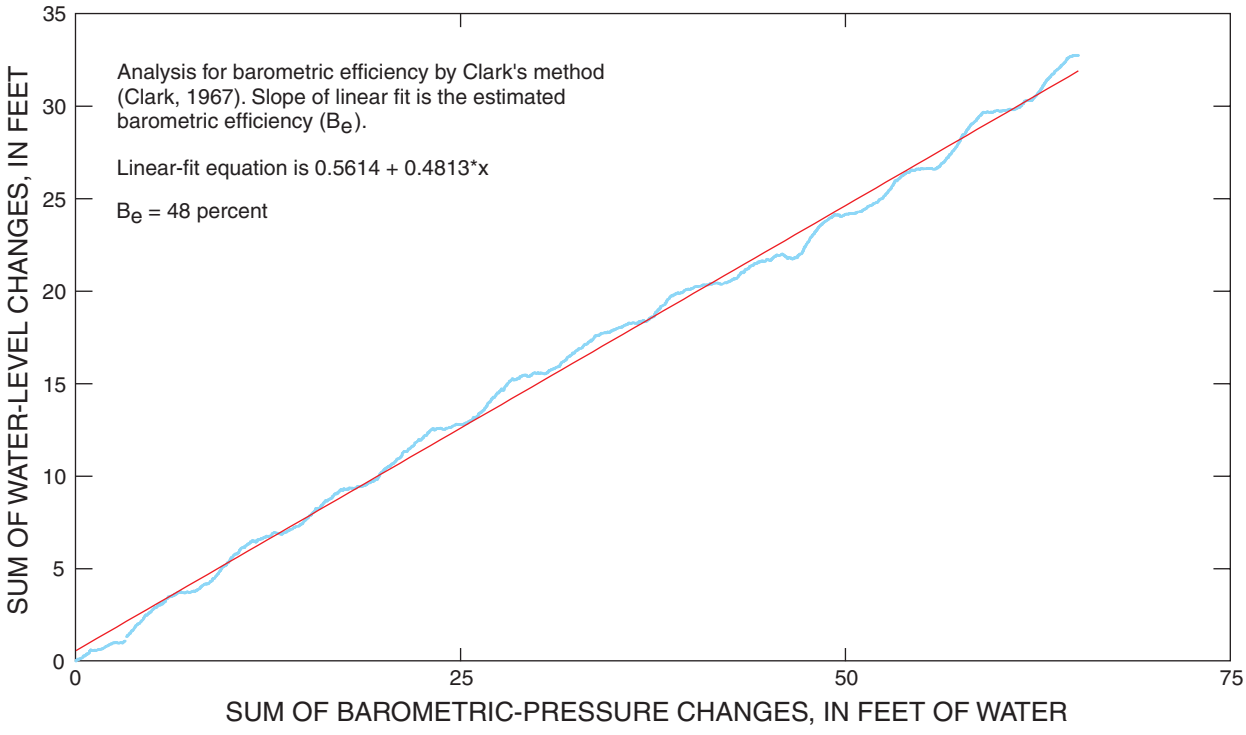

Figure 10. Computation of barometric efficiency based on measured-head data from MZ-4, well C-1112.

$$\sum_{j=1}^{j=i} \delta w_j = \sum_{j=1}^{j=i-1} \delta w_j + \delta w_i \quad \text{, and} \qquad (15)$$

$$h_i^c = h_i + \sum_{j=1}^{j=i} \delta w_j + COR \quad , \qquad (16)$$

where

δw_i is the estimated correction to the measured head value h_i, and

h_i^c is the corrected head value.

The corrected data (shown for November and December 1999 in fig. 11) are without the effects of long-term, aperiodic atmospheric-pressure fluctuations during that time period, although the head data show a decreasing trend caused by other environmental influences during that time period. The sudden drop in head readings (possibly erroneous data) of November 8-9 are not affected by the procedure. The periodic (diurnal and semidiurnal) head oscillations also are altered, but some periodic oscillations remain because of the influence of earth tides. Because of the latter influence, it is difficult to determine the extent to which the periodic head oscillations caused by periodic atmospheric-pressure oscillations have been corrected.

The method was applied to data from MZ-3 (1,700-1,880 ft bls), with the same period of record as MZ-2, and a barometric efficiency estimate of 71 percent was obtained (table 3). The corrected plot was smoother than the original, but the correction process did not appear as effective for MZ-3 as for MZ-2. A barometric efficiency of 48 percent was obtained from analysis of data from MZ-4 (2,200-2,300 ft bls), which were from a more limited period of record (April-September 1999). Atmospheric pressure-induced head fluctuations in this zone appeared to be subdued. The correction process appeared to smooth the raw data from the early part of the period of the data, but caused distortions in the raw data from the later part of the record period, when the raw data appeared to show almost no response to long-term, aperiodic atmospheric-pressure fluctuations.

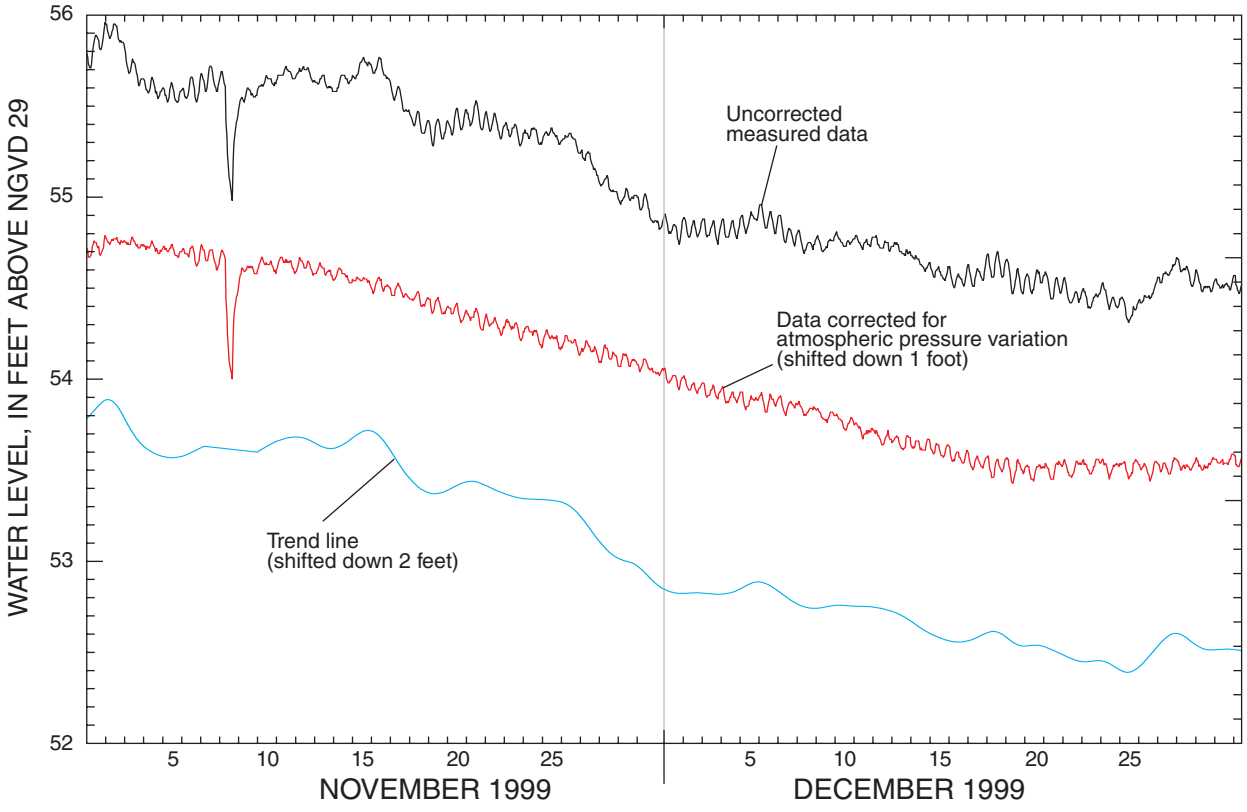

Figure 11. Uncorrected measured-head data from MZ-2, well C-1112, data corrected for the effect of long-term, aperiodic atmospheric-pressure fluctuations, and the trend line based on the data, November and December 1999.

Table 3. Barometric-efficiency and loading-efficiency determinations

[--, not estimated]

Monitor zone	Well	Barometric efficiency calculated by the Clark[1] method (in percent)	Barometric efficiency calculated by the trial-and-error method (in percent)	Loading efficiency calculated by the modified Clark method (in percent)	Loading efficiency calculated by the trial-and-error method (in percent)	Rock compressibility computed from loading efficiency (inverse pounds per square inch x 10^{-6})
MZ-1	C-1111 (I-75 Canal site)	83	--	17	--	0.24
MZ-2	C-1111 (I-75 Canal site)	74 to 86	--	26	--	.41
MZ-3	C-1111 (I-75 Canal site)	31	85	69	15	.21
MZ-2	C-1112 (Immokalee site)	63	--	37	--	.69
MZ-3	C-1112 (Immokalee site)	71	--	29	--	.48
MZ-4	C-1112 (Immokalee site)	48	--	52	80	--
MZ	HE-1087 (L-2 Canal site)	--	75	95	25 to 45	--

[1]Clark, 1967.

Clark's method was applied to head data (period of record November 1997-December 2000) from the three monitor zones in well C-1111 near Naples (figs. 12-14). Atmospheric data from the Naples NOAA station, beginning January 1, 1998, were used for the analysis. The linear fit computation of barometric efficiency worked well for MZ-1 (690-780 ft bls) and provided an estimate of 83 percent. Most of the variation in the head data caused by aperiodic, long-term atmospheric-pressure variations was removed in the correction process. The linear-fit plot was somewhat variable for MZ-2 (905-1,050 ft bls). An overall linear-fit value of 74 percent was computed for barometric efficiency, but two sections of the plot having a slope of 86 percent were separated by a section of nearly zero slope. Both values produced good results when used in the correction process, and results from use of the two values could not be easily distinguished from one another.

Data between December 1999 and June 2000 were absent from the record of heads from MZ-3 (2,300-2,350 ft bls) and only data from the period between January 1998 and December 1999 were used in the analysis. The slope of the plot of the head-increment sum as a function of the barometric-pressure increment sum (fig. 14) was quite variable, and ranged from less than zero to about 90 percent in various sections. The overall computed slope (estimate of barometric efficiency) was only 28 percent. Correcting the raw data using a barometric efficiency estimate of 28 percent was ineffective. A value of 85 percent was found to be appreciably more effective in the correction process.

Unsatisfactory results occurred when the Clark method was applied to head data from the monitor zone in HE-1087 (1,400-1,810 ft bls). The data were measured between September 1998 and December 1999. The atmospheric-pressure data used for the analysis were measured at the Clewiston Field Station weather site (CFSW) operated by the SFWMD. The plot of the sum of head increments as a function of the barometric-pressure increment sum (fig. 15, no time lag) has a slope of about 43 percent until mid-April 1999, at which time the slope becomes negative. A detailed examination of the data reveals that it was somewhat noisy, which could serve to make the relation between incremental changes in atmospheric pressure and heads less well defined than if the data were free of noise. There was also a strong downward, and then upward, trend in the atmospheric-pressure data between March and June 1999, but this did not appear correlated with the trend of the sums in the Clark method analysis.

It was found that the slope could be reversed if several hours were added to or subtracted from the time coordinate of the head data. The software was

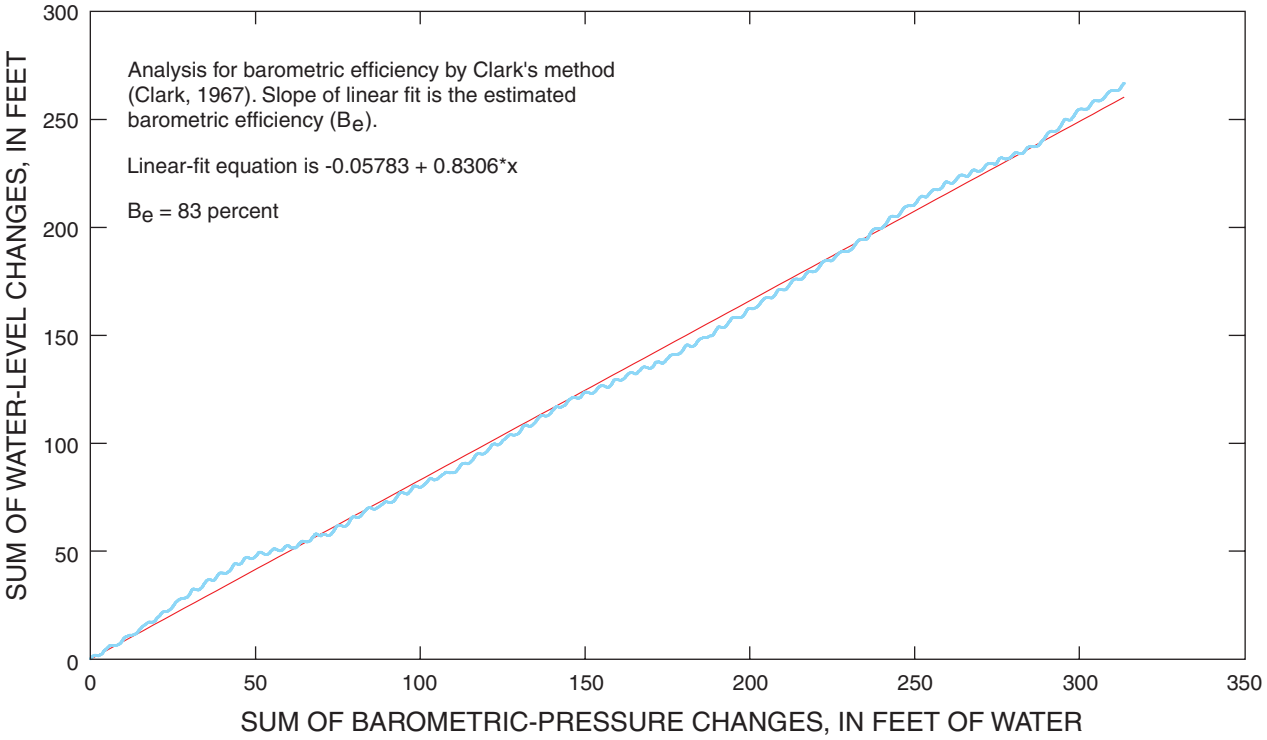

Figure 12. Computation of barometric efficiency based on measured-head data from MZ-1, well C-1111.

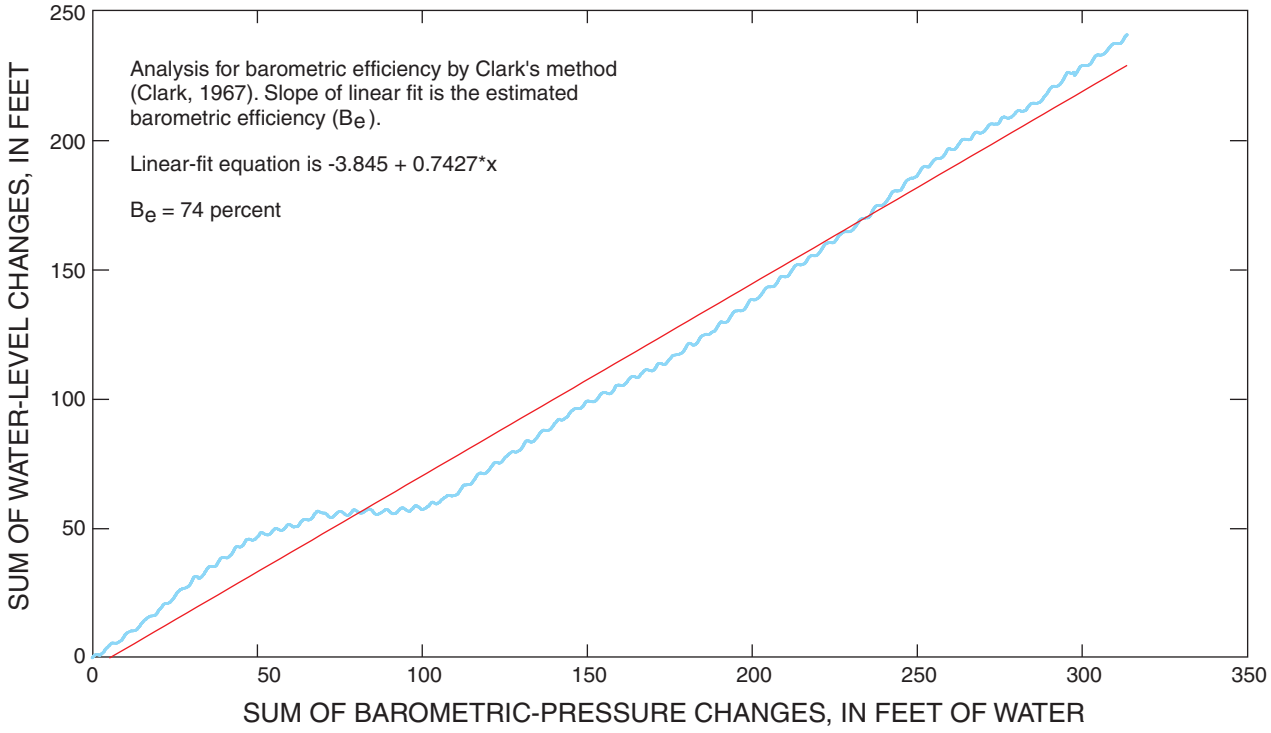

Figure 13. Computation of barometric efficiency based on measured-head data from MZ-2, well C-1111.

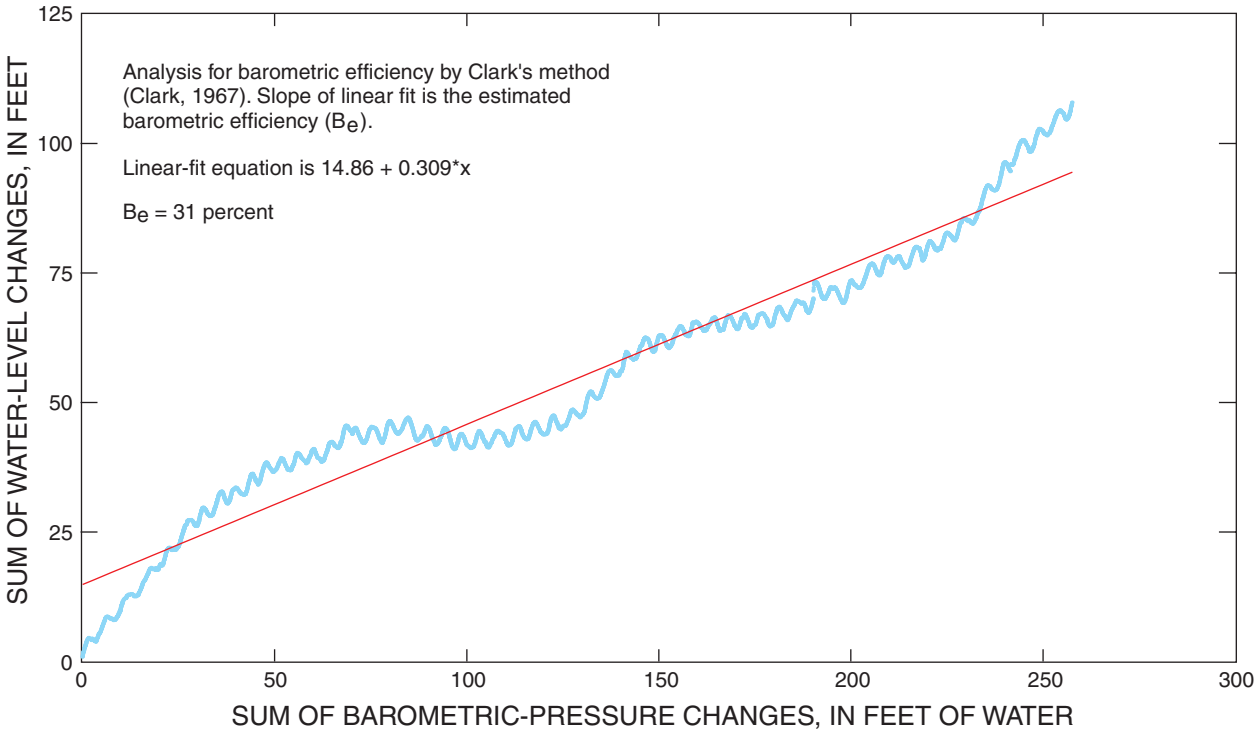

Figure 14. Computation of barometric efficiency based on measured-head data from MZ-3, well C-1111.

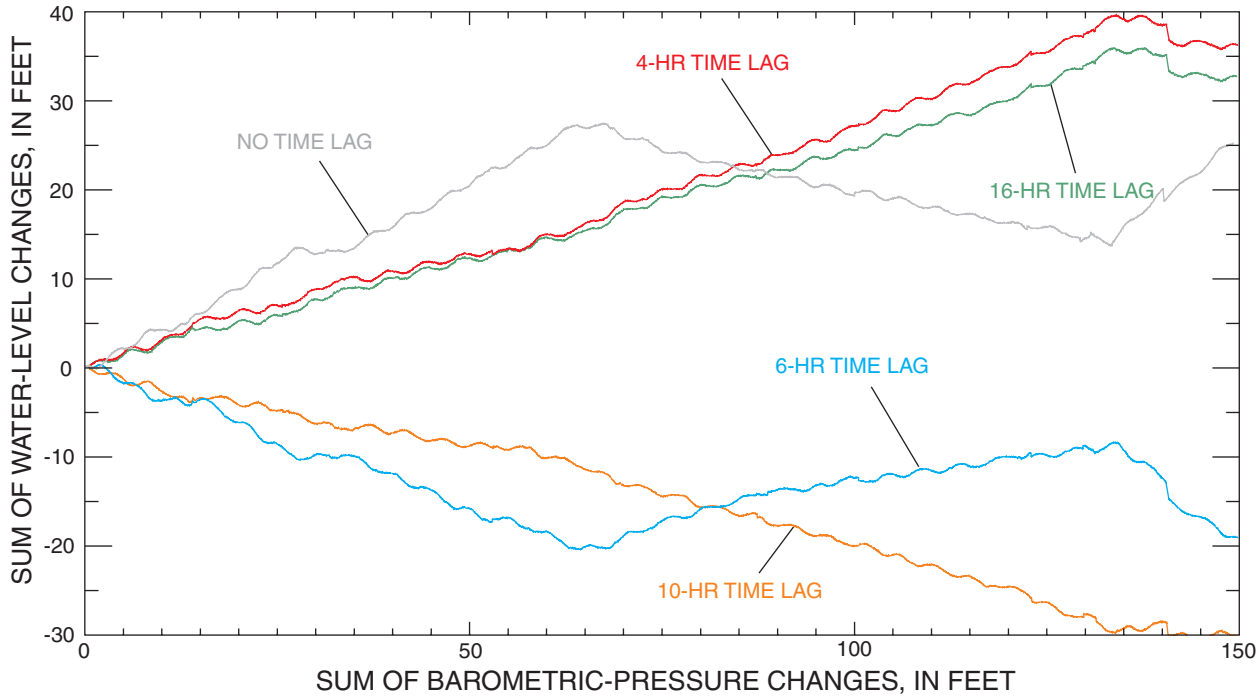

Figure 15. Head increment sums in data from the monitor zone in well HE-1087 as a function of barometric-pressure increment sums.

modified to provide for a bias of the time of the head data, and various lengths of time were used in trial computations. The plot of the sum of head increments as a function of the barometric pressure sum became a straight line for a 4-hour time lag (fig. 15), but the slope of the graph was only about 27 percent. For a time lag of 6 hours, the positive and negative slopes of the original graph became reversed. The plot was straight with a negative slope for a 10-hour time lag, but became straight with a positive slope again for a time lag of 16 hours, where the slope of the plot was 24.5 percent. Correcting the head data assuming a barometric efficiency of 24-27 percent, however, was not effective in removing the atmospheric-pressure influence.

Because of the failure of the Clark method to provide a realistic estimate of barometric efficiency for the monitor zone in well HE-1087, an alternative trial-and-error method was implemented. Trial-and-error was mentioned by Clark (1967) as one method of determining barometric efficiency, and his computational method provided a more efficient and precise statistical alternative for obtaining estimates. Barometric efficiency values of 43, 75, and 95 percent were assumed in attempts to correct the head data (fig. 16). From viewing the figure, the first of these values appears to be too low, and the third appears to be too high, resulting in an overcorrection for the atmospheric pressure effect. The value of 75 percent appears to be nearly correct, and the trend of the corrected head data appears to be largely free of the influence of long-term, aperiodic atmospheric-pressure variations.The trial-and-error method also was applied successfully to data from MZ-3, well C-1111, but not to data from MZ-4.

It is concluded that the Clark method can be an effective tool for determining barometric efficiency when the head data are of high quality. But the method does not appear to be entirely robust, and can provide values that are too low in some data sets that might be affected by a high degree of noise, strong trends, or timing inaccuracy. The method provided values that were too low in data sets that did not have obvious problems of these kinds. It seems prudent to apply a

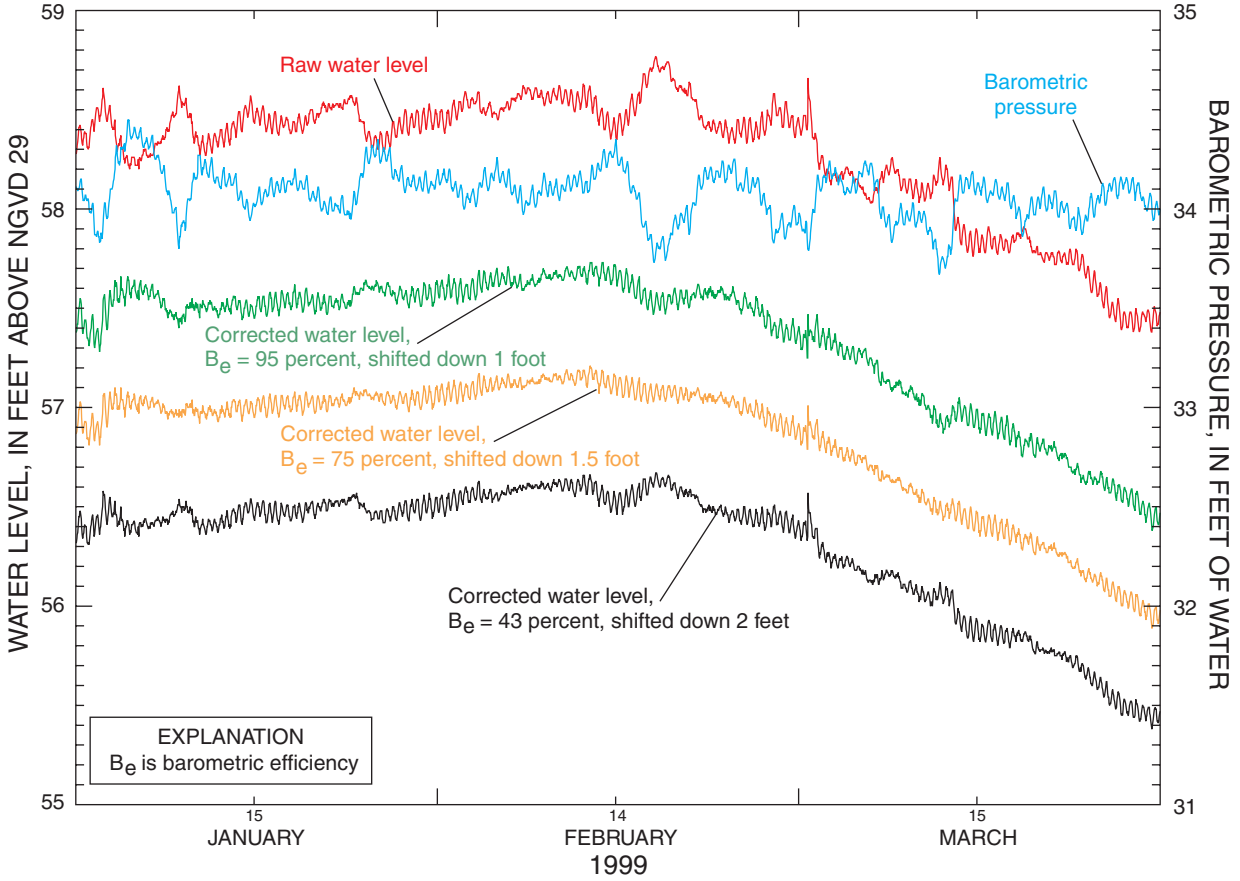

Figure 16. Application of trial-and-error method for correcting measured-head data from the monitor zone in well HE-1087 for the influence of long-term, aperiodic atmospheric-pressure variations.

process of actually correcting head data sets to determine whether barometric efficiency values determined by the Clark method are correct. If they are not correct, or if the method yields ambiguous results, the trial-and-error method should be applied, in which a process of arbitrarily selecting a value and using it for correction is repeated until results are satisfactory.

Determination of loading efficiency by Clark's method

One of the physical properties most often used in analytic methods for basing aquifer parameter estimates on measured tidally influenced data is the loading efficiency (L_e). From equation 6, it is straightforward to estimate loading efficiency once an estimate of the barometric efficiency (B_e) is obtained. It was desirable, however, to verify such estimates by applying a modified version of Clark's method to the time series of total pore pressure-head values, obtained by summing values of water level from the vented pressure transducers and the measured barometric pressure, converted to feet of water, at each time for which both were available. Because the total pore pressure and barometric pressure were positively correlated, the sign of the conditional relation was changed in equations 11-12, that is, the absolute value of Δh_i was added to the sum if $\beta_i > 0$ and subtracted from the sum if $\beta_i < 0$. This is equivalent to reversing the sign of β_i, or Δb_i (or reversing Clark's sign convention). If h_i is the measured pressure head used in equation 8 and h_i^t is the corresponding total pressure head, loading efficiency will be a regression line drawn through the plot of:

$$\frac{\sum_{j=0}^{j=i} \Delta h_i^t}{\sum_{j=0}^{j=i} \Delta b_i^t} = \frac{\sum_{j=0}^{j=i} (\Delta h_i - \Delta b_i)}{\sum_{j=0}^{j=i} (-\Delta b_i)} = 1 - \frac{\sum_{j=0}^{j=i} \Delta h_i}{\sum_{j=0}^{j=i} \Delta b_i}. \quad (17)$$

This result suggests that the modified Clark method should produce the result predicted by equation 6. The values obtained by applying the modified Clark method to the time series of measured data (table 3) confirm equation 6. The plots of S_h as a function of S_b for the monitor zone in HE-1087 showed no sections of negative slope, even when the entire record was used.

Estimates were checked by using them to correct fluctuations in the time series of total pressure head induced by long-term aperiodic atmospheric-pressure fluctuations. Such fluctuations were not clearly defined in the data from the three monitor zones in well C-1111 in Naples. It was difficult to evaluate the effects of the small corrections (17 and 26 percent) applied to data in MZ-1 and MZ-2. The 69-percent correction applied to MZ-3 data clearly was too large; a correction of 15 percent seemed more appropriate, but again, results were difficult to evaluate.

The estimated 37- and 29-percent corrections were successfully applied to total head data from MZ-2 and MZ-3 in well C-1112 at Immokalee, but a 52-percent correction appeared inadequate for data from MZ-4. Because the latter part of the 6-month record of measured heads showed no response to aperiodic atmospheric-pressure fluctuations, adding the atmospheric-pressure values to generate the total head data caused strong aperiodic atmospheric-pressure fluctuations in the latter. An 80-percent correction applied to the data successfully removed the fluctuations caused by atmospheric pressure, but appeared to amplify periodic oscillations. The raw data and correction results from MZ-4 appeared anomalous and are not considered highly reliable. A 95-percent correction applied to the data from the monitor zone in HE-1087 (in the center of the peninsula) clearly was too great. Corrections ranging from 25 to 45 percent were more effective for various parts of the data record.

The estimated loading efficiencies that appeared realistic or that were used successfully to correct for long-term, aperiodic atmospheric-pressure effects were used for estimates of rock compressibility (α) for comparison with literature values cited previously. These values are shown in table 3. All computed compressibility values are based on loading efficiencies computed by the modified Clark method, except for MZ-3, well C-1111, where the trial-and-error value (0.15) was used. The values computed generally are within the ranges cited by Domenico and Schwartz (1997), Birch (1966), and Rhoads and Robinson (1979).

Harmonic Structure of Tidal and Atmospheric Stresses

Ocean and earth tides, being of solar and lunar origin, are periodic, as are the motions of those astronomical bodies relative to the earth. Because these motions are complex and have many components of different frequencies and level of influence, the tides also are a combination of periodic components of different frequencies and amplitudes. These components are expressed as distinct "harmonics," sinusoidal functions of given amplitude and frequency and phase relation to some common time reference. Many of the harmonics that are part of daily tidal oscillations are listed in table 4 together with the symbols usually used to refer to them and their associated frequencies. These frequencies are known with great precision based on decades of astronomical observations (Hanson and Owen, 1982, table 1). The frequencies are common to all ocean and earth tide data, but the amplitudes and phase relations for each component are a characteristic of each individual set of tide data. Further information about tides can be obtained from Melchior (1983) and Godin (1972).

Bredehoeft (1967) cites Melchior (1964) in stating that, of all the harmonic components, only five (M_2, S_2, N_2, K_1, and O_1) are of importance geophysically, together accounting for approximately 95 percent of the tidal potential. Several other minor components have frequencies so close to those of one of the other harmonics that they often cannot be resolved from the other harmonic at a high probability level by harmonic analysis (S_2-K_2, K_1-P_1, N_2-$2N_2$, O_1-Q_1, Q_1-$2Q_1$, and K_1-J_1). Such resolution becomes possible at a lower probability level only when a long time series of relatively error-free data is available. P_1 and K_2 are major components, but usually are combined with K_1 and S_2, respectively, in analyses. Hanson and Owen (1982, fig. 1) illustrate the relative position and amplitude of minor tidal components Q_1, $2Q_1$, $2N_2$, J_1, and K_2. Nowroozi and others (1969) show Q_1, $2Q_1$, OO_1, $2N_2$, and μ_2, but all are stated to be resolved at less than a 95-percent confidence level.

Analysis of time-series data to determine the presence of harmonics (spectral analysis) is usually accomplished using the discrete Fourier transform technique (Shumway, 1988). A range of frequencies is subdivided into increments, and for each frequency

Table 4. Harmonic components of tides

Symbol	Angular frequency (radians/hour)	Frequency (cycles/day)	Period (hours)	Explanation
O_1	.24335189	.92953574	25.819341	Main lunar diurnal
K_1	.26251618	1.00273794	23.934469	Lunar-solar diurnal
M_2	.50586804	1.93227356	12.420602	Main lunar semidiurnal
S_2	.52359878	2.00000000	12.000000	Main solar semidiurnal
N_2	.49636693	1.89598199	12.658348	Lunar elliptic (lunar semi-diurnal component caused by monthly variation in moon's distance)
P_1	.26108260	.99726206	24.065891	Main solar diurnal
K_2	.52503234	2.00547579	11.967235	
Q_1	.23385075	.89324406	26.868357	
ν_2	.49763845	1.90083884	12.626005	
M_1	.25301504	.96644625	24.833249	
J_1	.27201730	1.03902954	23.098477	
μ_2	.48813732	1.86454720	12.871758	
L_2	.51536918	1.96856524	12.191620	
T_2	.52288202	1.99726218	12.016449	
$2N_2$	.48686579	1.85969031	12.905375	
OO_1	.28168047	1.07594013	22.306074	
$2Q_1$	.22434962	0.85695241	28.006223	

(increased incrementally), the sine and cosine functions are integrated with the data over the period of record used (Fourier transform). Where the data have a periodic component corresponding to the frequency, a Fourier transform value results that is substantially different from zero. A graph of the results of these computations with frequency as the abcissa is called a periodogram and shows the frequencies of the harmonics present in the data. This method of analysis was applied to data collected for this study to verify and demonstrate the presence of the usual harmonics.

This technique was applied to hourly tidal stage data measured by NOAA at Naples, Florida, for nearly 4 years (January 1997-November 2000). The software used was the PFFT program included in Microsoft Fortran Power Station, Professional Edition. An application program was written to input the data set and to use PFFT and various other supporting utility programs for the analysis and storage of the results. A graph showing the resulting periodogram (fig. 17) clearly indicates the large Fourier transform values obtained at frequencies nearly equal to those of the major harmonic components of ocean and earth tides (the O_1, K_1-P_1, M_2, and S_2-K_2 components). For convenience, the K_1-P_1 and S_2-K_2 components are labeled as the larger of the two components in each set (K_1 and S_2). The N_2 component is small, but is clearly shown at a slightly lower frequency than the M_2 component.

In this analysis, the availability of a lengthy data set of reasonably good quality has provided a good signal-to-noise ratio in the results of the analysis that enhances their graphical interpretation. At a larger scale (figs. 18-19), the Q_1 component is clearly indicated, and the P_1 and K_2 components can be separated from the K_1 and S_2 components, respectively. The M_1, J_1, $2N_2$, μ_2, and ν_2 components are also visible, with Fourier series values ranging from 0.3 to 3.0. A slight spike in the graph at the correct frequency might be the L_2 component. Only the $2Q_1$ and OO_1 components cannot be found, and the T_2 component cannot be distinguished from the S_2 component.

The Fourier transform technique also is applied to atmospheric-pressure data from station FPWX collected at quarter-hour intervals between January 1998 and November 2000 (fig. 20). The periodogram indicates that the harmonic components are strictly diurnal

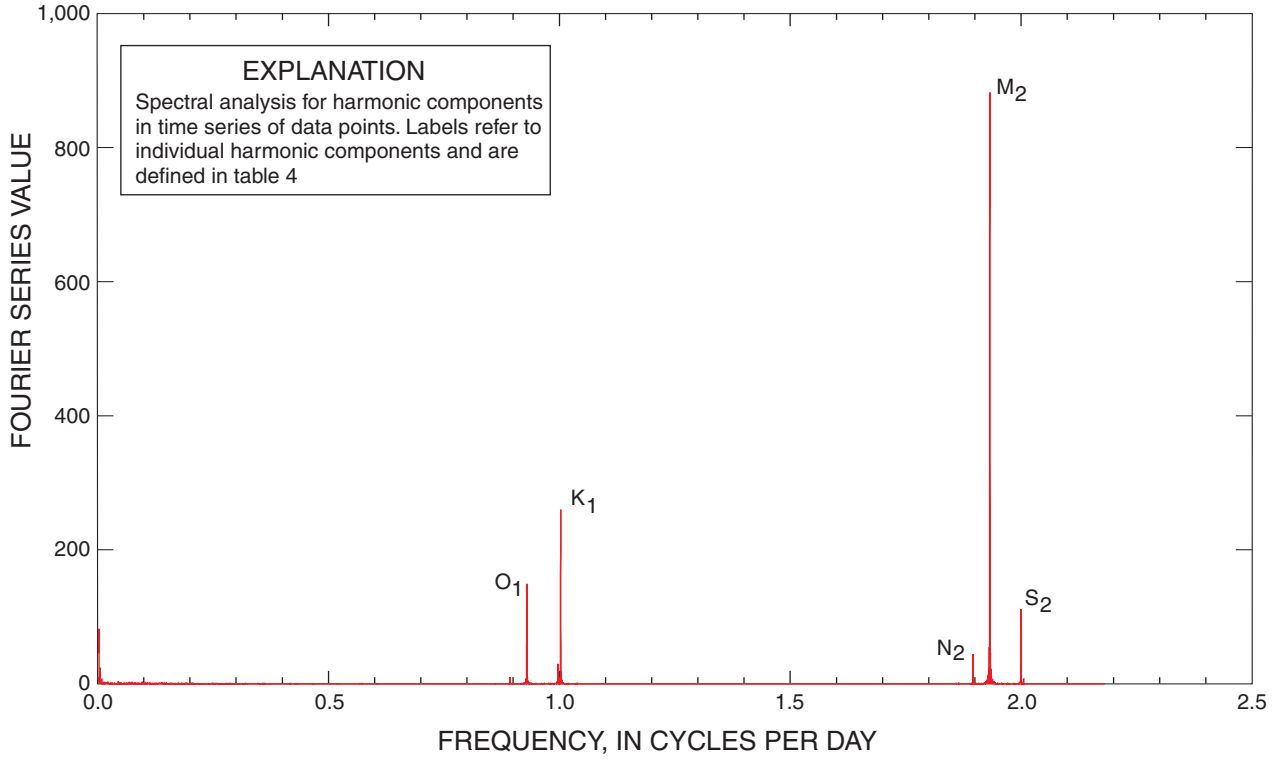

Figure 17. Periodogram of harmonic frequencies present in ocean-tide data collected by the National Oceanic Atmospheric Administration at Naples, Florida.

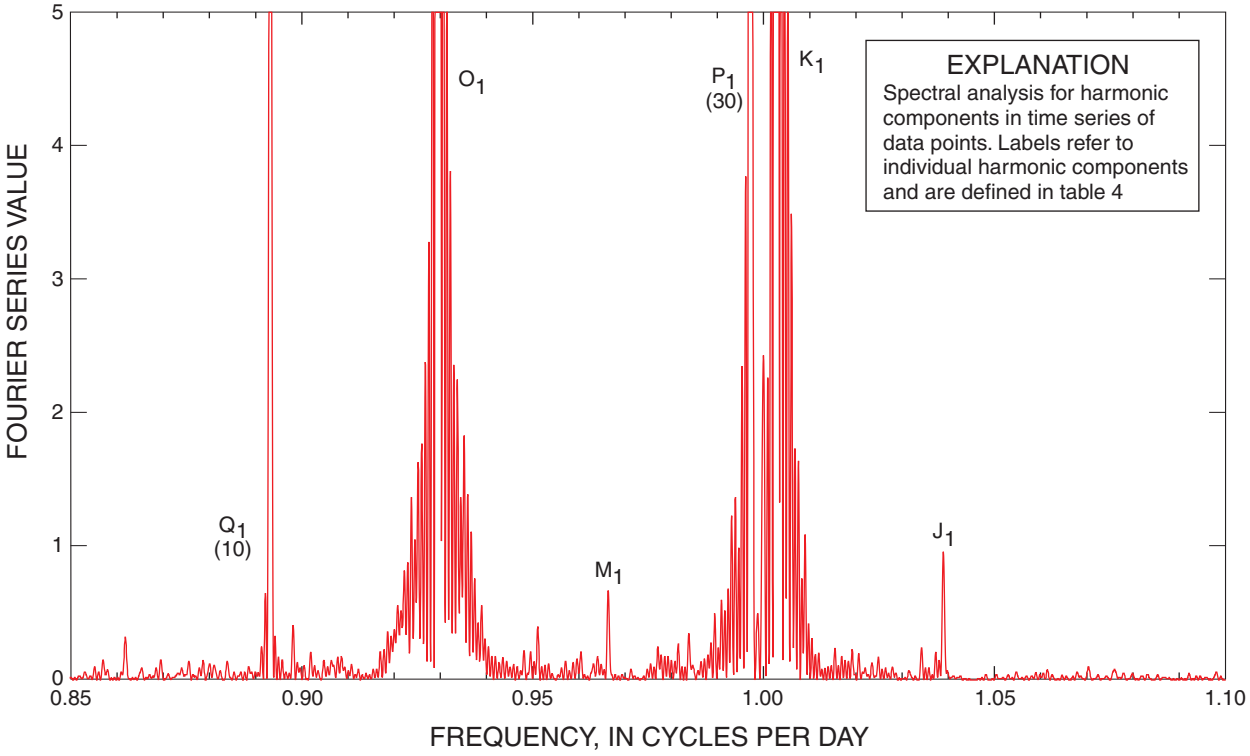

Figure 18. Detail of Naples ocean-tide periodogram showing minor harmonics having frequencies nearly equal to one cycle per day.

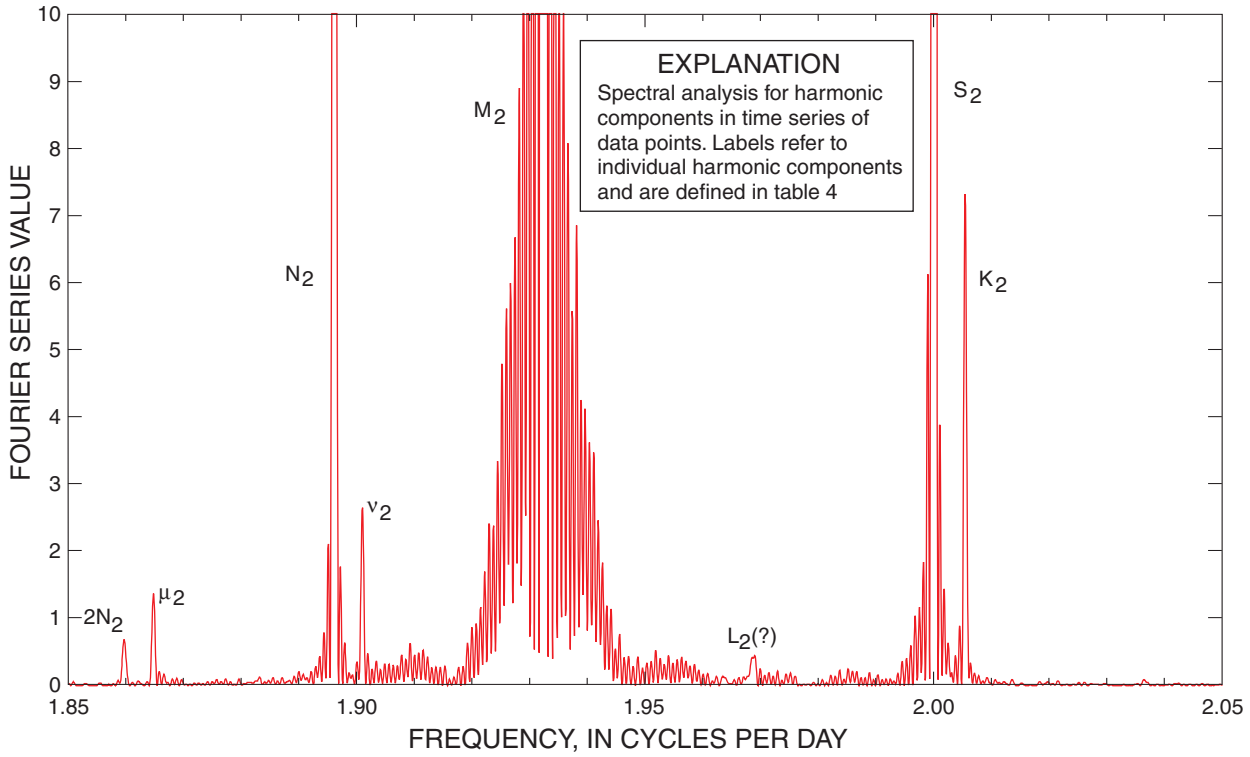

Figure 19. Detail of Naples ocean-tide periodogram showing minor harmonics having frequencies nearly equal to two cycles per day.

or semidiurnal at frequencies of one and two cycles per day. There seems to be a slight signal at a frequency of three cycles per day. It has been customary for some authors (Hsieh and others, 1987) to label the two major components S_1 and S_2. The S_1 component has nearly the same frequency as K_1 of the Naples ocean-tide analysis, and the S_2 component of the atmospheric-pressure analysis has the same frequency (2.00) as the S_2 component from the ocean-tide analysis. Large Fourier series values between frequencies of 0 and 0.5 are caused by aperiodic atmospheric-pressure fluctuations lasting for days or weeks that are treated by the Fourier transform analysis as harmonics having a long period (low frequency). The fact that the periodogram does not show harmonic components having lunar tidal frequencies confirms that the diurnal and semidiurnal atmospheric-pressure oscillations are not caused by the gravitational effects of lunar movements. Given this fact, it also is unlikely that the lesser gravitational effects of solar movements affect the data. The tidal oscillations in the atmospheric-pressure data are more likely the result of solar heating and other factors in the earth's environment.

Application of the Fourier series technique to head data from wells C-1111, C-1112, and HE-1087 (figs. 21-23) reveals a full suite of the major solar and lunar harmonic components that are found in the Naples ocean-tide data. The Fourier series values for the harmonics in the head data from monitor zone MZ-3 in well C-1111 (table 2), only 4.9 miles from the ocean near Naples, are high compared to those from monitor zones in the other two wells because of the strong ocean-tide influence. This influence is small or negligible at the inland wells C-1112 and HE-1087, as will be discussed later.

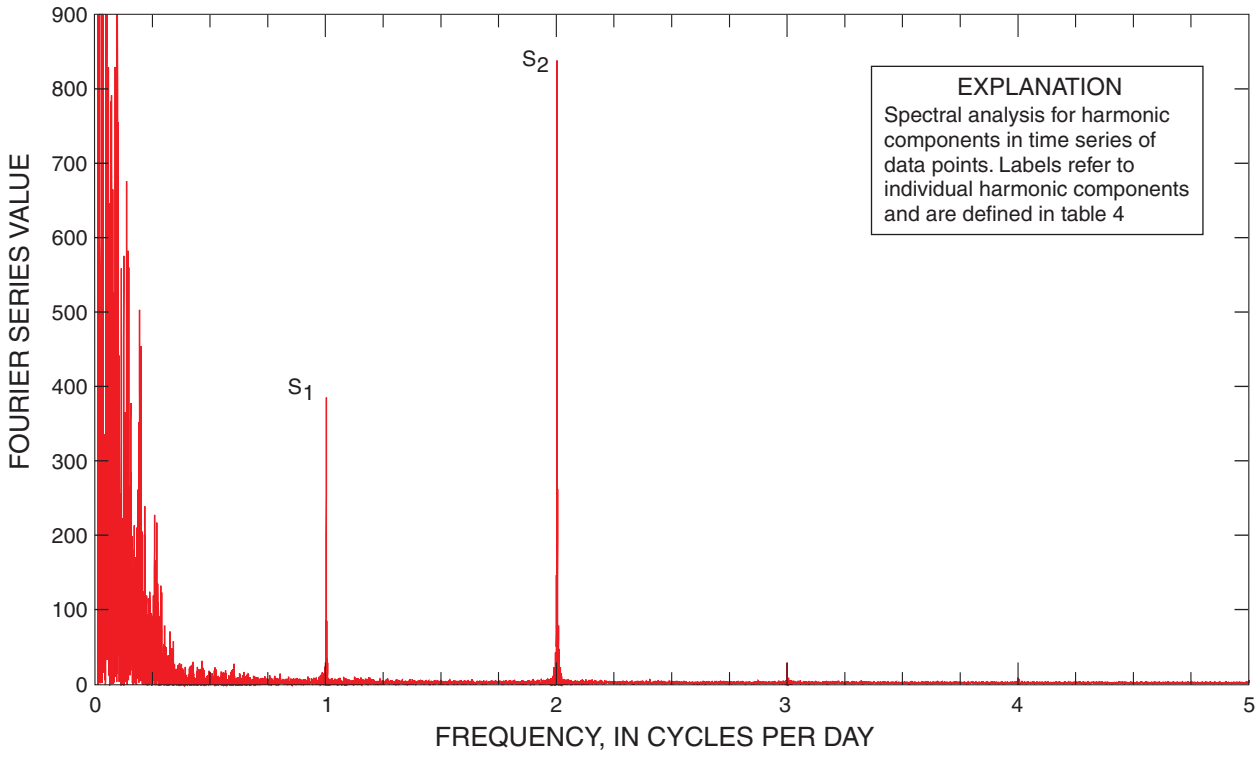

Figure 20. Periodogram of harmonic frequencies present in atmospheric-pressure data collected at South Florida Water Management District station FPWX.

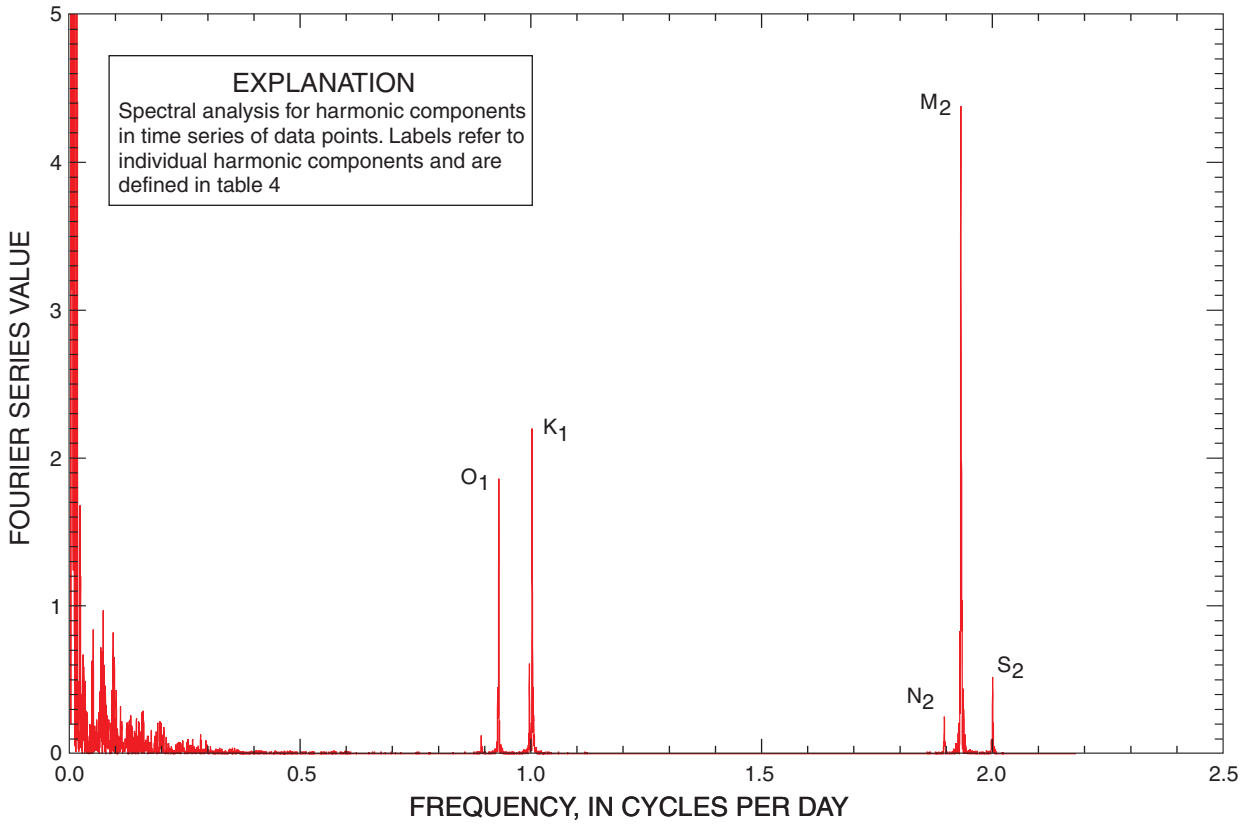

Figure 21. Periodogram of harmonic frequencies present in head data from MZ-3, well C-1111.

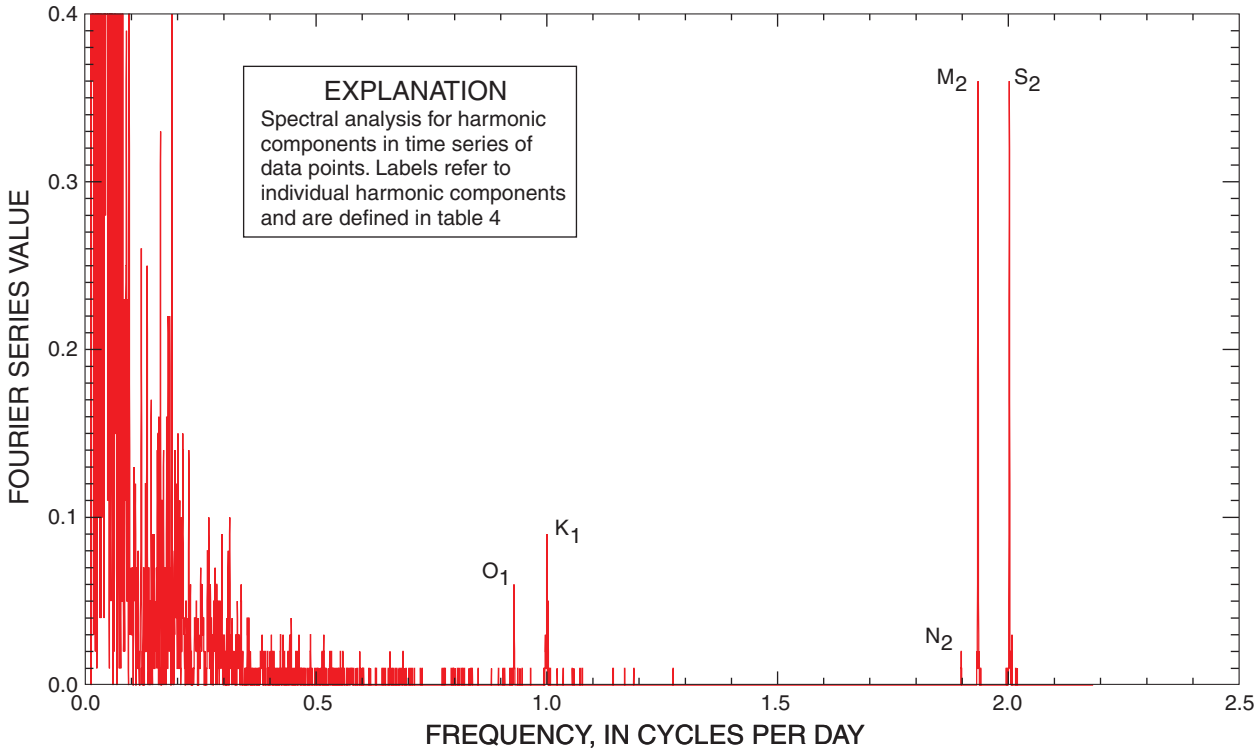

Figure 22. Periodogram of harmonic frequencies present in head data from MZ-2, well C-1112.

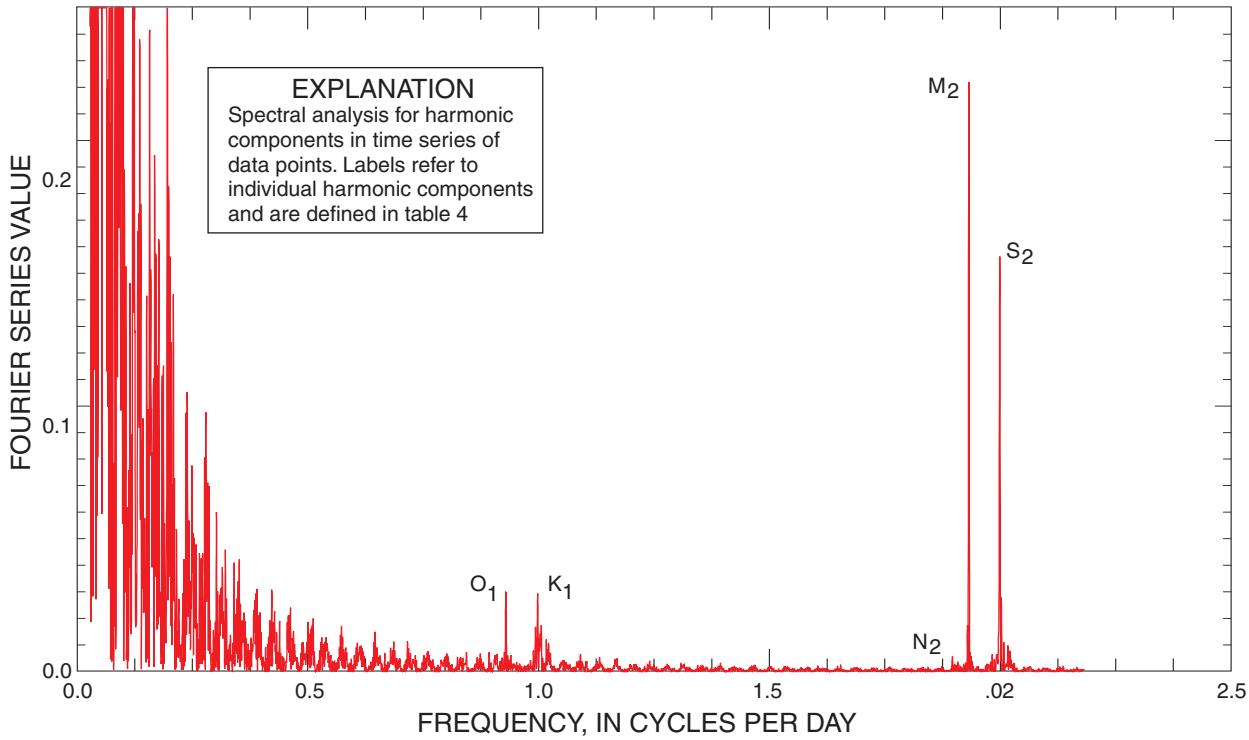

Figure 23. Periodogram of harmonic frequencies present in head data from the monitor zone in well HE-1087.

At inland locations, the amplitude of tidally influenced head oscillations in wells is largely influenced by the local hydraulic characteristics of the formations open to the wells, so variations in Fourier series values between C-1112 and HE-1087 do not have a global interpretation. The presence of the lunar harmonics, O_1 and M_2, in head data from the inland wells shows the influence of earth tides, as the influence of ocean tides should be negligible and the periodic oscillations in atmospheric pressure do not have lunar harmonics (fig. 20). The lunar harmonics at this inland site can be regarded as almost entirely caused by earth tides. On the other hand, the solar harmonics, K_1 and S_2, contain the combined influence of earth tides and diurnal and semidiurnal atmospheric-pressure oscillations. This fact is important for the application of analytic procedures for determining aquifer properties.

The solar and lunar harmonics in head data can alternately augment and interfere with one another. For instance, the lunar and solar periods for the principal diurnal components are about 25.82 and 23.93 hours, respectively. If the two are in phase, complementing each other, at time t_0, they will be exactly out of phase when the daily difference in period, about 1.885 hour, sums to 12.91 hours, half the longer period. This will occur in about 6.85 of the longer periods, or at time t_0 + 7.39 days. The principal lunar and solar semidiurnals periods are 12.42 and 12.00 hours, respectively. Again, if in phase at time t_{00}, they will be exactly out of phase when the difference in period (0.42 hour) sums to half the longer period (6.21 hours). This will occur in 14.79 of the 12.42-hour periods, or at time t_{00} + 7.65 days. Thus, both the principal solar and lunar components of the tide will go in and out of phase in 7-8 days, although the two interactions (solar and lunar) will not always be in phase with one another. This might be observable as increases and decreases of tidal amplitude in graphical representations of the tide.

An example is obtained from the data used for this study (fig. 24). The measured and total heads in July and August 1999, are from MZ-2 in well C-1112. An analysis, described in the following section, which makes possible the reconstruction of an estimated tide in MZ-2, was used to determine when the solar and

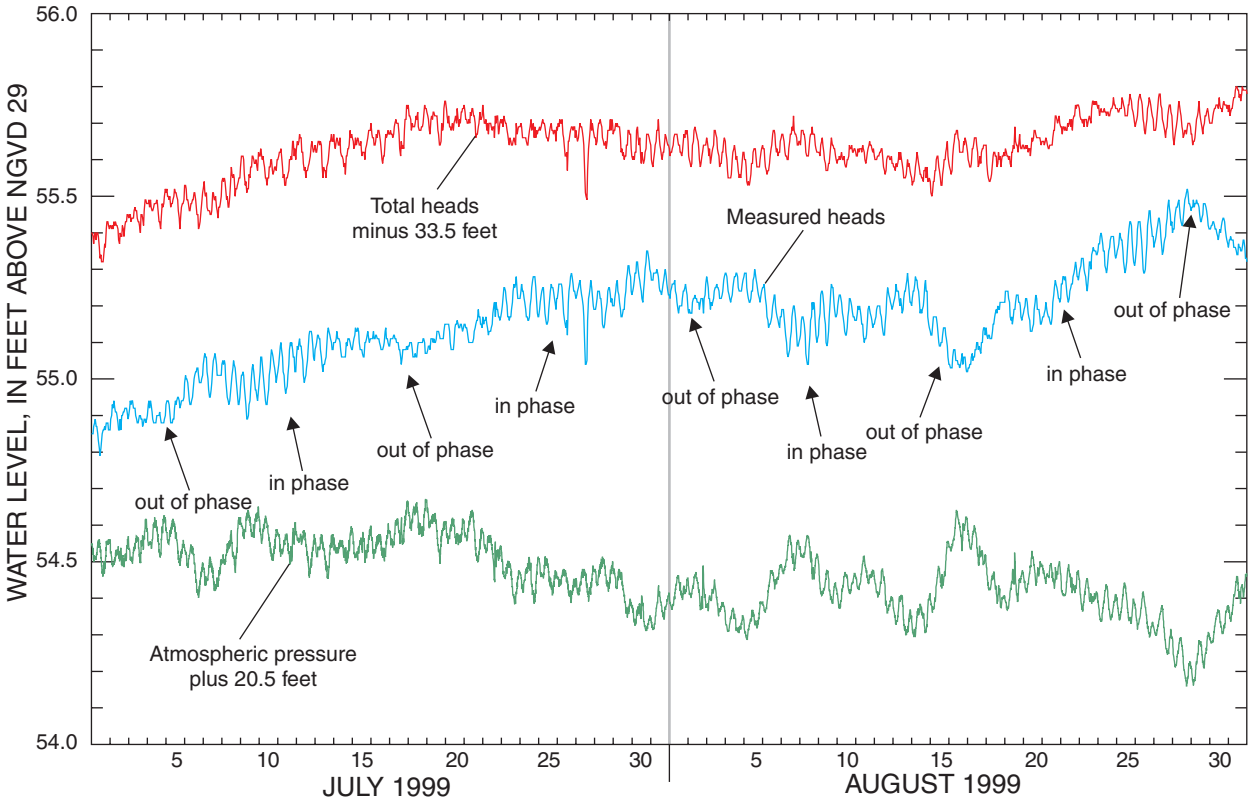

Figure 24. The measured and total heads in MZ-2, well C-1112, and atmospheric pressure at station FPWX for July and August 1999.

lunar diurnal tidal components were in and out of phase, and when the solar and lunar semidiurnal components were in and out of phase. The arrows in figure 24 show when the lunar (O_1) and solar (K_1/S_1) diurnal components were in and out of phase. Generally, the tidal amplitude diminishes when these components are out of phase and increases when they are in phase. There did not seem to be an evident correlation of tidal amplitude with the relative phases of the lunar (M_2) and solar (S_2) semidiurnal components in this data set.

The best estimates of the barometric and loading efficiencies in MZ-2, well C-1112, computed by the Clark method, were 63 and 37 percent, respectively (table 3), and 2 months of total head and atmospheric pressure data, converted to feet of water, are shown in figure 24. Because the barometric efficiency is relatively high and the loading efficiency is relatively low, the effect of atmospheric-pressure fluctuations should be more apparent in the measured-head data than in the total-head data. That this hypothesis is actually the case is shown in figure 24.

Analysis for amplitude and phase of harmonic components

The analysis of specific tidally influenced data sets for estimates of aquifer properties depends largely on being able to resolve the amplitude and phase of the various harmonic components. In particular, the amplitude and phase of the five harmonic components (O_1, K_1, N_2, M_2, and S_2) that comprise approximately 95 percent of the tidal potential must be determined. A means for doing this is by regression analysis, as described by Nowroozi and others (1966). This method was encoded in Fortran by Hsieh and others (1987), and the program was used in the present study. The program can estimate the amplitude and phase of up to 16 components (table 4), but in this study was used generally to estimate amplitudes and frequencies of only the five principal components. The frequencies (ω_j) of the components are entered as input. As previously noted, these frequencies are known precisely from many years of astronomical observations, and it was not necessary to determine them by spectral analysis.

The least squares method minimizes the sum of squares of a set of residuals (S):

$$S = \frac{1}{n}\sum_{i=1}^{n}\left[x_i - \frac{a_0}{2} - \sum_{j=1}^{P}(a_j\cos\omega_j t_i + b_j\sin\omega_j t_i)\right]^2 , \quad (18)$$

where:

n is the number of data points $x_i(t_i)$ (measured or total well pressure heads),

t_i is the time of the i^{th} data point,

ω_j is the frequency of the j^{th} tidal component,

P is the number of tidal components considered in the analysis, and

a_0, a_j, and b_j are the $2P+1$ unknown coefficients.

Equation 18 is differentiated with respect to the $2P+1$ unknown coefficients, and the $2P+1$ resulting equations are each set equal to zero to minimize the sum of the squares (S). The resulting system of linear equations is solved by matrix inversion to obtain the values of the $2P+1$ unknown coefficients. The amplitude (α_j) and phase (ϕ_j) of each harmonic component is determined by:

$$\alpha_j = (a_j^2 + b_j^2)^{1/2} , \text{ and} \quad (19)$$

$$\phi_j = \text{atan}(b_j/a_j) . \quad (20)$$

The j^{th} tidal component ($h_j(t)$) is estimated by:

$$h_j(t) = \alpha_j\cos(\omega_j t + \phi_j) . \quad (21)$$

The tidal height ($h(t)$) is estimated by:

$$h(t) = \frac{a_0}{2} + \sum_{j=1}^{P} h_j(t) = \frac{a_0}{2} + \sum_{j=1}^{P}\alpha_j\cos(\omega_j t + \phi_j) . \quad (22)$$

This analysis was applied to the ocean tide at Naples and to the tidally influenced head data in each monitor zone in wells C-1111, C-1112, and HE-1087. The analysis requires specification of an arbitrary initial time as a reference for the phase computation. To facilitate the comparison of various tidal data sets as part of analyses that are described in the following pages, the initial time for all analyses for amplitude and phase was midnite, the beginning of January 1, 1998. As a modification to the original software, all time coordinates in tidal or tidally influenced data sets were referenced to this time. Following the original software configuration, time values were converted to hours.

Before tidal or tidally influenced data could be analyzed by the regression analysis, it was necessary to detrend the data so that fluctuations in the data would be strictly tidal in origin. Besides long-term, aperiodic atmospheric-pressure effects, possible causes of trends in head data in wells include temporal variations in aquifer recharge, regional changes in potentiometric level, and effects of pumping. The detrending procedure generally was done in two steps: (1) estimate a trend line by use of a low-pass filter; and (2) compute the detrended data set by subtracting the trend line from the raw data.

The low-pass filter (that removes high-frequency harmonics from the time series) was applied by use of a program prepared as part of this study. This program computes a revised time series as the midpoints of successive 25 data-point averages of the original hourly time series. This computation was performed twice, first on the raw (total head) data set, then again on the first revised data set. In the notation of Godin (1972), this filter is $\frac{1}{25^2}A_{25}^2$. An example of a trend line computed by this procedure is shown for head data from MZ-2 in well C-1112 (fig. 11). The detrended data for this 2-month time interval (November-December 1999) is shown in figure 25. This two-step filter was used instead of the somewhat more complex filter $\frac{1}{24^2}\frac{1}{25}A_{24}^2A_{25}$ used by Hsieh and others (1987) because a study of the results of a third filter pass using the filter programmed for this study (the combined three passes being $\frac{1}{25^3}A_{25}^3$) showed the third smoothing to have a negligible effect on the result.

Observations made by Serfes (1991) suggest a possible source of error in the filtering procedure described above. As previously noted, Hsieh and others (1987) used the filter $\frac{1}{24^2}\frac{1}{25}A_{24}^2A_{25}$ that involved smoothing three times, two 24-point averages followed by a 25-point average. Serfes (1991) cites Godin (1972) as explaining that the 25-point average

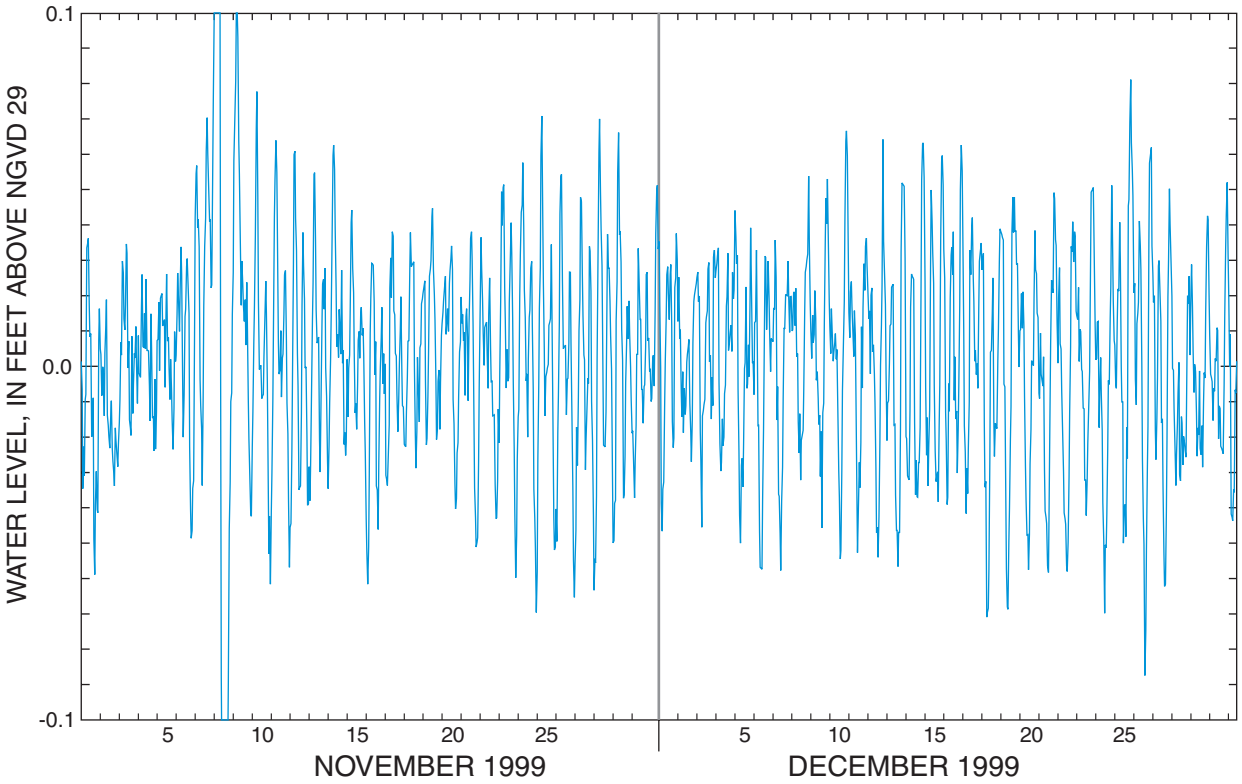

Figure 25. Detrended tidally influenced and barometrically influenced total-head data from MZ-2, well C-1112, for November and December 1999.

is the best filter for the lunar components of the tidal oscillation but does not filter all of the solar variation, and that the 24-point average is the best filter for the solar components but does not filter all of the lunar variation. To test for the possibility of error in the procedure used in this study, two measured-head data sets, from MZ-1 in well C-1111 and from MZ-2 in C-1112, were filtered using the method of Hsieh and others (1987) and analyzed for amplitude and phase of the five major components by the least-squares analysis. Differences in amplitude and phase values were negligible in MZ-1, C-1111, and negligible to slight (0.5 percent) in MZ-2, C-1112.

Data collected from the monitor zones in C-1111, C-1112, and HE-1087 contained time gaps of several weeks to several months, and several abrupt positive and negative discontinuities of more than a foot were present. The latter appeared to be related either to the servicing of instrumentation at the site (because they coincided with an reinitialization of the elapsed time channel), or to unexplained abrupt changes in the values from the temperature and/or pressure channels of the sensor. The consequences for the data analysis was that the computation of a trend line would have misleading results in the neighborhood of the these time gaps or data discontinuities. The resulting detrended data would show unusual fluctuations in these time periods, leading to unrealistically high variance values in the solution for amplitude and phase of tidal harmonics.

To avoid this undesirable result, each data set was subdivided into smoothly varying subsets, continuous in time, for computation of individual trend lines. The resulting individual trend lines were then successively appended to produce a single trend line before subtraction from the raw data. The procedure caused time gaps to occur about the previous data discontinuities because smoothed data values were not computed for the first and last 12 points of each subset in each stage of the filtering, but this did not appreciably affect the results of the analysis for amplitude and phase.

At first, the detrending procedure and the analysis for amplitudes and phases were applied to data sets of measured heads that were corrected for long-term, aperiodic atmospheric-pressure fluctuations. Semidiurnal solar (S_2) component amplitudes computed from

these detrended time series were substantially less (by 40-80 percent) than the S_2 amplitudes computed from data sets of measured heads not corrected for atmospheric-pressure fluctuations. The estimated phases for S_2 also differed substantially. The cited differences were greatest for the upper Floridan monitor zones. Possibly, the atmospheric-pressure correction had the effect of removing a part of the S_2 component caused by diurnal and semidiurnal atmospheric-pressure fluctuations. Amplitudes and phases computed for other harmonic components were nearly the same for data sets corrected and not corrected for atmospheric-pressure fluctuations.

Next, the detrending steps and least-squares analysis were applied to the data sets of total pore pressure heads (sums of contemporaneous values of barometric pressure and measured head) not corrected for atmospheric-pressure fluctuations. Except for the S_2 component, resulting amplitudes and phases were virtually the same as for the raw measured head data (corrected and uncorrected for atmospheric-pressure fluctuations). The new S_2 amplitudes in the total head data were substantially smaller than S_2 amplitudes of the measured-head data uncorrected for atmospheric-pressure fluctuations, and phases also differed substantially. It is believed that the reduced S_2 amplitudes in the total head data reflected the relatively low loading efficiencies of the formations. The measured-head data (high barometric efficiencies) contained a higher dependence on the atmospheric-pressure fluctuations and would be expected to have a solar semidiurnal (S_2) signal of greater amplitude than the total head data. Amplitude and phase values from the analysis of the total head data (table 5) were the ones used in the application of algorithms described in later sections of this report. Another result of the detrending procedure was that the tidal oscillations were oriented about the value of zero, so estimates of a_0 (equations 18 and 22) were expected to be (and were) nearly equal to zero.

Of the Naples ocean-tide data, only data after December 31, 1997, were used for estimating amplitudes and phases of harmonic components. The time series contained a gap of most of August and September 2000. Tidal harmonic components in the Naples ocean-tide data (table 5) are substantially higher in amplitude than those in head data from any of the well monitor zones. Among the latter, the amplitudes are significantly greater in the data from well C-1111 than in data from C-1112 and HE-1087 because of the strong ocean-tide influence at C-1111.

Table 5. Amplitudes and phases of the five major harmonic components in Naples ocean-tide data and in total-head data from monitor zones in wells C-1111, C-1112, and HE-1087

[Amplitude in feet (phase in degrees). M, mean square of fit in square feet; V, variance of data in square feet. Negative degrees (-d) are equivalent to negative degrees + 360 (-d+360)]

Source	Time period	O_1 component	K_1 component	M_2 component	S_2 component	N_2 component	M/V
Naples ocean tide	January 1998 - November 2000	0.38326 (0.87)	0.45690 (-69.51)	0.89004 (65.16)	0.30864 (-0.85)	0.18478 (5.48)	93.3
Well C-1111, MZ-1	January 1998 - December 2000	0.03981 (42.13)	0.04861 (-26.15)	0.06259 (146.70)	0.00695 (83.52)	0.01328 (79.78)	84.9
Well C-1111, MZ-2	January 1998 - December 2000	0.03754 (49.58)	0.04733 (-15.60)	0.05445 (158.68)	0.00187 (158.95)	0.01126 (90.66)	77.9
Well C-1111, MZ-3	January 1998 - December 2000	0.05586 (22.30)	0.06740 (-47.08)	0.09859 (106.87)	0.02228 (2.14)	0.02198 (43.86)	83.0
Well C-1112, MZ-2	April 1999 - December 2000	0.01074 (-112.90)	0.01124 (168.42)	0.02476 (-105.79)	0.01081 (-91.40)	0.00416 (-140.11)	50.9
Well C-1112, MZ-3	April 1999 - December 2000	0.01278 (-113.96)	0.01500 (166.78)	0.03022 (-105.73)	0.00883 (-110.68)	0.00477 (-141.94)	64.3
Well C-1112, MZ-4	April 1999 - September 1999	0.00978 (-111.43)	0.01283 (155.64)	0.02679 (-121.79)	0.00659 (-103.14)	0.00396 (-155.94)	46.1
Well HE-1087, MZ	September 1998 - June 2000	0.00961 (-85.35)	0.00691 (-167.14)	0.01991 (-85.26)	0.03232 (-91.16)	0.00327 (-130.53)	50.4

Amplitudes and phases of tidal components for MZ-1 and MZ-2 in well C-1111 were generally similar, but amplitudes for MZ-3 were greater and the phase differences with the ocean-tide components were less than those of MZ-1 and MZ-2. As shown later, this indicates that the transmissivity of MZ-3 is higher than that of the other zones. For each (j^{th}) harmonic component, the percent of variance (Pv_j) was computed, according to:

$$Pv_j = \frac{\alpha_j^2}{2V}, \text{ where } V \text{ is the variance of the data:} \quad (23)$$

$$V = \frac{1}{n}\sum_{i=1}^{n}(x_i - a_0/\ 2)^2 . \quad (24)$$

The values of Pv_j can be used to indicate the relative significance of the j^{th} harmonic component in the tidal or tidally influenced data set. The sum of the Pv_j values is a ratio (*M/V*), the mean square of fit (*M*) divided by the variance of the data (*V*):

$$\frac{M}{V} = \sum_{j=1}^{P} Pv_j = \frac{1}{2V}\sum_{j=1}^{P}\alpha_j^2 . \quad (25)$$

M/V can be used as an indicator of the degree of success with which the tidal components identified by the regression analysis explain the variance in the data set. In this study, *M/V* was multiplied by 100 and expressed as a percent (table 5). The *M/V* value for the Naples ocean-tide data was 93 percent. *M/V* values for the monitor zones in C-1111 range from 77.9 to 84.9 percent. In decreasing order of magnitude of the Pv_j values are the components M_2, K_1, O_1, N_2, and S_2.

When the analysis was run on measured head values, S_2 values were only slightly less than O_1 amplitudes on MZ-1 and MZ-2. Using measured head data, the analysis for MZ-1 was rerun with components P_1, K_2, Q_1, and T_2 added to the solution. The *M/V* value increased about 4 percent, but only the P_1 and Q_1 components added appreciably to the *M/V* value. When 16 of the 17 harmonic components listed in table 4 were included in the analysis, the additional 7 components added negligibly to the *M/V* value. When the original five components were solved for and the data set length was changed by deleting the first year of data, the change in estimated amplitudes varied from negligible to 5 percent, the change in estimated phases varied from negligible to 8 degrees of arc, and the *M/V* value increased slightly.

In analyzing data from well C-1112, amplitudes computed for MZ-3 based on analysis of total heads are generally slightly greater than those for MZ-2 and MZ-4. The computed phases for MZ-2 and MZ-3 are similar. The amplitude of M_2 is appreciably higher than the others. *M/V* values range from 46.1 to 64.3 percent. The amplitudes of the S_2 components were only slightly less than that of M_2 when measured head data were used for the analysis.

An *M/V* value of 50.4 was obtained when analyzing total-head data from HE-1087. When the analysis was restricted to the time period (April-September 1999) before a suspected time bias (one time series shifted in time relative to the other) may have affected the data, the *M/V* value improved to 70.6, and the phases for K1 and S2 changed significantly. The largest amplitude was for the M_2 components.

To partially verify the results of the component analysis and to check for errors, a program was written to construct a time series by summing the values of the five principal tidal components computed at successive times from the amplitudes and phases estimated by the least-squares analysis. This “simulated (detrended) tide” was graphically superimposed on the detrended-tide time series based on the field data so that comparisons could be made in various time periods of the data for error checking. An example plot (fig. 26), for MZ-2 in well C-1112, shows estimated and measured tides for 7 days in November 1999. The match seems to be slightly better when tidal oscillations are greatest, as during November 24-26, than when tidal oscillations are small and affected by noise not removed by the detrending procedure, as in the first 2 days of this plot.

Another view of the harmonic structure of the tide is obtained by computing time series of the individual harmonics and graphically superimposing them. The example plot shown in figure 27, for the same data and time period as the previous plot in figure 26, shows the complex interplay between the harmonics over a 7-day period. At the beginning, the lunar diurnal (O_1) and the lunar-solar diurnal (K_1) are partly out of phase, but, between the 25th and 26th of the month, they are exactly in phase. Similarly, the lunar and solar semidiurnals (M_2 and S_2) begin the 7-day time period partly out of phase, but are almost completely in phase on the 25th.

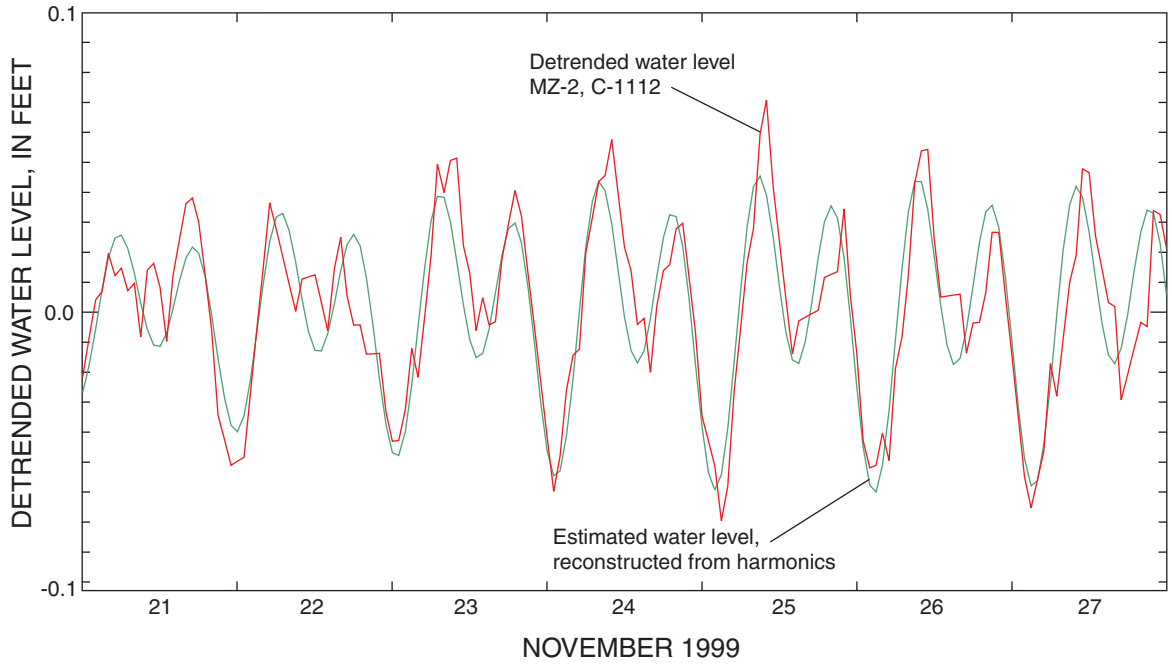

Figure 26. Detrended total-head data from MZ-2, well C-1112, and head oscillations estimated from regression analysis for November 21-27, 1999.

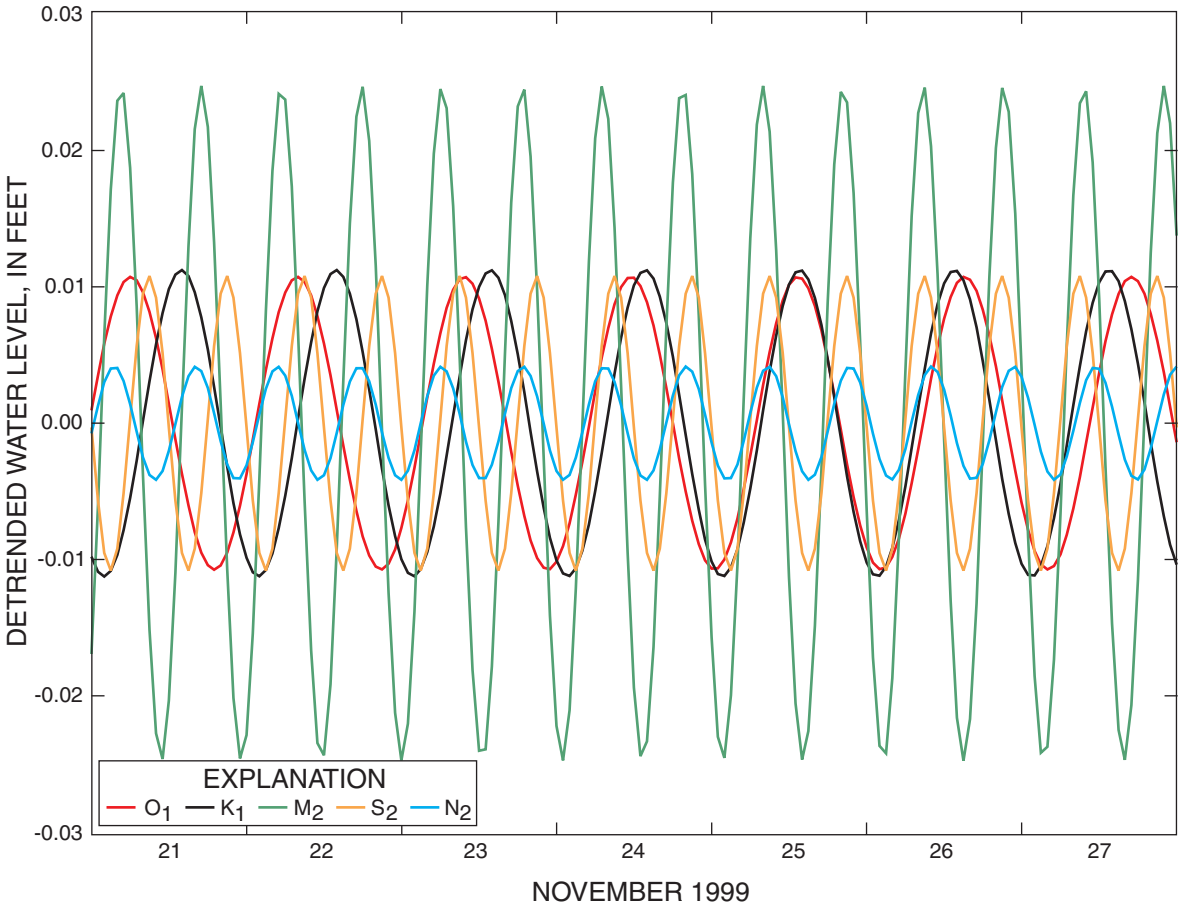

Figure 27. Individual harmonic components determined by regression analysis of total-head data from MZ-2, well C-1112, for November 21-27, 1999.

ANALYTICAL METHODS FOR COMPUTING AQUIFER PROPERTIES FROM NATURALLY FORCED PERIODIC DATA

Research into the analytical use of tidally influenced and other naturally forced head fluctuations to estimate values of aquifer properties tends to segregate into four principal categories: (1) use of heads influenced by ocean tides to estimate aquifer diffusivity (transmissivity divided by storage coefficient); (2) use of heads influenced by earth tides or atmospheric-pressure oscillations for estimating specific storage and porosity; (3) use of water levels from open wells penetrating a confined aquifer and influenced by earth tides or atmospheric-pressure oscillations to estimate aquifer transmissivity and storage coefficient; and (4) use of water levels or pressure heads in a vertical diffusion equation to determine vertical hydraulic conductivity. The order of the four categories corresponds generally to the sequence in time in which these categories were the principal avenue of research.

The second research category primarily involves aquifer pressure changes caused by surface loading or dilatation of the aquifer material. Since the head changes are not associated with water movement, except possibly on a microscopic scale (Van der Kamp and Gale (1983) and other authors refer to these as "undrained processes"), they cannot serve as the basis for the estimation of properties such as transmissivity that describe water movement in the aquifer. For this reason, most of the research in category three involves a consideration of the well-aquifer system problem, in which pressure oscillations cause macroscopic water movement (a "drained process"), in this case, movement of water into and out of a well.

The first three research categories involve a comparison of pressure heads or water levels with other data: category 1 - with ocean-tide measurements; category 2 - with the theoretical tide potential; and category 3 - with background pressure data, dilatometer data, or the theoretical tidal potential. As will be shown, application of many of the derived equations reduces to a comparison of theoretical and observed amplitude ratios and phase shifts.

Using Heads Influenced by Ocean Tides for Estimates of the Hydraulic Diffusivity of an Aquifer

Ferris (1951) presented one of the first analytical solutions to the problem of calculating the theoretical head oscillations in a well near enough to the ocean to be influenced by ocean tides. The solution was developed mainly for the case in which the aquifer crops out at or near the coastline (fig. 28a). In this case, the oscillation of sea level corresponds to an equal oscillation of head at the subsea outcrop, and water is forced into and out of the aquifer, causing heads in the aquifer (h(x,t)) to fluctuate with an amplitude that diminishes with distance (x) away from the subsea outcrop as the time lag of a given maximum increases. The solution assumes that the aquifer is homogeneous and of uniform thickness and of infinite extent shoreward. The subsea outcrop is straight and the X-coordinate direction is normal to it. The effects of atmospheric-pressure fluctuations and earth-tide oscillations are ignored in the theoretical development. Citing analogous problems of determining the transmission of thermal energy in solids, and assuming that the tidal oscillation is a simple harmonic, Ferris (1951) represented the problem with the following differential equation, previously presented by Jacob (1950):

$$\frac{\partial^2 h(x,\ t)}{\partial x^2} = \frac{S}{T}\frac{\partial h(x,\ t)}{\partial t}, \qquad (26)$$

subject to the boundary conditions:

$$h(x,\ t) = h_0 \sin \omega t \text{ at } x=0, \text{ and} \qquad (27)$$

$$h(\infty,\ t) = 0, \qquad (28)$$

where:

t is time (T),
h_0 is the amplitude or half range of the tidal harmonic oscillation (L),
ω is the frequency of the harmonic oscillation (T^{-1}),
S is the aquifer storage coefficient (unitless),
T is the aquifer transmissivity (L^2/T),
L is a length unit, and
T is the time unit.

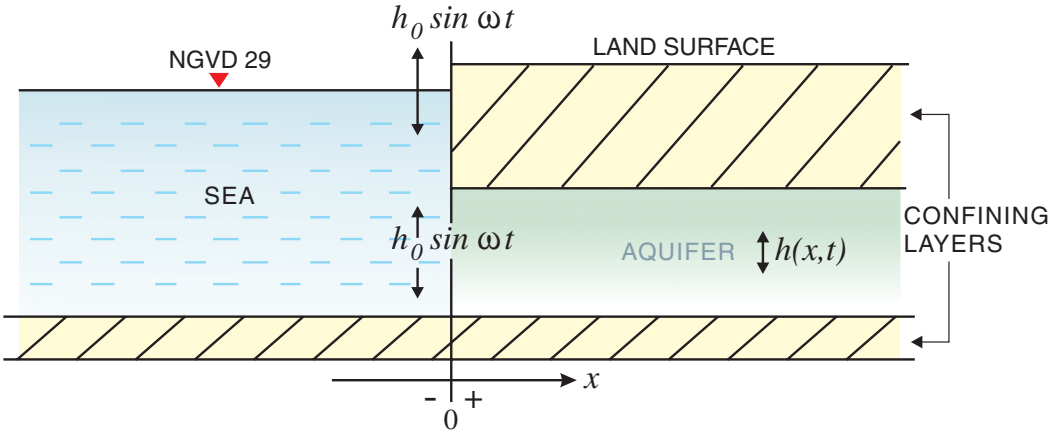

(a) Model of Jacob (1950) and Ferris (1951) - aquifer and overlying confining layer crop out at or near coastline.

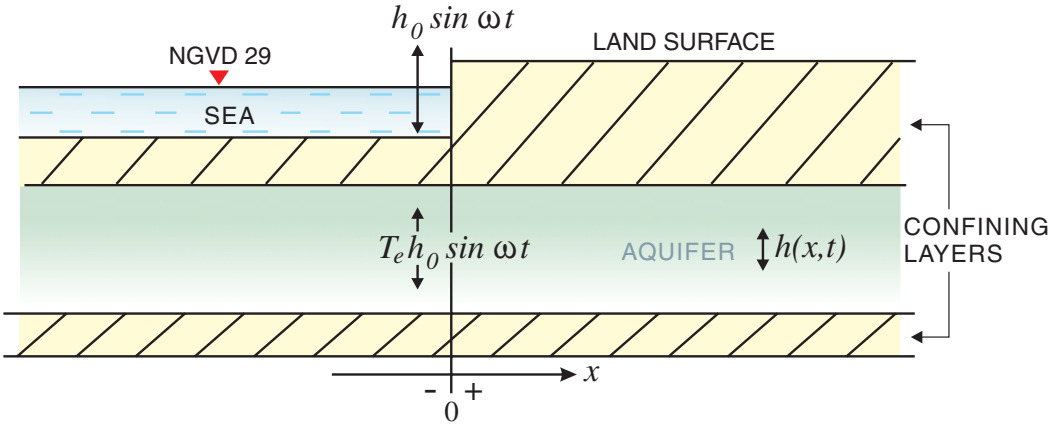

(b) Model of Van der Camp (1972) - a completely confined aquifer extending under the sea.

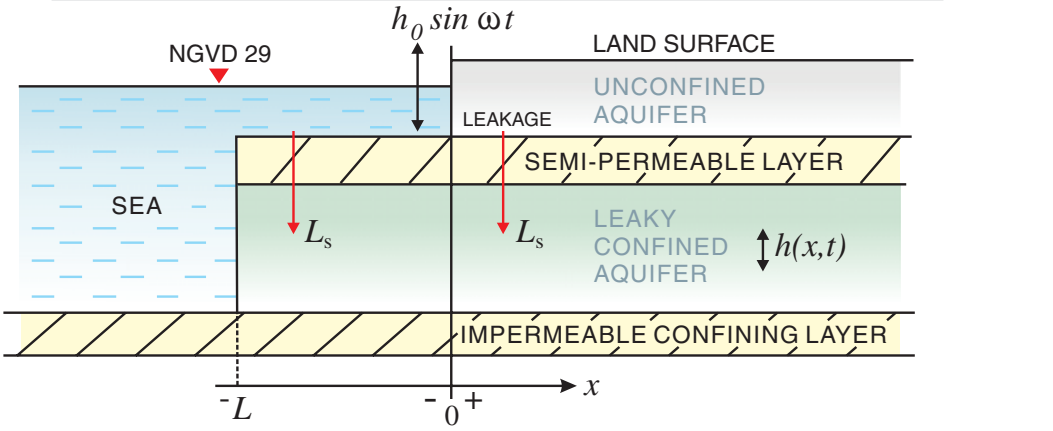

(c) Model of Li and Jiao (2001a) - a leaky contained aquifer system extending under the sea for a distance L.

Figure 28. Sea-aquifer models for which solutions for head ($h(x)$) as a function of distance inland (x) have been derived.

The solution to the equation and boundary conditions is:

$$h(x,\ t) = h_0 e^{-x\sqrt{\frac{\omega S}{2T}}} \sin\left(\omega t - x\sqrt{\frac{\omega S}{2T}}\right) = h_0 e^{-x\sqrt{\frac{\pi S}{\tau T}}} \sin\left(\omega t - x\sqrt{\frac{\pi S}{\tau T}}\right), \quad (29)$$

where

τ is the period of the harmonic oscillation (T).

This solution is a harmonic function with a phase shift that increases with distance inland (x) and with an exponential damping term that reduces the amplitude of the harmonic function with distance inland.

The use of a simple harmonic representation of the ocean tide in the analysis is not limiting, as the ocean tide was previously shown to consist of a number of harmonics superimposed on one another, only five of which are dominant. Equation 26 is linear, so that solutions for simple harmonics can be added together, or tides can be analyzed for component amplitudes and phases, and equation 29 can be applied to individual components.

Although figure 28a portrays an aquifer confined to or near the subsea outcrop, Ferris (1951) did not restrict the solution to that case, stating that the solution will apply to aquifers under water-table conditions where appreciable vertical flows do not occur and where the saturated thickness of the aquifer is sufficiently large. The storage coefficient (S) may be four or more orders of magnitude greater for unconfined aquifers than confined ones, so the exponential damping term will quickly reduce the amplitude of tidally forced head oscillations with distance from the ocean in surficial aquifers (Jiao and Tang, 1999). For this reason, some authors discount the use of analytical methods depending upon tidally forced water levels in surficial aquifers, but these methods have been applied successfully in certain cases (Erskine, 1991). Even so, Erskine (1991) reported that tidal oscillations in an unconfined aquifer were unmeasurable farther inland than 400 meters from the shore. Referring again to equation 29, however, if the transmissivity (T) is exceptionally high, as in the surficial Biscayne aquifer of south Florida, then measurable tidal effects may be observable inland even farther than 400 meters.

Neither did Ferris (1951) ignore the case (fig. 28b) in which the aquifer confinement extends under the sea, stating that "if . . . the aquifer is confined by an extensive aquiclude, the rise and fall of the surface-water stage changes the total weight upon the aquifer. Resultant variations in compressive stress are borne in part by the skeletal aquifer and in part by its confined water." Ferris (1951) stated that "when the aquifer response is due to loading rather than head change at the suboutcrop, the amplitude factor should be reduced (Jacob, 1950, p. 365) by the factor $\alpha/(\alpha+\eta\beta)$, where α is the vertical compressibility of the skeletal aquifer, β is the compressibility of the water, and η is the porosity of the sand." This is the factor presented as the loading efficiency (L_e) (equation 1). (However, it was shown by Van der Kamp, 1972, that the tidal efficiency at the coast was only half the factor proposed by Jacob and Ferris.)

The assumption inherent in this case and in equation 29 is that head oscillations in a confined aquifer beneath the ocean at the coast are reduced in amplitude by the "tidal efficiency" (T_e) from the amplitude of the ocean tide without any change in phase or frequency; from this location, the head oscillations reduced in amplitude by the factor T_e are transmitted into the aquifer inland from the ocean with an exponential decrease in amplitude with distance, with a change in phase (time lag) that increases with distance, but with no change in frequency.

The sea-aquifer model shown in figure 28b was considered in detail by Van der Kamp (1972) in order to obtain a solution for subaquaeous formations separated from the overlying water body by a confining layer. The particular objective of Van der Kamp (1972) was to derive a solution for narrow tidal channels, but the solution has wider applicability. The previous assumptions regarding aquifer homogeneity, extent, and uniformity remain in effect. As in the previous analysis of Ferris (1951), "it is assumed that changes in hydraulic potential and of the stresses on the solid skeleton can be transmitted horizontally only by water movement and not directly through the solid skeleton independent of water movement," an assumption that simplifies "treatment of the complex interactions at the land-sea boundary due to the abrupt difference of compressive load" (Van der Kamp, 1972). Thus, Van der Kamp's generalization of the physical process was similar to that of Jacob and Ferris in assuming that, at the coast, the amplitude of the oscillations of head in the confined aquifer are reduced from the amplitude of

the ocean-tide oscillations by the tidal efficiency factor, and the resulting lesser oscillations are transmitted inland within the aquifer only hydraulically, as described by Darcy's Law.

Van der Kamp (1972) stated separate governing equations and boundary conditions for the inland ($x > 0$) and subsea ($x < 0$) parts of the confined aquifer. The inland equation (equation 26) remained the same, but the subsea equation had an additional term:

$$\frac{\partial h(x,\ t)}{\partial t} = L_e h_0 \omega \cos \omega t + \frac{T}{S} \frac{\partial^2 h(x,\ t)}{\partial x^2} . \qquad (30)$$

The boundary condition for the subsea region was:

$$h(x,\ t) = L_e h_0 \sin \omega t \text{ at } x = -\infty. \qquad (31)$$

Solutions were required to match at the coastal boundary between the two regions, resulting in the following equations for tidally influenced heads in the inland and subsea regions:

$$h(x,\ t) = \frac{1}{2} L_e h_0 e^{-x\sqrt{\frac{\omega S}{2T}}} \sin\left(\omega t - x\sqrt{\frac{\omega S}{2T}}\right) \text{for } x > 0, \text{ and} \qquad (32)$$

$$h(x,\ t) = L_e h_0 \sin \omega t + \frac{1}{2} L_e h_0 e^{x\sqrt{\frac{\omega S}{2T}}} \sin\left(\omega t + x\sqrt{\frac{\omega S}{2T}} + \pi\right) \quad \text{for } x < 0. \qquad (33)$$

Equation 32 represents a modification of the result of Jacob (1950) and Ferris (1951) for the inland region. Van der Kamp (1972) interprets this modification as the result of considering both the subsea and inland parts of the aquifer and the fact that a damped wave of water moving in and out of the inland part is matched by a damped wave of opposite phase moving in the opposite direction into the subsea part of the aquifer. Equation 32 reduces the tidal efficiency at the coast (T_e) to half the loading efficiency (L_e): $T_e = \frac{1}{2} L_e$. The first term on the right-hand side of equation 33 for the subsea region is the ocean tide reduced in amplitude by the loading efficiency value (L_e).

Application of the theory is most efficiently done by comparing the amplitudes and phases of harmonic components in the well head data with those of the ocean tides. The theoretical harmonic component amplitude ($A(x)$) and phase lag (t_{lag}) in a well at a distance x inland from the coast are:

$$A(x) = \frac{1}{2} L_e h_0 e^{-x\sqrt{\frac{\omega S}{2T}}} = \frac{1}{2} L_e h_0 e^{-x\sqrt{\frac{\pi S}{\tau T}}}, \text{ and} \qquad (34)$$

$$\omega t_{lag} = x\sqrt{\frac{\pi S}{\tau T}} . \qquad (35)$$

The amplitude ratio of the corresponding harmonic components of the head in a well at a distance inland x_0 and the ocean tide is expressed by dividing $A(x_0)$ by the ocean-tide amplitude h_0. Setting the result equal to the observed amplitude ratio r and rearranging the equation, an equation is obtained that relates transmissivity (T) to storage coefficient (S) based on data from the well:

$$T = \frac{\pi {x_0}^2}{\tau \left[\ln\left(\frac{2r}{L_e}\right)\right]^2} S . \qquad (36)$$

Recognizing that the exponential term in equation 34 cannot have values greater than one, equation 36 is only valid for values of L_e greater than 2r.

If the difference between the phases of a particular harmonic component of the head in the well and the ocean tide is denoted Φ and converted to units of radians (2π radians = 360 degrees of arc) and set equal to the right-hand side of the equation for ωt_{lag} (equation 35), then the expression for the time lag, or phase shift, leads to a second, independent equation relating T to S:

$$T = \frac{\pi {x_0}^2}{\tau \Phi^2} S . \qquad (37)$$

The actual difference in phase could be Φ plus a multiple of 2π. Whether or not this is true requires hydrologic intuition on the part of the analyst and data from additional wells, if available. Equation 37 has an advantage relative to equation 36 in that it does not contain a dependence on the loading efficiency (L_e), for which estimates might not be available. Equations similar to equations 36-37 were presented by Meyer (1974), which is the only publication known to the author that applies the theory of Van der Kamp (1972) to a set of field data.

An intermediate case in which a non-leaky confining layer extends a finite distance (L) under the sea was considered by Li and Chen (1991). However, their solution for damped tidal oscillations in a fully confined aquifer caused by an assumed simple harmonic ocean-tidal oscillation was corrected by Li and Jiao (2001a). Jiao and Tang (1999) considered the case of a leaky, confined aquifer separated from an overlying unconfined aquifer by a semipermeable layer. The assumption of a non-varying head at mean sea level in the unconfined aquifer was considered an adequate approximation of cases normally observed in real-world aquifer systems. The semiconfining layer and semiconfined aquifer were assumed to terminate at the shoreline with no extension under the sea. Flow was assumed to be horizontal in the aquifer, and storage within the semiconfining layer was neglected as vertical leakage occurred.

Li and Jiao (2001a) combined these cases into a more general solution. The coastal aquifer system (fig. 28c) consists of a leaky semiconfining layer separating an overlying unconfined aquifer from an underlying semiconfined aquifer. The aquifer and semiconfining layer (referred to by Li and Jiao (2001a) as the "roof of the aquifer") extend for a finite distance (L) under the sea. As above, the water level in the unconfined aquifer is assumed constant at mean sea level, vertical leakage (at a rate denoted L_s) occurs through the semiconfining layer, and storage effects in the latter are ignored. Flow in the semiconfined aquifer is horizontal. The governing equations, boundary conditions, and solution equations are as follows.

Governing equations:

Inland (x > 0):

$$S\frac{\partial h(x,\ t)}{\partial t} = T\frac{\partial^2}{\partial x^2}h(x,\ t) - L_s h(x,\ t)\ . \qquad (38)$$

Offshore aquifer (-L < x < 0):

$$S\frac{\partial h(x,\ t)}{\partial t} = T\frac{\partial^2}{\partial x^2}h(x,\ t) + ST_e\frac{\partial h_s(t)}{\partial t} + L_s[h_s(t) - h(x,\ t)]\ . \qquad (39)$$

Boundary conditions:

$$h(-L,\ t) = h_s(t) = h_0\cos\omega t \text{ and } h(\infty,\ t) = 0\ , \qquad (40)$$

where

$h_s(t)$ is a harmonic component of the ocean tide having amplitude h_0 and angular frequency ω.

Also, the inland and offshore functions for $h(x,t)$ and their x-derivatives must match at the boundaries between the two regions. The solutions are expressed in terms of u and a, where u is a dimensionless leakage parameter and a, referred to by Li and Jiao (2001a) as the "tidal propagation factor," was used before in equations 29 and 32-35:

$$a = \sqrt{\frac{\omega S}{2T}} = \sqrt{\frac{\pi S}{\tau T}}, \text{ and} \qquad (41)$$

$$u = \frac{L_S}{\omega S}\ . \qquad (42)$$

Only the solution for the inland region is presented here:

$$h(x,\ t) = h_0 C_e e^{-pax}\cos(\omega t - qax - \varphi), \text{ where} \qquad (43)$$

$$0 < C_e = \sqrt{(R_1 + \lambda/\ 2)^2 + (\ I_1 - \mu/\ 2\ )^2} \le 1\ , \qquad (44)$$

$$\lambda = \frac{u^2 + L_e}{u^2 + 1} \text{ and } \mu = -\frac{(1 - L_e)u}{u^2 + 1}, \qquad (45)$$

$$R_1 = e^{-paL}[(1-\lambda)\cos(qaL) - \mu\sin(qaL)] + \frac{1}{2}e^{-2paL}[\lambda\cos(2qaL) + \mu\sin(2qaL)]\ , \qquad (46)$$

$$I_1 = e^{-paL}[(1-\lambda)\sin(qaL) + \mu\cos(qaL)] + \frac{1}{2}e^{-2paL}[\lambda\sin(2qaL) - \mu\cos(2qaL)], \quad (47)$$

$$p = \sqrt{\sqrt{1+u^2}+u} \text{ and } q = \sqrt{\sqrt{1+u^2}-u}, \text{ and} \quad (48)$$

$$\varphi = \operatorname{atan}\frac{2I_1 - \mu}{2R_1 + \lambda} . \quad (49)$$

Li and Jiao (2001a) use the notation T_e instead of L_e in equation 45, and refer to the parameter as "tidal efficiency" without additional explanation. The correct parameter, however, is assumed to be the loading efficiency (L_e) defined as "tidal efficiency" by Jacob (1940).

Li and Jiao (2001a) consider special cases represented by extreme values of solution parameters. For instance, the special case in which leakage is zero ($L_S = 0$) and the extent of the aquifer and "roof" under the sea are infinite (L = ∞) is the case considered by Van der Kamp (1972). The solution of Li and Jiao (2001a) reduces to that of Van der Kamp (equation 32) when these parameter values are used (C_e reduces to $L_e/2$, $p = q = 1$, and $\varphi = 0$). When leakage is zero ($L_s = 0$) and the aquifer and confining zone terminate at the shoreline (L = 0), the solution reduces to that of Ferris (1951) presented in equation 29, as $C_e = 1$, $p = q = 1$, and $\varphi = 0$.

As before, application of the theory is most effectively done by comparing measured harmonic-component amplitudes and phases of heads in wells with those of the ocean tides. The expressions for the amplitude ratio and phase lag at an inland well (for a given harmonic component) are:

$$A(x) = h_0 C_e e^{-pax}, \text{ and} \quad (50)$$

$$t_{lag}(x) = \frac{1}{\omega}(qax + \varphi) . \quad (51)$$

Using the logic for comparing theoretical and measured amplitude ratio (r) and phase shift (Φ) that led to equations 36 and 37, the following two independent relations between T and S at inland location x_0 are obtained:

$$T = \frac{\pi p^2 x_0^2}{\tau\left[\ln\left(\frac{r}{C_e}\right)\right]^2} S , \text{ and} \quad (52)$$

$$T = \frac{\pi q^2 x_0^2}{\tau(\Phi + \varphi)^2} S . \quad (53)$$

Substituting the values of C_e, p, q, and φ that correspond to the Van der Kamp case, these relations reduce to equations 36 and 37.

Li and Jiao (2001a) applied their theory to theoretical cases only, and no publication known to the author describes an application to field data. In a second paper, Li and Jiao (2001b) treat the aquifer system, as before, as a semiconfined aquifer separated from an overlying unconfined aquifer by a leaky semiconfining layer, but there is no extension under the sea (L = 0). Other assumptions are as before, with the exception that storage within the leaky semiconfining layer is accounted for in the governing equation.

Inland extent of ocean-tide influence

The equation of Van der Kamp (1972) was used to show approximately how far inland from the coast near Naples that ocean-tide oscillations propagate before the exponential damping term reduces the tidal amplitude to 10 percent and 1 percent of the ocean-tide amplitude measured at the coast. Van der Kamp (1972) assumed that a homogeneous, fully confined aquifer of uniform thickness extended both inland and, with confinement, beneath the ocean. The justification for adopting this assumption for analysis of Naples observation-well data is discussed in the next section.

The relation for tidal amplitude at inland locations within the confined aquifer (equation 34) was adapted for this application. The amplitude of tidal oscillations at inland distance x, $A(x)$, is divided by the ocean-tide amplitude h_0 to obtain an expression for the amplitude ratio r, and then solved for the distance x at which this amplitude ratio will, theoretically, be observed:

$$x = -\sqrt{\frac{\tau T}{\pi S}}\ln\frac{2r}{L_e}, \quad (54)$$

where all symbols are as previously defined.

This equation is applied to lunar harmonic components O_1 and M_2. Results (figs. 29-30) are presented as functions of the hydraulic diffusivity (transmissivity (T) divided by the storage coefficient (S)). If a 10-ft-thick artesian zone having hydraulic conductivity of 10,000 feet squared per day (ft^2/d) is considered, the estimated storage coefficient should be of the order of 1×10^{-5}, based on the rule of thumb offered by Lohman (1979, p. 8) for confined aquifers (1×10^{-6} per foot of thickness). The hydraulic diffusivity would be $1 \times 10^{+9}$ ft^2/d. This aquifer scenario generally is representative of thin, discrete flow zones found within the Upper Floridan aquifer. If the aquifer were considered to be 100 ft thick and to have a transmissivity of 100,000 ft^2/d, as is sometimes characterized in models, a value of 1×10^{-4} might be representative of the storage coefficient according to Lohman (1979, p. 8). The resulting value of diffusivity is again, $1 \times 10^{+9}$ ft^2/d.

For the O_1 component (fig. 29) and the cited value of hydraulic diffusivity ($1 \times 10^{+9}$ ft^2/d), a 90-percent reduction in tidal amplitude occurs at 0.8 miles inland when loading efficiency (L_e) is 25 percent, at 3.2 miles inland when is L_e = 50 percent, and at 4.6 miles inland when L_e = 75 percent. A 99-percent reduction in tidal amplitude occurs at 8.9 miles inland when L_e = 25 percent, at 11.3 miles inland when L_e = 50 percent, and at 12.7 miles inland when L_e = 75 percent. Because the period of the K_1 component of the tide is similar to that of the O_1 component, the required distances for K_1 would be similar.

Results are somewhat different for the M_2 component because the period (τ) is about half that of the O_1 and K_1 components. For the M_2 component (fig. 30) and the cited value of hydraulic diffusivity, a 90-percent reduction in tidal amplitude occurs at 0.5 miles inland when L_e = 25 percent, at 2.2 miles inland when L_e = 50 percent, and at 3.2 miles inland when L_e = 75 percent. A 99-percent reduction in tidal amplitude occurs at 6.1 miles inland when L_e = 25 percent, at 7.8 miles inland when L_e = 50 percent, and at 8.8 miles inland when L_e = 75 percent. Because the period of the S_2 component of the tide is similar to that of the M_2 component, the required distances for S_2 would be similar.

Assuming a hydraulic diffusivity of $1 \times 10^{+9}$ ft^2/d for the aquifers used as monitor zones in the present study, lunar tide components induced by the ocean tide at well C-1111, 4.9 miles from the coast, would probably be reduced to less than 10 percent of the ocean-tide variation. The M_2 components would likely be reduced

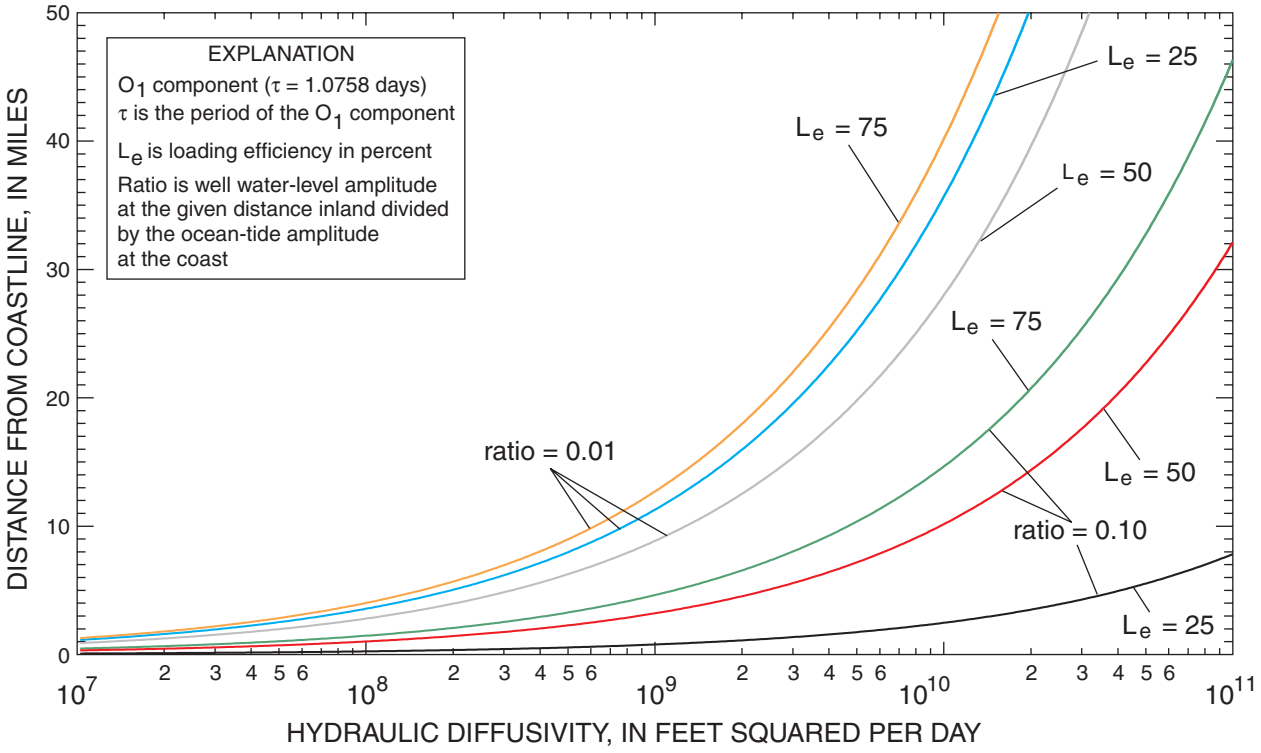

Figure 29. Distance from the coastline at which 90 and 99 percent reductions of the amplitude of the O_1 component of the ocean tide would be observed in wells in a confined aquifer, based on the equation of Van der Kamp (1972).

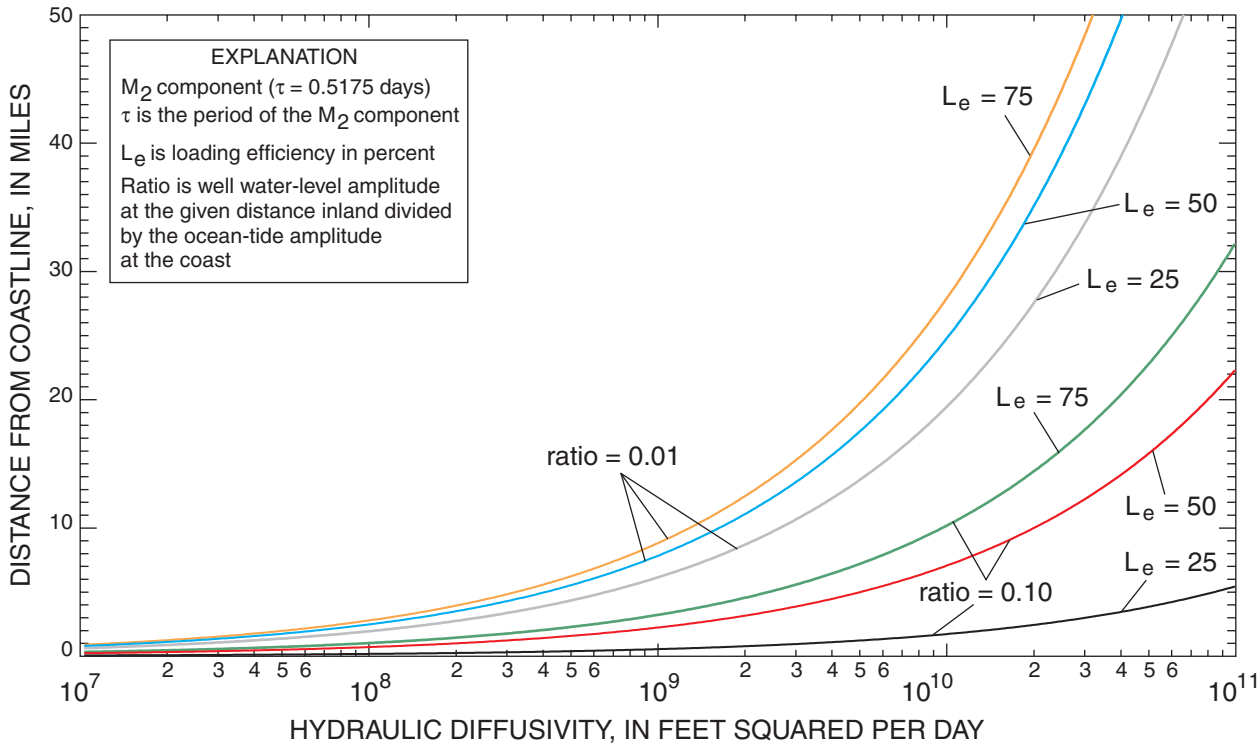

Figure 30. Distance from the coastline at which 90 and 99 percent reductions of the amplitude of the M_2 component of the ocean tide would be observed in wells in a confined aquifer, based on the equation of Van der Kamp (1972).

to a greater extent than the O_1 components. Wells C-1112 (28 miles inland) and HE-1087 (57 miles inland) are sufficiently far from the coast that the lunar component amplitudes induced by the ocean tide would be less than 1 percent of the ocean-tide variation—negligible for purposes of this study. Lunar tidal components measured at C-1112 and HE-1087 would chiefly be the result of the earth-tide influence.

Choice of method for estimating hydraulic diffusivity

Several solutions have been presented for estimating aquifer properties from ocean-tide data that differ with respect to the assumed nature of the aquifer-sea interface. In this section, the characteristics of the aquifer and confining layer in the vicinity of well C-1111 near Naples, Florida, and the tidal Gulf of Mexico are evaluated to determine the best solution for making aquifer parameter estimates based on the head data from this well.

Formations open to the monitor zones in C-1111 are overlain by numerous confining beds of the intermediate aquifer system (fig. 2). MZ-1 is at the base of the Hawthorn Formation, MZ-2 is within the Suwannee Formation, and MZ-3 is within the undifferentiated Avon Park-Oldsmar Formation (Reese, 2000). Regional studies (Meyer, 1989; Ryder, 1985; Miller, 1986) show that the Hawthorn Formation is extensive across the Floridan Peninsula to the east and southeast. To the north, the Hawthorn Formation, Suwannee and Ocala Limestones, and Avon Park Formation rise and thin until the Ocala Limestone is at land surface in central Florida. The confining beds of the Hawthorn Formation pinch out more than 100 miles to the north of the site of C-1111.

Because the aquifers and confining beds are of regional extent to the north, east, and southeast, and are assumed not to vary appreciably in thickness near the study area, theoretical assumptions of uniform aquifer thickness and confinement are assumed to be approximately satisfied in those directions. To the south and west, the Gulf of Mexico extends over a submerged part of the Florida Platform, an extension of the Continental Shelf. The edge of the shelf (indicated by the 6,000-ft depth contour in fig. 31) is about 200 miles west of Naples and about 160 miles south of Naples (Uchupi, 1966), where it bottoms in the shallower Straits of Florida at depths ranging between 3,000 and 6,000 ft. The top of the platform (bottom of the Gulf) is about 650 feet below present-day sea level about 165 miles west of Naples (fig. 31), a depth

higher than the top of any monitor zones providing data for this study. The top of the platform is about 2,300 ft deep, lower than any of the monitor zones, about 25 miles farther to the west. To the south of Naples, depths of 650 ft or greater are found only south of Key West, about 125 miles south of Naples. To the east, the shelf drops steeply east of Ft. Lauderdale, about 110 miles east of Naples, but bottoms at about 2,400 ft. From south and west of Key West, to the east and north around the southern tip of Florida, the bottom of the Straits of Florida rises from a depth of over 6,000 ft until it reaches a depth of 2,400 ft east of Ft. Lauderdale. These distances make the location of the edge of the Continental Shelf at Ft. Lauderdale, to the east of Naples, the closest to Naples.

Information is not known to exist on the stratigraphy of the Floridan aquifer system beneath the submerged part of the Florida Platform to the west and south of present-day peninsular Florida. Oil test wells have been drilled in the eastern Gulf of Mexico and near the Florida Keys, but normally, cuttings are not collected for examination at shallow depths. For this study, it is assumed that aquifer and confining zone depths and thicknesses found beneath present-day Florida continue uniformly westward and southward until the zones crop out at the edge of the Florida Platform. This assumption, together with previous assumptions, is equivalent to a hypothesis that the confinement of the monitor zones in C-1111 is extensive over a broad region, and that theoretical solutions assuming a confining zone of infinite extent (Van der Kamp, 1972; the special case of Li and Jiao, 2001a) are approximately valid for the analysis of tidally influenced head data inland of Naples.

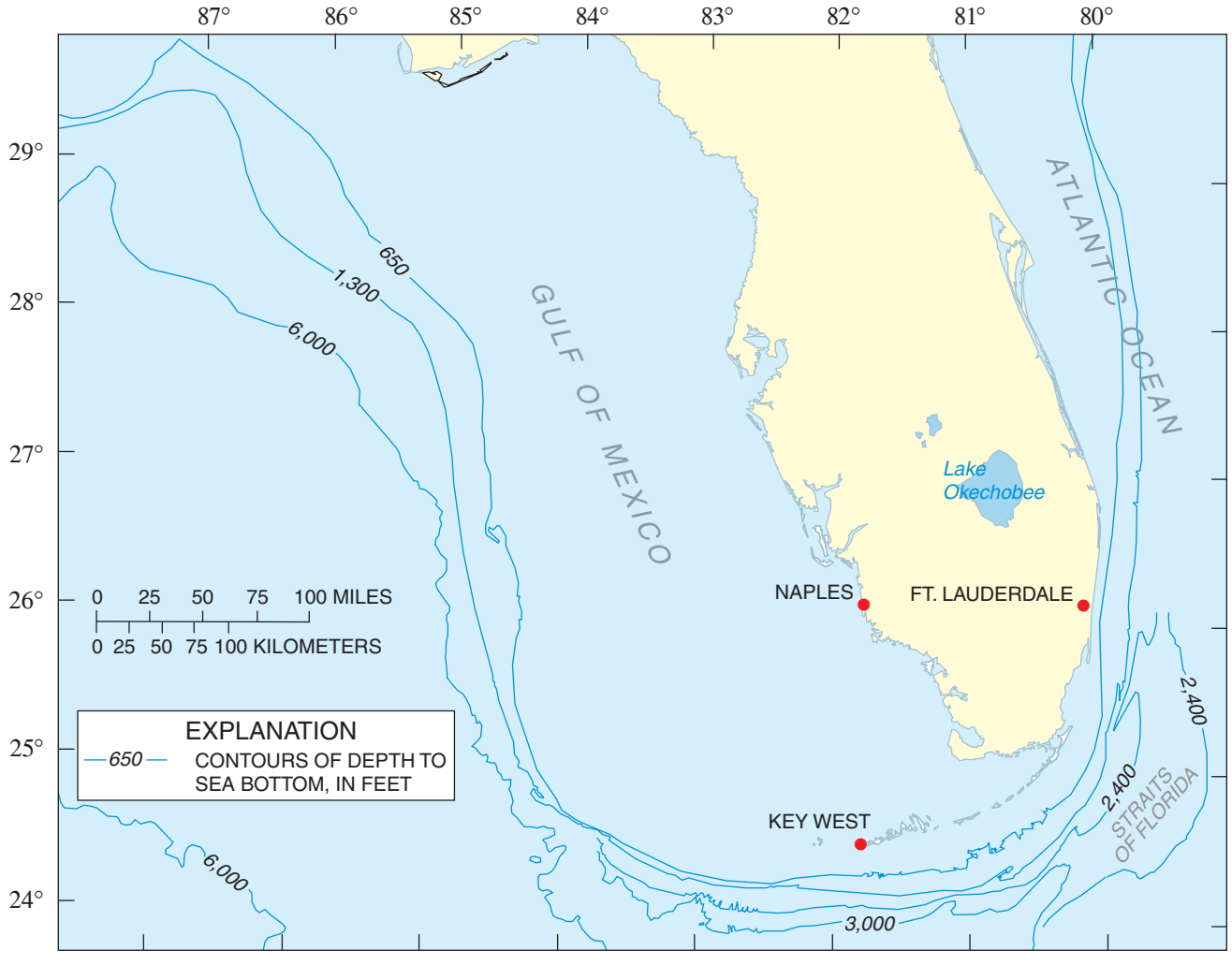

Figure 31. Peninsular Florida and contour lines showing the extent and slope of the Florida Platform.

The intermediate confining unit, comprised largely of clastics of low permeability of the Hawthorn Formation, has a low vertical conductivity in southern Florida. Heads in the Upper Floridan aquifer at C-1111 range from 34 to 35 ft above NGVD 29. Because land surface is only 10 ft above sea level at the C-1111 wellhead (Bennett, 2001b), the high heads maintained in the upper Floridan demonstrate the effectiveness of the confining layer. Depending upon geographical location, the thickness of the overlying surficial aquifer system, and the presence or absence of an intermediate aquifer system, the thickness of confining materials overlying the Upper Floridan aquifer could range from 500 to 1,000 ft.

In a highly generalized model of the aquifer systems underlying the southern part of the Floridan peninsula (Merritt, 1997), a realistic head distribution in the Upper Floridan aquifer was obtained by using vertical hydraulic conductivity values of 0.01 ft/d or less for the intermediate confining unit. Leakance values for 500 and 1,000 ft, respectively, would be 1×10^{-5} to 2×10^{-5} d^{-1}. Such values were needed to confine the aquifer under pressure and prevent substantial loss of head in the aquifer due to upward leakage. These values were applied regionally. If upward leakage occurs at discrete locations, vertical hydraulic conductivity values would be lower at a distance from the locations of leakage.

In the "mega-model" constructed by Sepúlveda (2002), the intermediate aquifer system in northern Charlotte County, about 60 miles north of C-1111, consists of an aquifer bounded above and below by confining units, to which ranges of leakance values are assigned (1×10^{-6} to 1×10^{-5} d^{-1} for the lower and 1.1×10^{-5} to 6×10^{-5} d^{-1} for the higher). Using the two lower values, and using the harmonic mean, a single combined leakance value of 0.9×10^{-6} d^{-1} is obtained. Using the two higher values, a combined value of 0.86×10^{-5} d^{-1} is obtained. In a model of the Floridan aquifer system in west-central Florida, Ryder (1985) specified leakance values ranging from 1×10^{-7} to 7×10^{-5} d^{-1} for what was termed "the lowermost intermediate confining bed." For purposes of this study, the leakance of the intermediate confining unit (intermediate aquifer system) is considered to lie within a range of values from 1×10^{-6} to 2×10^{-5} d^{-1}.

The cited analytical methods all assume an impermeable layer beneath the confined aquifer for which parameter estimates are made. Merritt (1997) assumed a vertical hydraulic conductivity of 1 foot per day (ft/d) or greater for the middle confining unit underlying a layer representing the Upper Floridan aquifer, but this value was assumed to apply regionally, and could have represented leakage at discrete locations. The 1-ft/d value was chosen because few if any vertical hydraulic gradients in the Floridan aquifer system have been documented, and vertical pressure gradients within the aquifer system generally are related to temperature and density variations. Locally, zones of massive limestone underlying solution-riddled flow zones might have lower vertical hydraulic conductivity, but still might not be completely confining.

As a first approximation for the present study, equations 36-37, based on the solution of Van der Kamp (1972) that assumes a completely non-leaky confining unit of infinite extent, were applied to data from the three monitor zones. As noted above, however, few if any confining layers in Florida, including the intermediate confining unit and middle confining unit of southern peninsular Florida, are entirely non-leaky, and it remains of interest to determine whether the estimated low leakance values could have an appreciable effect on estimates of hydraulic diffusivity derived from Van der Kamp's solution. Therefore, data from the two higher monitor zones (MZ-1 and MZ-2) were reanalyzed using the formulas of Li and Jiao (2001a) (equations 41-49), assuming a finite leakance. Leakance from below the monitor zone providing the tidally influenced data was assumed to be represented, together with leakance from overlying layers, by the leakance term used in the solution.

Estimates of hydraulic diffusivity

In applying the method of Van der Kamp (1972) for estimates of hydraulic diffusivity, only the lunar diurnal (O_1), lunar semidiurnal (M_2), and lunar elliptic (N_2) data were used, because the solar components (K_1 and S_2) contained both atmospheric-pressure and ocean-tide influences. A nominal value for S, 1×10^{-5}, was assumed for computational purposes. Lohman (1979, p. 8) states that the storage coefficient (S) of many aquifers is about 1×10^{-6} per foot of thickness multiplied by the thickness. The cited storage coefficient value might, therefore, represent an aquifer 10 ft thick, which is characteristic of the thin, discrete flow zones commonly found in the Floridan aquifer system. Because estimates of transmissivity (T) are linear in the value of S, T values for thicker aquifers would be proportional multiples of the values

computed for thinner aquifers. For instance, if the aquifer were 100 ft thick, 1 x 10^{-4} would be a typical S value for the aquifer, and T estimates would be 10 times those shown in the figures. A value of 4.9 miles is used for x_0.

The phase lag relation (equation 37) is applied by using the periods for the O_1, M_2, and N_2 harmonic components (table 4) and the measured differences in phase of the components (table 5). For instance, the computation for T of MZ-1 based on the O_1 component uses a period value of 1.0758 days and the difference (41.26 degrees) between phases (42.13 degrees for MZ-1 and 0.87 degrees for the ocean tide). The phase difference must be converted to radians (divide by 57.2957795).

The amplitude ratio relation (equation 36) requires specification of the dimensionless measured ratio of the amplitudes of the corresponding harmonic components of the heads in the wells and the ocean tide. In the example above (O_1 component, MZ-1), the amplitudes are 0.03981 and 0.38326, respectively, and the ratio is 0.103872. For the M_2 component in MZ-1, the amplitude ratio is 0.070323. (As previously predicted, the O_1 component was reduced to about 10 percent of the ocean-tide amplitude, and the M_2 component amplitude reduction was even greater.) Equation 36 also requires specification of a value for loading efficiency (L_e). In this study, L_e was varied from 0 to 100 percent in increments of 5 percent to obtain a series of estimates of T based on the series of values of L_e. However, no estimates were made for values of L_e less than twice the amplitude ratio. As previously noted, such values of L_e were invalid.

The two relations (equations 36-37) for the three components (O_1, M_2, and N_2) give six independent estimates of T as a function of the specified value of S for each monitor zone. Values are plotted (figs. 32-34) as a function of valid values of L_e. Because the phase difference relation is not a function of L_e, these estimates plot as horizontal lines. T values computed based on the M_2 phase lags are about half those computed based on the O_1 phase lags. From equation 37, this occurs because the measured M_2 phase lags are about twice the O_1 phase lags and the M_2 period is about half the O_1 period. This difference in estimates may not substantially detract from their usefulness, however, as T estimates from aquifer tests in solution-riddled carbonate aquifers can differ by as much as an order of magnitude. The period of N_2 is slightly longer than that of M_2. The N_2 phase lag estimates of T (figs. 32-34) are slightly higher than the M_2 estimates.

A more serious problem is manifest in the results of the estimates based on the amplitude ratio. It is observed that the previously estimated value of loading efficiency for MZ-1 (table 3, 17 percent) is less

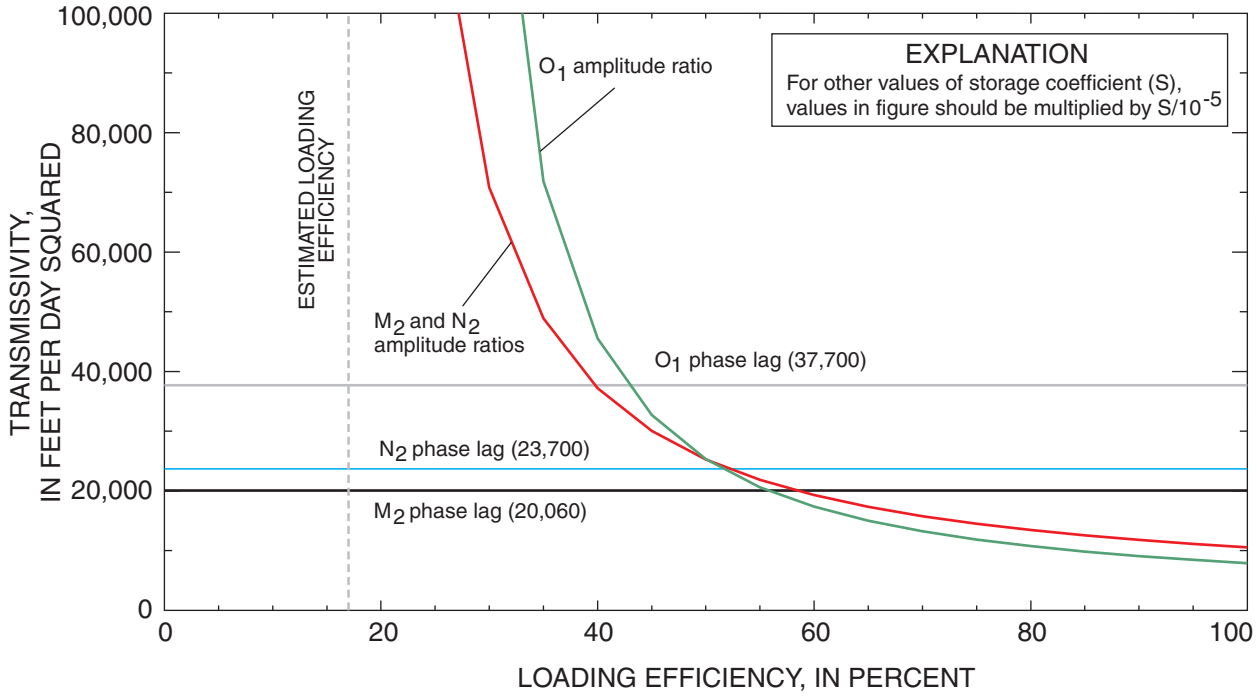

Figure 32. Estimates of transmissivity based on total-head data from MZ-1, well C-1111, assuming a storage coefficient of 1 x 10^{-5} and zero leakance, by the method of Van der Kamp (1972).

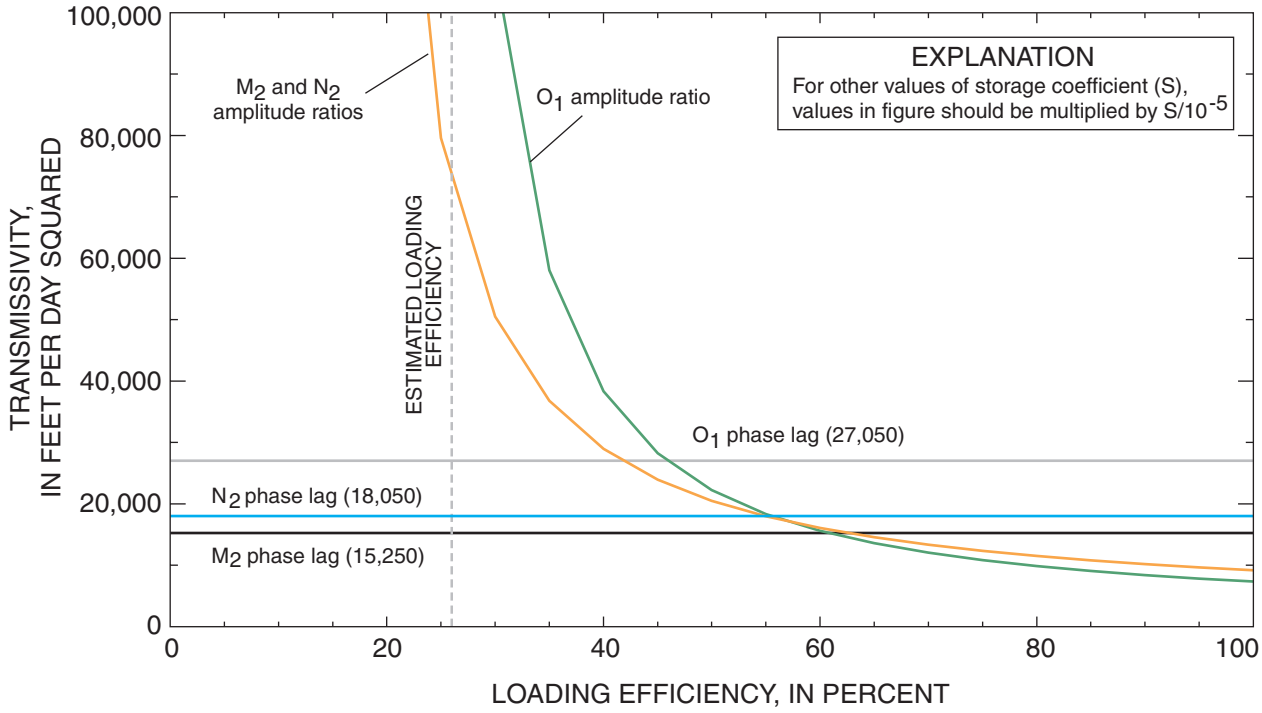

Figure 33. Estimates of transmissivity based on total-head data from MZ-2, well C-1111, assuming a storage coefficient of 1 x 10^{-5} and zero leakance, by the method of Van der Kamp (1972).

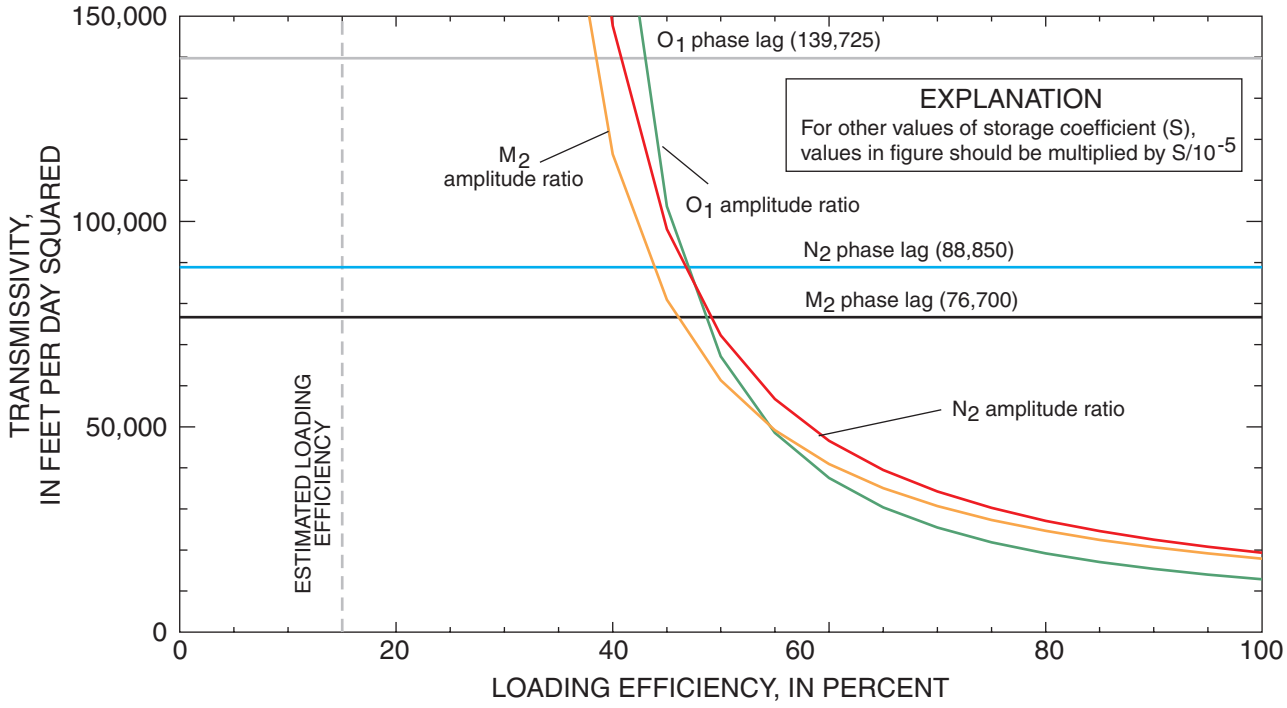

Figure 34. Estimates of transmissivity based on total-head data from MZ-3, well C-1111, assuming a storage coefficient of 1 x 10^{-5} and zero leakance, by the method of Van der Kamp (1972).

than the range of loading efficiency estimates considered valid according to equation 32. Given a loading efficiency value of 17 percent, equation 34 predicts that the amplitude of tidal oscillation in the monitored formation at the coast (x = 0) should be 8.5 percent of the tidal amplitude in the ocean. However, the amplitude ratios of tidal components O_1 and M_2 measured in well C-1111, 4.9 miles inland, are 10 and 7 percent, respectively, of the ocean-tide range. Thus, the loading efficiency estimates (table 3) are not consistent with results of the amplitude ratio analysis. A re-examination and reanalysis of the atmospheric-pressure and head data did not resolve this issue. The estimated component amplitudes (table 5) are consistent with the tidal range observed in the ocean and in the total-head time series for MZ-1, in which the daily range of variation reaches a maximum of about 0.34 ft in early July 1999.

Resolution of this problem would require additional analysis beyond the scope of this study, and possibly additional well drilling and data collection. It might be possible that loading efficiency is greater under the sea at the coast than at the location of well C-1111, 4.9 miles inland, or that loading efficiency estimates based on atmospheric-pressure loading data are not valid for ocean-tide analysis. It is unlikely that the unsaturated zone separating the atmosphere from the water table can reduce the loading efficiency of a confined layer, considering the results of Rojstaczer (1988). The unsaturated zone is probably less than 10 ft thick at each of the wells (C-1111, C-1112, HE-1087) providing tidally influenced water-level data for the study.

Amplitude ratio analyses based on the N_2 components also were made. For MZ-1 and MZ-2 data, computed values were almost exactly the same as those of the M_2 component, and results from the analyses based on the two components are plotted as a single line (figs. 32-33). Estimates of T for MZ-3 based on the N_2 component are slightly higher than M_2 estimates (fig. 34).

Depending mainly on results of the phase lag analysis, the results shown in figs. 32-34 can be interpreted to suggest that estimates of T for the three monitor zones range between 20,000 and 38,000 ft^2/d (MZ-1), between 15,000 and 27,000 ft^2/d (MZ-2), and between 75,000 and 140,000 ft^2/d (MZ-3). As previously noted, if the storage coefficient (S) is different from 1×10^{-5}, these estimates should be modified by the factor $S/10^{-5}$.

Aquifer performance tests in MZ-1 and MZ-2 were performed by the SFWMD in 1996-1997 (Bennett, 2001b). The data were analyzed using a procedure developed by Moench (1985) for large diameter wells in leaky semiconfined aquifers with storative semiconfining layers and a wellbore skin. For MZ-1 and MZ-2, estimated T values were 15,560 and 7,018 ft^2/d, respectively; estimated storage coefficients were 1.7×10^{-5} and 2.3×10^{-5}, respectively; and estimated leakance values were 3.1×10^{-4} and 2.2×10^{-4} d^{-1}, respectively. Using the SFWMD values for storage coefficient, the estimated T values determined by the Van der Kamp method would range between 34,000 and 65,000 ft^2/d for MZ-1 and between 34,000 and 62,000 ft^2/d for MZ-2.

The measured amplitude ratios and phase shifts of the O_1 and M_2 components determined from the head data from the three well monitor zones were reanalyzed using the analytical method of Li and Jiao (2001a) and previously cited leakance values (1×10^{-6} to 2×10^{-5} d^{-1}) that were obtained from the literature. As before, the leaky semiconfining layer was considered to be of infinite extent ($L = \infty$). This means that R_1 and I_1 (equations 46-47) are zero. The procedures involved in the calculation, therefore, are: (1) to calculate the dimensionless leakage u (equation 42); (2) to calculate the intermediate variables p and q from the value of u (equation 48); (3) to calculate the intermediate variables λ and μ (equation 45) from the values of u and loading efficiency L_e; (4) to calculate the value of C_e related to loading efficiency and leakage (equation 44); (5) to calculate the leakage-related phase shift φ (equation 49) from the values of λ and μ; and (6) to compute T as a function of S by using the amplitude ratio and phase shift relations (equations 52-53).

Using a value for S of 1×10^{-5}, as before, and a leakance value of 1×10^{-6} d^{-1} (fig. 35), valid amplitude ratio estimates are obtained only for L_e values much larger than estimated, as before. The estimate based on the phase lag is now a weak function of loading efficiency (L_e) and no longer plots as a straight line. Phase lag estimates are slightly lower than when a zero leakance was used, especially for low values of L_e. For a L_e of 50 percent, the range of estimates of T from the phase lag analysis is now 20,000 to 35,000 ft^2/d. When the leakance is increased to 2×10^{-5} d^{-1} (fig. 36), estimates based on both amplitude ratio and phase lag are lower. For $L_e = 50$ percent, the amplitude ratio estimates are in a narrow range of 26,500-28,000 ft^2/d

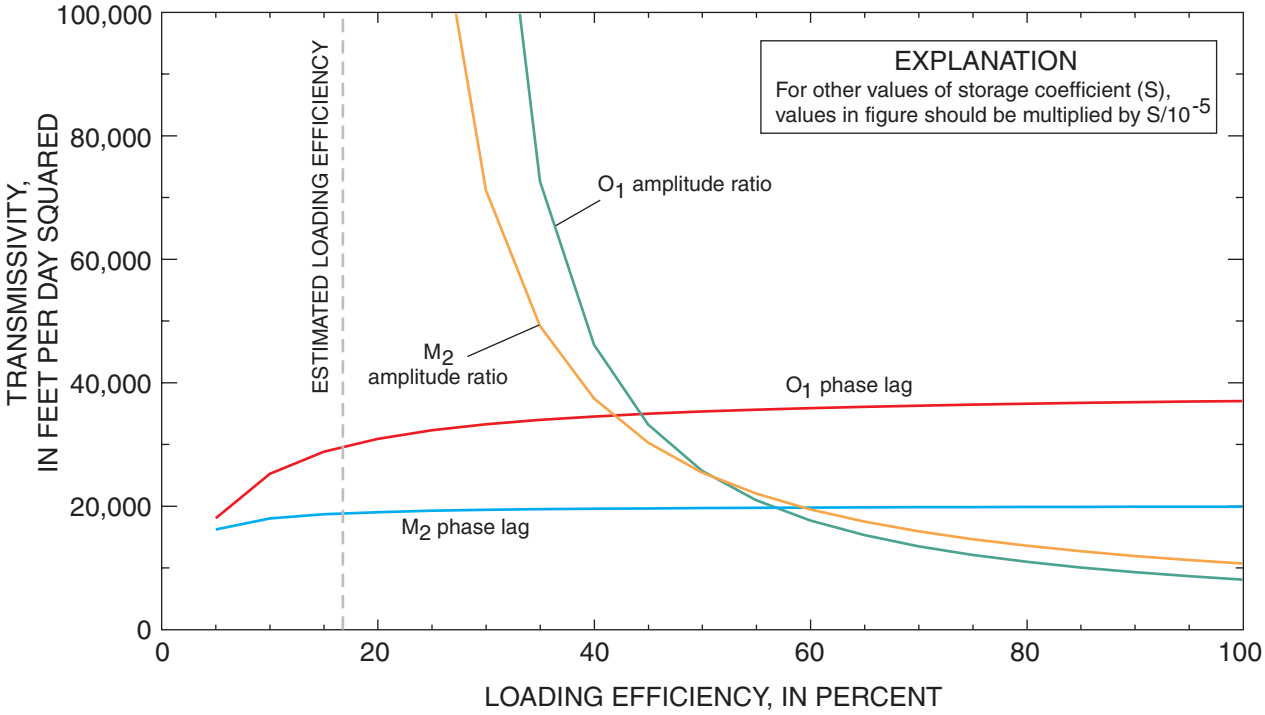

Figure 35. Estimates of transmissivity based on total-head data from MZ-1, well C-1111, assuming a storage coefficient of 1 x 10^{-5} and a leakance of 1 x 10^{-6} d^{-1}, by the method of Li and Jiao (2001a).

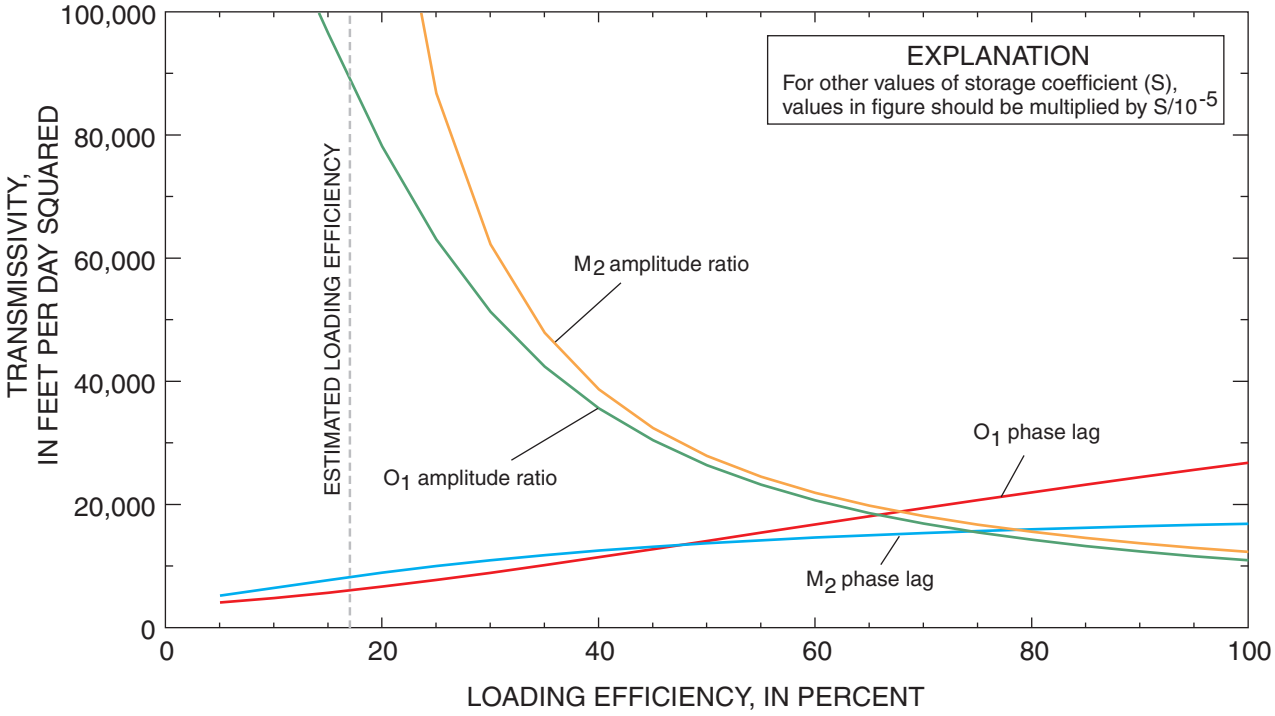

Figure 36. Estimates of transmissivity based on total-head data from MZ-1, well C-1111, assuming a storage coefficient of 1 x 10^{-5} and a leakance of 2 x 10^{-5} d^{-1}, by the method of Li and Jiao (2001a).

and the phase lag estimates are almost identical at 14,000 ft^2/d. For the estimated L_e value of 17 percent, the phase lag estimates range from 6,000 to 8,000 ft^2/d. Using the leakance value of 2 x 10^{-5} d^{-1} to analyze the data from MZ-2 (fig. 37), and assuming L_e to be 50 percent, the amplitude ratio analysis provides T estimates of 23,000-24,000 ft^2/d, and the phase lag analysis provides estimates of 11,000 ft^2/d for both O_1 and M_2 components. When the estimated loading efficiency of 26 percent is used, valid amplitude ratio estimates of 51,000-59,000 ft^2/d are obtained, but the phase lag estimates are only 7,000-8,000 ft^2/d. When the leakance coefficient is increased further by an order of magnitude (to 2x10^{-4} d^{-1}), the O_1 and M_2 amplitude ratio curves for MZ-1 flatten, with T values over an L_e range of 5 to 100 percent ranging from about 44,500 to 37,750 ft^2/d (M_2) and 58,300 to 55,300 ft^2/d (O_1). The phase lag curves also flatten, but at values less than one-tenth of the amplitude ratio curves. Values for an L_e range of 5 to 100 percent are about 3,000 to 5,600 ft^2/d (M_2) and 2,800 to 5,400 ft^2/d (O_1). Although valid amplitude ratio estimates are obtained for the estimated L_e value, there is no value of L_e for which there is even near agreement between the amplitude ratio and phase lag estimates.

Using the method of Li and Jiao (2001a) with a leakance value large enough to permit a small degree of leakage into the aquifer provides T estimates based on the phase lag analysis that are mutually consistent and appreciably lower than those from the non-leaky Van der Kamp method, and closer to the SFWMD estimates. Application of this method appears promising; however, its application requires an estimate of the rate of leakage into the aquifer through confining layers, a property for which accurate estimates are typically scarce or unavailable.

The results of the various analyses using the phase lag calculation methods of Van der Kamp (1972) and Li and Jiao (2001a), rounded to the nearest thousands, are summarized in table 6. Also included, in parentheses, are the values of loading efficiency for which the amplitude ratio calculations would have provided approximately the same estimates. The listed loading efficiencies fall in a narrow range (0.42 to 0.60) for the non-leaky method of Van der Kamp (1972) and for the low value of leakance using the method of Li and Jiao (2001a). When the higher leakance value is used in calculations with the method of Li and Jiao (2001a), the estimated transmissivities are substantially lower and the listed loading efficiencies are substantially higher.

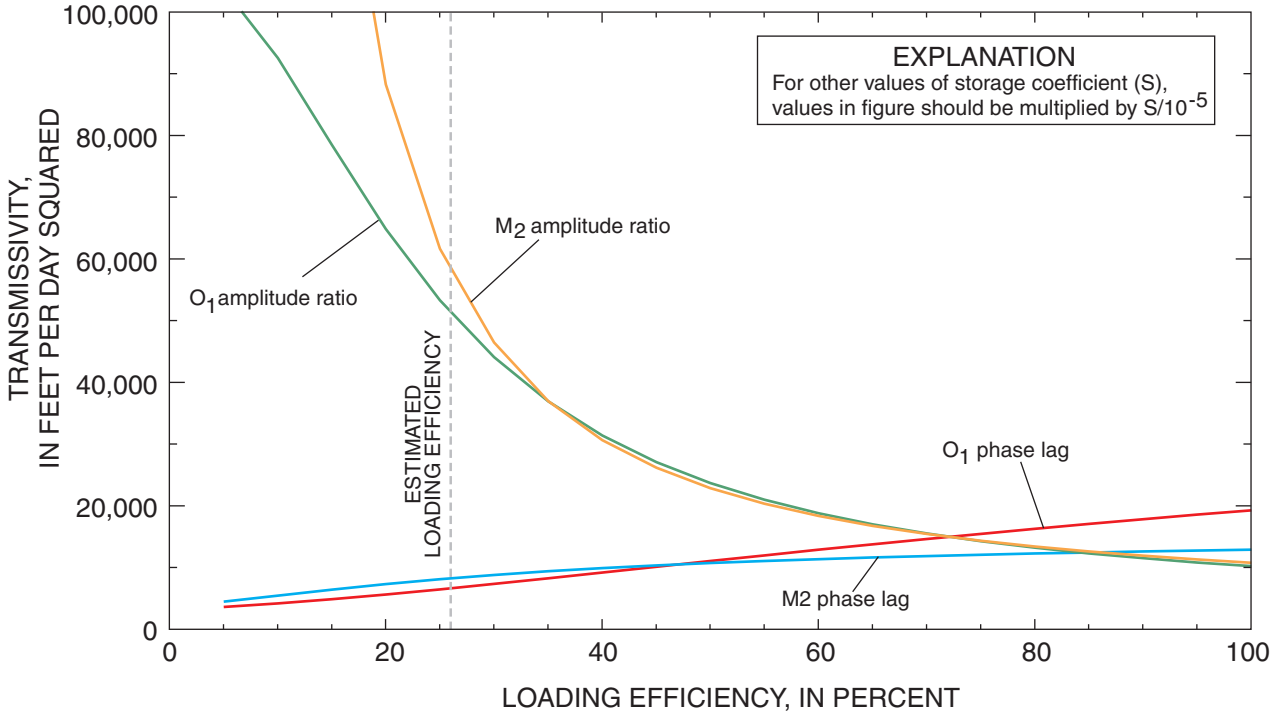

Figure 37. Estimates of transmissivity based on total-head data from MZ-2, well C-1111, assuming a storage coefficient of 1 x 10^{-5} and a leakance of 2 x 10^{-5} d^{-1}, by the method of Li and Jiao (2001a).

Table 6: Summary of transmissivities computed for the three monitor zones in well C-1111 using the phase lag calculation methods of Van der Kamp (1972) and Li and Jiao (2001a), and the values of loading efficiency at which the amplitude ratio calculation would yield the same estimate, in parentheses

[d, day; ft, feet; s, second; --, not calculated]

Method of analysis	Estimated leakance (d^{-1})	Monitor zone designation	Transmissivity in $ft^2/s \times 10^3$ (loading efficiency in percent)		
			O_1	M_2	N_2
Van der Kamp (1972)	0.0	MZ-1	38 (0.42)	20 (0.60)	24 (0.53)
Van der Kamp (1972)	0.0	MZ-2	27 (0.43)	15 (0.60)	18 (0.55)
Van der Kamp (1972)	0.0	MZ-3	140 (0.42)	77 (0.44)	89 (0.47)
Li and Jiao (2001a)	1.0×10^{-6}	MZ-1	35 (0.45)	20 (0.60)	--
Li and Jiao (2001a)	2.0×10^{-5}	MZ-1	20 (0.66)	17 (0.78)	--
Li and Jiao (2001a)	2.0×10^{-5}	MZ-2	16 (0.72)	12 (0.84)	--

It is of interest to examine the amplitudes developed from the least-squares analysis (table 5) to determine the accuracy of the assertion of Gregg (1966) that ocean and earth tides are 180 degrees out of phase at the coast. It is noted that inland wells C-1112 and HE-1087 are 0.24 and 0.44 degrees west of C-1111 at Naples. (The longitude dependence of tidal amplitude is of the form $\cos(A+\phi)$ or $\cos(A+2\phi)$, where ϕ is the longitude and A is the sum of other arguments (Doodson and Warburg, 1941).) Because of the proximity of the latitudes, and because the inland wells are not appreciably affected by ocean tides, the lunar components in those wells are caused solely by earth tides, and Gregg's hypothesis would imply that lunar tidal components at the inland wells should be approximately 180 degrees out of phase with the ocean tides. The M_2 tidal components in the two shallower monitor zones in well C-1112 are 171 degrees out of phase with the ocean tide at Naples; however, the O_1 components are only 114-115 degrees out of phase. The M_2 and O_1 components in well HE-1087 are 150 and 86 degrees out of phase, respectively, with the ocean-tide components. The data do not appear to support Gregg's hypothesis. Why the amplitudes and phases of the lunar components in wells C-1112 and HE-1087 are not approximately the same remains unexplained.

Additional accuracy could be obtained in the estimates of hydraulic diffusivity if the effects of earth tide were filtered from the C-1111 head data. This was attempted by Meyer (1974), using a method developed for that study by H. H. Cooper (U.S. Geological Survey, written commun., March 15, 1973) but not described in detail. The method was specialized to their application and did not appear to be useful for this study. Amplitudes of the lunar components of tides in the monitor zones of inland wells C-1112 and HE-1087 were of the order of 0.010-0.013 ft (O_1) and 0.020-0.030 ft (M_2) (table 5). These lunar components are the result of earth tides and are not caused by semidiurnal atmospheric-pressure oscillations. The O_1 component amplitudes generally are about 17-34 percent of those in the upper monitor zones of well C-1111, and the M_2 components generally are about 20-55 percent of those in the upper monitor zones of well C-1111. These percentages suggest that earth tides could have an appreciable influence on the water-level data used for the ocean-tide analysis. Substantial effort was expended during this study to develop a method to correct the C-1111 well data for the earth-tide effect; however, this objective was not achievable within the timeframe of the study.

Analysis with numerical model

A numerical model was applied for the purposes of: (1) using another means to illustrate the response of a coastal aquifer to ocean-tide loading; (2) investigating additional aspects of the effects of tidal forces on pressure heads in the monitor zones; and (3) demonstrating an application of a numerical model to the problem of aquifer response to ocean-tide loading. The model application was not intended to verify the analytic methods nor to replicate the values obtained from application of those methods.

The model code applied was the version of MODFLOW released by the USGS in 1996 (Harbaugh and McDonald, 1996a and 1996b). A cross-sectional grid design was devised in which ocean-tide oscillations were represented as specified-head boundary conditions on the left-hand side of the grid. The remainder of the grid represented a system of aquifers and confining layers inland of the coast. The simulation of observed data was not attempted. Rather, comparison runs (sensitivity analyses) were made to test the theoretical response of the system to variations in hydraulic characteristics represented by model parameters. Computed heads were relative to a fixed value of 0 ft at the upper vertical surface of the model.

A conceptual model was developed to represent a system of flow zones and less-permeable layers that generally resemble the system of aquifers and

confining layers present in the vicinity of the C-1111 test well, 4.9 miles inland of the coast of the Gulf of Mexico near Naples, Florida. This conceptual model was based on the geologic description (section titled Hydrogeologic Framework) provided by Bennett (2001b) for well C-1111. Apparent differences in lithology and permeability were used to delineate thicknesses and depths of 20 distinct layers (fig. 38). Hydraulic conductivities for the layers were hypothesized based on knowledge of hydraulic characteristics of similar lithologies in other parts of southern Florida.

The model was discretized horizontally, proceeding from the left side (assumed to correspond to the coast) into 10 columns 1 mile wide, a column 1.5 miles wide, and 5 columns 10 miles wide. Confining zones associated with the Hawthorn Formation (layers 2, 4, 6, and 8), known to consist of clastics of low permeability, were assigned an isotropic hydraulic conductivity of 0.001 ft/d. This value was sufficiently low to maintain a hydraulic head difference of 35 ft between the surficial layer and flow zones (layers 9, 11, 13, 15, 17, and 19) within the Floridan aquifer system. A single value of isotropic hydraulic conductivity was assigned to confining zones (layers 10, 12, 14, 16, 18, and 20) associated with the Floridan aquifer system. This value was varied in model tests to test the influence of this parameter on the propagation of oceanic-tide oscillations into the aquifer flow zones.

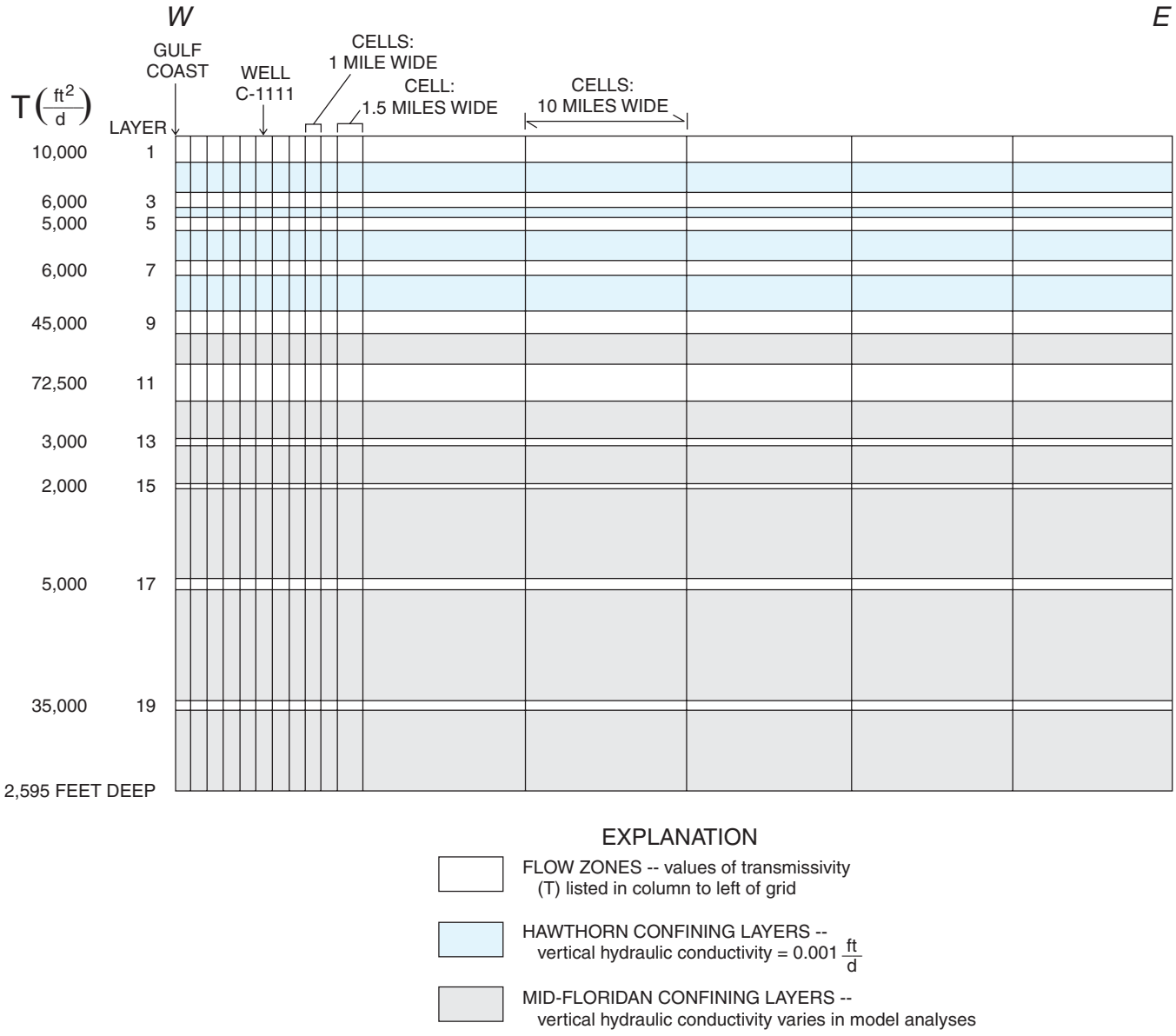

Figure 38. Model grid design used for testing concepts related to the inland influence of ocean tides on pressure heads in wells.

Layers 9 and 11 were associated with monitor zones MZ-1 and MZ-2, respectively, and were assigned a horizontal hydraulic conductivity of 500 ft/d, which was equivalent to transmissivities of 45,000 and 72,500 ft^2/d, respectively. Layer 19 was associated with MZ-3 and was assigned a horizontal hydraulic conductivity of 1,000 ft/d (transmissivity of 35,000 ft^2/d). Other flow zones were assigned a horizontal hydraulic conductivity value of 100 ft/d. Vertical hydraulic conductivities for the flow zones were a tenth of the horizontal values. The input to MODFLOW-96 required the specification of vertical leakances; these were computed from the specified layer thicknesses and vertical hydraulic conductivities. Confined storage coefficients were estimated by using layer thicknesses and the rule-of-thumb value, 0.000001 per foot of thickness, suggested by Lohman (1979).

MODFLOW does not simulate pressure loading from the surface. Tidal oscillations specified as a surface boundary condition in layer 1 would not have been transmitted hydraulically across Hawthorn confining layers tight enough to maintain a pressure-head difference of 35 ft. Therefore, the tidal-pressure oscillations were represented by specified-head conditions for all layers along the vertical ocean boundary in column 1 using module FHB (Leake and Lilly, 1997). This was exactly analogous to the conceptual models of Ferris (1951) and Van der Kamp (1972) that postulate that pressure loading from the surface occurs beneath the ocean seaward of the shoreline, but is not transmitted vertically inland of the shoreline. The specified tide was a simple harmonic of amplitude 0.38 ft and with period 25.819341 hours. Both specifications are parameters of the main lunar diurnal (O_1) in the ocean tide at Naples. The tidal oscillations were normalized about 0 ft in layers 1-8, but were increased by an additive constant of 35 ft in layers 9-20 to correspond to the presumed head difference across the Hawthorn. There is actually a head gradient through the vertical thickness of the Hawthorn, but this assumption simplified the model design without affecting the objectives of the exercise.

The model was run for 100 simulation days with 240 time steps per day. Some aperiodic hydraulic trends were evident in early time steps as the model simulated the hydraulic adjustment to some degree of vertical leakage in parts of the grid. Simulated water levels at horizontal and vertical grid locations corresponding to monitor zones in well C-1111 were downloaded to special files for graphical representation.

The first experiments performed with the model were to test the response of water levels at the monitor-zone locations to variations in the vertical hydraulic conductivity of the confining layers in the layers (9-20) representing the Floridan aquifer system. The uniform specification of this parameter value in these layers was given values of 0.1, 0.05, 0.01, and 0.001 ft/d (fig. 39). Given the lowest specified value, a strong tidal response occurs at the position (column 6, layer 19) of the lowest monitor zone (MZ-3) approximately normalized about the value of 35 ft used as a base value to the boundary tidal specification. With increasing specified values for the parameter, however, the tidal response lessens and the average pressure-head value declines. When the specified vertical hydraulic conductivity is 0.1 ft/d, the tidal variation is barely detectable, and the average pressure-head value is about 33.4 ft.

The explanation for these results is that higher values of vertical hydraulic conductivity represent a loss of confinement for the permeable layer (aquifer). Oscillations in head caused by ocean tides are negligible in vertically adjacent confining layers because of their low transmissivity. If these confining layers are slightly permeable vertically, pressure oscillations propagating into the aquifers from the ocean dissipate vertically into them. This result highlights the importance of aquifer confinement in the theory of Ferris (1951) and Van der Kamp (1972), and the potential usefulness of a solution that accounts for vertical leakage (Li and Jiao, 2001a).

A second set of model runs was made to test the effect of aquifer transmissivity on the response of the water level at the location of MZ-3. Transmissivity values of 3,500, 35,000, and 350,000 ft^2/d were specified (35,000 ft^2/d was used in the previous set of model runs). The effect of the parameter variation is appreciable (fig. 40); the model illustrates that tidal response at inland locations is positively correlated to the aquifer transmissivity, as shown by Ferris (1951) and Van der Kamp (1972). When the transmissivity specified in the model run is 350,000 ft^2/d, the amplitude of simulated head oscillations at the monitor well location is more than half of that specified at the ocean boundary. But when the specified transmissivity is reduced to 3,500 ft^2/s, the head series is nearly flat, and tidal oscillations are barely discernible (fig. 40).

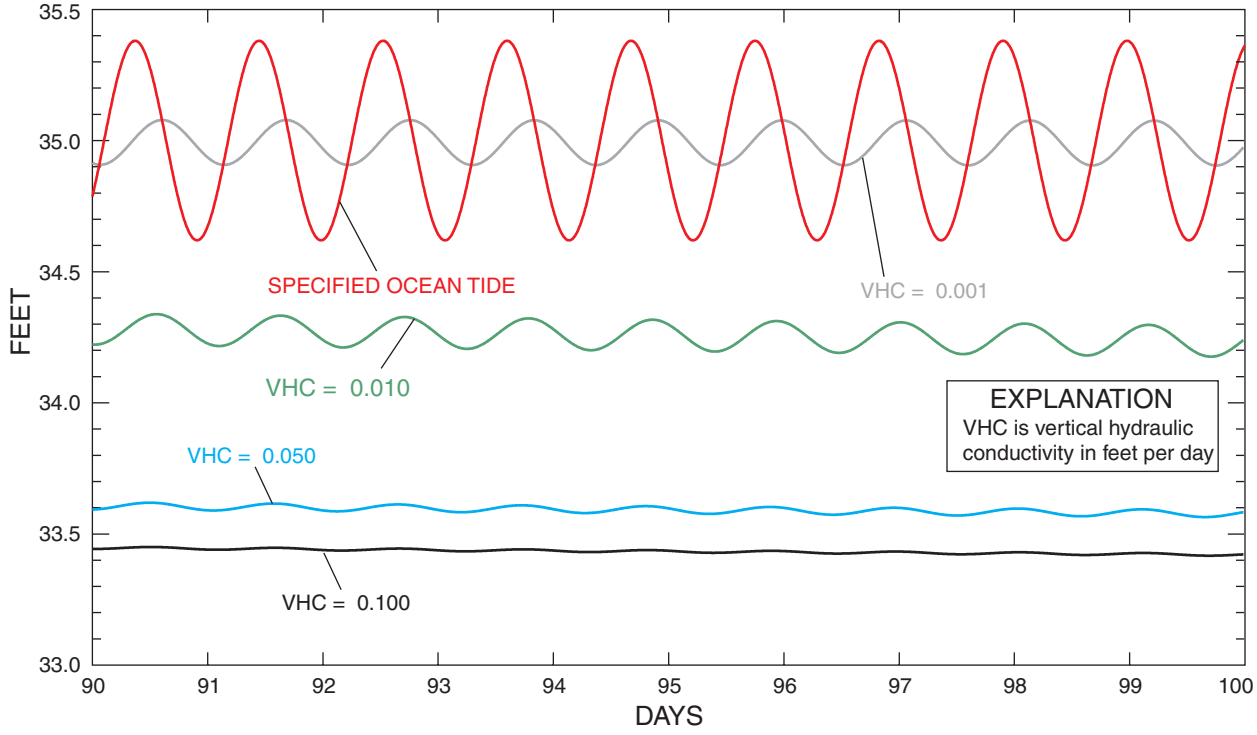

Figure 39. Simulated ocean-tide induced head oscillations in MZ-3 at the approximate inland distance of well C-1111 (5 miles), assuming various values of vertical hydraulic conductivity for overlying and underlying confining layers.

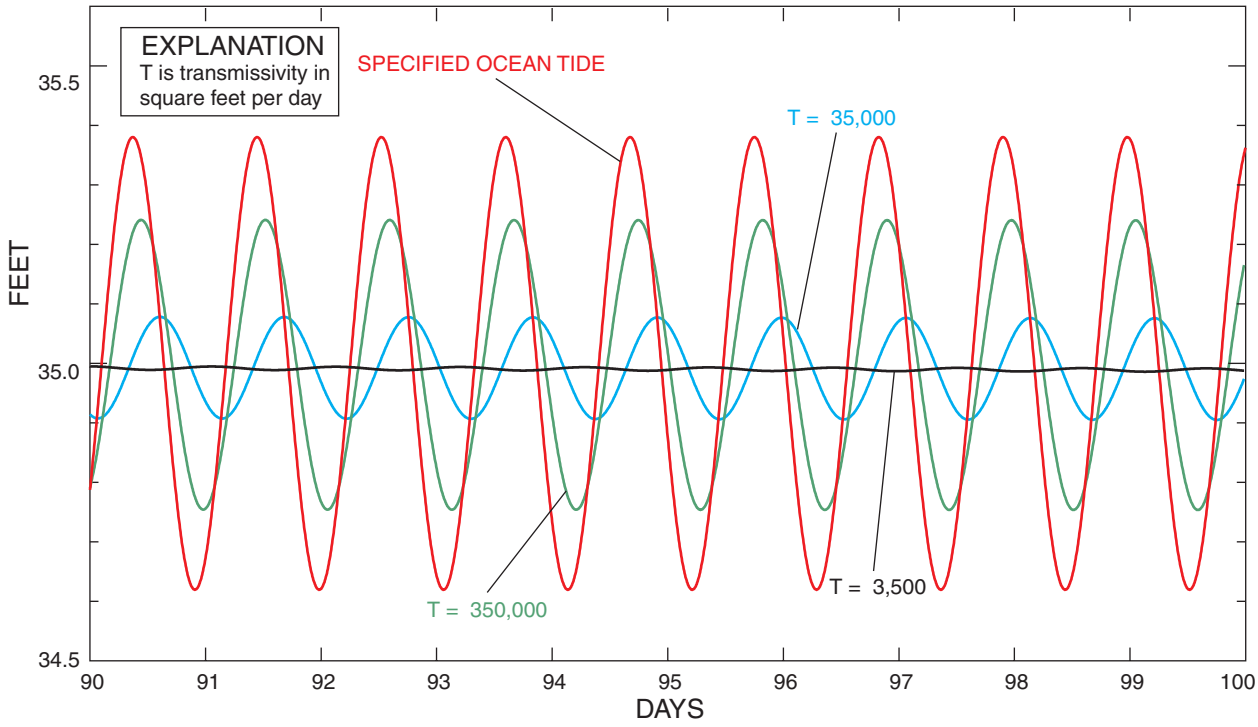

Figure 40. Simulated ocean-tide induced head oscillations in MZ-3 at the approximate inland distance of well C-1111 (5 miles), assuming various values of transmissivity for the aquifer.

Using Heads Influenced by Earth Tides for Estimates of Specific Storage, Porosity, and Bulk Modulus of the Aquifer

The second cited category of research is the use of inland head oscillations caused by earth-tide and periodic atmospheric-pressure oscillations to derive estimates of the elastic storage capacity of the aquifer. Because both forces are effectively uniform in magnitude over large lateral distances, the effect on the confined aquifer also would be uniform over large distances (assuming no areal variation of barometric efficiency) and would, therefore, not induce additional lateral flow in the aquifer. (The possibility of inducing vertical flow is discussed later.) Because lateral flow is not affected by the periodic stresses, no information can be derived regarding the horizontal transmissivity of the aquifer.

Jacob (1940) and Lohman (1979, p. 9) cite Theis (1938) for presenting the expression for the unitless storage coefficient (S) of an aquifer:

$$S = \rho\eta B\left(\beta + \frac{\alpha}{\eta}\right), \qquad (55)$$

where

ρ is weight density (pound-force/L^3),

η is porosity (unitless),

B is aquifer thickness (L), and

α and β are as defined for equation 1.

Dividing equation 55 by the thickness B results in the definition of specific storage (S_s) (L^{-1}) of the aquifer.

By considering the dilatation of the aquifer material and relating it to the specific storage of the aquifer (S_s) and to the tide-generating potential (W_2), Bredehoeft (1967) derived the following relation between specific storage, the tide-generating potential, and the head (h) oscillation observed in a well open to the aquifer:

$$S_s = -\left[\left(\frac{1-2\nu}{1-\nu}\right)\left(\frac{2\bar{h}-6\bar{l}}{ag}\right)\right]\frac{dW_2}{dh}, \qquad (56)$$

where

ν is the Poisson ratio of the aquifer material (dimensionless),

$\bar{h}$ and $\bar{l}$ are Love numbers at the surface of the earth (dimensionless),

a is the radius of the earth (L), and

g is the gravitational acceleration at the surface of the earth (L/T^2).

The Love numbers are used to relate the theoretical tidal potential to actual displacements at the earth's surface (Bredehoeft, 1967).The Love numbers have a theoretical basis but usually are determined experimentally.

The expression for the vertical tidal strain developed by Bredehoeft (1967) is re-derived by Hsieh and others (1988) using two approaches: (1) that of Bredehoeft and (2) one that follows the development of Van der Kamp and Gale (1983), but with the solid grains assumed incompressible. The functional form of the equation for the theoretical tidal potential (Munk and MacDonald, 1960) is obtained from a manual published by the British Navy (Doodson and Warburg, 1941):

$$W_2(\theta, \phi, t) = gK_m bf(\theta)\cos[\beta(\phi, t)], \qquad (57)$$

where

K_m is the general lunar coefficient, taking into account the masses of the earth and moon, the distance to the moon, and the earth's radius, and is equal to 53.7 cm (1,7618 ft);

b is an amplitude factor (unitless) that has a distinct value for each tidal component with period τ,

$f(\theta)$ is the latitude function (unitless); and

$\beta(\phi, t)$ is a phase term that depends on the longitude ϕ and the Greenwich Mean Time (GMT) t.

The terms W_2 and ag each have units of L^2/T^2. The dimensionless terms b, $f(\theta)$, and $\beta(\phi,t)$ were obtained for individual harmonic components of the tide from Munk and McDonald (1960) and Doodson and Warburg (1941) and are shown in table 7 for seven major tidal components (P_1 and K_2 are treated separately from K_1 and S_2, respectively, in the cited references and also are used in some of the subsequent calculations). The Munk and MacDonald reference contains several errors in the specifications of the functions $f(\theta)$ and $\beta(\phi,t)$. Because neither reference is organized for ease of use by hydrologists, it was found useful in this study to use both sources and to correlate their information.

Table 7. Some parameters for diurnal and semidiurnal equilibrium tides

[Periods, frequencies, and common names for tidal components are given in table 4. Symbols: θ, latitude; q, angular velocity of the Earth relative to the mean sun (15 degrees per mean solar hour); $\phi_s(t)$, longitude of the mean sun (increasing by 0.0411 per mean solar hour); $\phi_m(t)$, mean longitude of the moon (increasing by 0.549 degrees per mean solar hour); $\phi_p(t)$, mean longitude of lunar perigee (increasing by 0.0046 degrees per mean solar hour); and ϕ, longitude of the observation point. Further definitions of terms are provided in Munk and MacDonald (1960) and Doodson and Warburg (1941)]

Tidal component	*b*	*f*(θ)	$\beta(\phi,t)$
O_1	0.377	sinθcosθ	$qt + \phi_s(t) - 2\phi_m(t)$ - 169.8 degrees + ϕ
P_1	0.176	sinθcosθ	$qt - \phi_s(t)$ - 10.2 degrees + ϕ
K_1	0.531	sinθcosθ	$qt + \phi_s(t)$ + 10.2 degrees + ϕ
N_2	0.174	0.5 $\cos^2\theta$	$2(qt + \phi_s(t) - 1.5\phi_m(t) + 0.5\phi_p(t)$ - 79.8 degrees + ϕ)
M_2	0.908	0.5 $\cos^2\theta$	$2(qt + \phi_s(t) - \phi_m(t)$ - 79.8 degrees + ϕ)
S_2	0.423	0.5 $\cos^2\theta$	$2(qt + \phi)$
K_2	0.115	0.5 $\cos^2\theta$	$2(qt + \phi_s(t)$ - 79.8 degrees + ϕ)

The minus sign in equation 56 indicates that the head in the aquifer decreases as the tide-generating potential increases. The entire term in brackets is a constant. Values for the coefficients (n = 0.27, $\overline{h}$ = 0.60, $\overline{l}$ = 0.07, a = 6.371 x 10^8 cm (centimeters) = 2.0902 x 10^7 ft) were obtained from Marine (1975). The value of the gravitational constant was g = 979 cm/s^2 (centimeters per second squared) = 32.12 ft/s^2 at the latitudes (26-27 degrees) of the observation wells analyzed during this study. Although Marine's application was to sand, clay, crystalline basement rock, sandstone, and mudstone, P.A. Hsieh (U.S. Geological Survey, oral commun., 2002) states that the Poisson ratio does not vary much from 0.25 in any rocks in which it has been measured. Using the cited values, the value of the term in brackets is 0.788 x 10^{-12} (cm^2/s^2)$^{-1}$, or 0.7321 x 10^{-9} (ft^2/s^2)$^{-1}$.

Although equation 56 is written as a derivative, mathematically the instantaneous change of W_2 as a function of the instantaneous change of aquifer head (h), the derivative can be approximated by a finite differential, the change in W_2 (ΔW_2) when the aquifer head changes by an amount Δh. In the present study, the ratio of small finite changes ΔW_2 and Δh in a small time period Δt are considered to be proportional to the ratio of the corresponding amplitudes of the theoretical and observed tides.

Bredehoeft (1967) applies equation 56 to individual harmonic components of the head oscillations caused by earth-tide forcing. As previously noted, the solar components of the periodic head oscillations are caused partly by periodic atmospheric-pressure oscillations, so that their use in the equation 56 could lead to inaccurate results. Again, only the lunar components of the head oscillations (O_1 and M_2), considered to be caused wholly by earth tides, are used for the analysis. Heads from C-1111 are excluded from use in the analysis because the lunar components are primarily the result of the ocean tide.

If the amplitude of a harmonic component of W_2 is denoted $A_2(\tau,\theta)$, where τ is the period of the harmonic component, and the amplitude of a component of the head change of period τ is denoted $A_h(\tau)$, then an approximation of equation 56 is:

$$S_s = 0.7321x10^{-9}\left(\frac{ft^2}{s^2}\right)^{-1}\frac{A_2(\tau,\ \theta)}{A_h(\tau)}\ , \text{where} \quad (58)$$

$$A_2(\tau,\ \theta) = gK_m bf(\theta)\ . \quad (59)$$

$A_2(\tau,\theta)$ is a function of latitude (θ), but not of longitude (ϕ). Using equations 58-59, estimates of S_s range from 0.49 x 10^{-6} to 0.76 x 10^{-6} ft^{-1} and average 0.60 x 10^{-6} ft^{-1} (table 8). These values are lower than the rule-of-thumb estimate (1.0 x 10^{-6} ft^{-1}) suggested by Lohman (1979, p. 8). According to E.P. Weeks (U.S. Geological Survey, written commun., 2003), Lohman's estimate is based on data from unconsolidated aquifers, and specific storage values for consolidated rock should be lower. The estimates based on the O_1 and M_2 harmonic components of the measured earth-tide effect appear to be mutually consistent in each monitor zone.

Use of the theoretical tidal potential as a standard of comparison for well pressure-head observations is not without some uncertainty. Beaumont and Berger (1975) analyzed data from wells and determined that the actual tidal potential could differ appreciably from the predicted value as a result of topographical variations and geologic nonuniformities.

Table 8. Summary of calculations for specific storage (S_s) and porosity based on head data from monitor zones in wells C-1112 and HE-1087

Monitor zone	Latitude (θ) (degrees, minutes, seconds)	$f(\theta)$	τ (days)	b	$A_2(\tau)$ (ft^2/s^2)	$A_h(\tau)$ (ft)	S_s (ft^{-1} x 10^{-6})	B_e (percent)	Porosity (percent)
Well C-1112									
MZ-2	26° 24' 48"	0.3984	1.0758 (O_1)	0.377	8.4994	0.01074	0.58	63	25
MZ-2	26° 24' 48"	.4011	.5175 (M_2)	.908	20.6095	.02476	.61	63	27
MZ-3	26° 24' 48"	.3984	1.0758 (O_1)	.377	8.4994	.01278	.49	71	24
MZ-3	26° 24' 48"	.4011	.5175 (M_2)	.908	20.6095	.03022	.50	71	25
MZ-4	26° 24' 48"	.3984	1.0758 (O_1)	.377	8.4994	.00978	.64	49	22
MZ-4	26° 24' 48"	.4011	.5175 (M_2)	.908	20.6095	.02679	.56	49	19
Well HE-1087									
MZ	26° 36' 30"	.4004	1.0758 (O_1)	.377	8.5421	.00961	.65	75	34
MZ	26° 36' 30"	.3997	.5175 (M_2)	.908	20.5377	.01991	.76	75	39

Jacob (1940) derived an equation that relates porosity and specific storage:

$$\eta = \frac{B_e S_s}{\beta \rho} \quad . \qquad (60)$$

Equation 60 is obtained by combining equations 1 and 6 with equation 55. As before, B_e refers to the barometric efficiency measured from observations of the water level in a well open to the atmosphere. Parameter values are β (the compressibility of water) = 3.34 x 10^{-6} psi^{-1}, or 2.32 x 10^{-8} ft^2/pound-force, and ρ (the weight density of water) = 62.4 pound-force/ft^3. Using previously estimated values for barometric efficiency (table 3), a series of estimates of porosity can be made based on the computed values of specific storage (table 8). The values of these porosity estimates, ranging from 19 to 39 percent, appear to be mutually consistent within each monitor zone, and are consistent with typical values of porosity measured on cores and used in modeling applications. Numerous measurements of porosity on cores from the monitor zone in HE-1087 are cited by Bennett (2001a), and range from 20 to 43.5 percent, with the majority of values falling between 30 and 40 percent.

Recent research into methods of estimating specific storage, porosity, and bulk modulus

Another relation between specific storage, porosity, and bulk modulus that can be implemented by the acquisition of the appropriate field data was derived by Robinson and Bell (1971). Their theory "extends the development of Bredehoeft (1967) by considering the separate aquifer dilatations caused by the barometric tide and the ocean tide (in coastal areas) as well as the solid earth tide" (Rhoads and Robinson, 1979). Rhoads and Robinson (1979) refine the derivation. Using a definition of barometric efficiency due to Bear (1972), Rhoads and Robinson (1979) provide additional equations for estimating porosity and the aquifer matrix bulk modulus (inverse of compressibility).

Cooper and others (1965) stated that "when the aquifer is compressed, the change in volume of the solid material due to deformation of the individual particles is small in comparison with the change in volume of the water." Thus, compressibility of the solid fraction is assumed to be negligible ($1/K_s = 0$) in the development of equation 56 and "volume changes of the formation are taken as equal to changes of the pore volume" (Van der Kamp and Gale, 1983). Cooper and others (1965) do note, however, that "This assumption is apparently valid for granular aquifers,

but, depending on the pore geometry and Poisson's ratio, it may not be valid for such aquifers as limestone and basalt."

Van der Kamp and Gale (1983) developed expressions for specific storage (S_s) and its relation to earth-tide strain that include the effect of the compressibility of the solids because "the compressibility of solids may not be negligible for many common formations, especially if they have low compressibility and low porosity." Their "expression for the coefficient of specific storage with vertical deformation only, including the effect of compressibility of solids" is:

$$S_s = \rho g\left[\left(\frac{1}{K}-\frac{1}{K_s}\right)(1-\lambda)+\eta\left(\frac{1}{K_f}-\frac{1}{K_s}\right)\right], \text{ where} \quad (61)$$

$$\lambda = \frac{2(1-2\nu)}{3(1-\nu)}\left(1-\frac{K}{K_s}\right) . \quad (62)$$

As before,

K is the bulk modulus of elasticity of the formation,

K_f and K_s are the bulk moduli of elasticity of water and "the solid fraction including the effect of unconnected pores" (Van der Kamp and Gale, 1983),

ν is Poisson's ratio, and

η is the interconnected porosity of the formation.

If the compressibility of solids is considered to be zero ($1/K_s = 0$), equation 61 reduces to a form that Van der Kamp and Gale (1983) consider equivalent to the storage coefficient derived by Jacob (1940), when the confined modulus of elasticity (K') (equation 5) is used in place of the bulk modulus (K).

Finally, Van der Kamp and Gale (1983) derive the relation between aquifer-pressure oscillations and the earth-tide strain. Inserting the relation between earth-tide strain (dilatation) and the theoretical tidal potential (W_2) assumed by Bredehoeft (1967), and solving for S_s in terms of the corresponding changes in W_2 and pressure-head in the aquifer (h), a more precise expression for S_s results:

$$S_s = -\left[\left(1-\frac{K}{K_s}\right)\left(\frac{1-2\nu}{1-\nu}\right)\left(\frac{2h-6l}{ag}\right)\right]\frac{dW_2}{dh} , \quad (63)$$

where all terms have been previously defined.

As the bulk modulus of the formation (K) is less than the bulk modulus of the solid fraction (K_s) (bulk modulus is the inverse of compressibility and increases as compressibility decreases), the first term in parentheses in equation 63 is always between 0 and 1. If the solid fraction is incompressible, as assumed by Bredehoeft (1967), this term is unity and equation 63 reduces to equation 56. No attempt was made to apply this relation in the present study because of the lack of information available to support estimates of K_s. However, assuming some compressibility of the solid fraction of the carbonate aquifers in the study area, using equation 63 would have resulted in some reduction of the previously calculated estimates of specific storage.

Rojstaczer and Agnew (1989) followed Van der Kamp and Gale (1983) in assuming that the solid portion of the aquifer matrix was compressible to some extent. Rojstaczer and Agnew (1989) also removed the assumption of previous papers that uniform surface loading caused only vertical deformation of the aquifer material. The theory analyzes water levels in an open well penetrating a confined aquifer for responses to earth-tide and atmospheric loading. Accounting for lateral deformation leads to an iterative procedure for determining matrix compressibility, after which the porosity can be determined. Given these parameters, specific storage can also be determined.

Dual porosity in aquifers, where a permeable fracture network is embedded in a less permeable porous matrix, and where the aquifer is isotropic and homogeneous at the continuum scale, was studied by Desbarats and others (1999). Water-level and atmospheric-pressure fluctuations are analyzed for barometric efficiency. Independent estimates are required for the porosities of the fractured and porous parts of the aquifer. Distinct pressure fields are generated in the fractures and the pore space by changes in atmospheric pressure that may take an appreciable amount of time to equilibrate. The theory is used for estimates of specific storage.

Using Heads in Open Wells Penetrating Confined Aquifers for Estimates of the Transmissivity and Storage Coefficient of an Aquifer

The well-aquifer system has been a productive scenario for theoretical and applied hydrologic studies from the early days of scientific hydrology. In most theoretical developments, the well is assumed to be open to the atmosphere, and the well is assumed to be either screened (or open) throughout the thickness of a confined aquifer and cased to the top of the aquifer (fig. 41). When oscillations of pressure head in the aquifer occur, water moves into or out of the screened or open part of the well. This causes an oscillation of the water surface in the open well, which, depending on aquifer and well characteristics, might be damped or lagged in time relative to the pressure-head oscillations, although the frequency will remain the same.

Characteristics of the oscillation of the water level in the open well in response to a pressure-head disturbance in the aquifer are a function of the periodicity of the disturbance, the aquifer parameters (transmissivity and storativity), as well as inertial and storage effects affecting water movement in the well and the air pressure at the water surface in the well (atmospheric pressure). Given adequate field data, mathematical solutions for the well-aquifer interaction can be used to estimate values of aquifer coefficients.

Jacob (1940) used the open artesian well scenario to define concepts of barometric and tidal efficiency and the response of well water levels to periodic pressure-head variations originating at a remote line source within the aquifer (the ocean-tide theory previously described). A relation between the motion of water within an open wellbore (taking into account the inertia of water within the wellbore) and pressure-head oscillations in the confined aquifer was developed by Cooper and others (1965) with the objective of describing mathematically the water-level response to seismic waves. The resulting equation established a relation between the amplitude and phase lag of oscillations of the water level in the well to the amplitude of oscillations of pressure-head in the aquifer. Bredehoeft (1967) showed that the inertial effects were negligible when the transmissivity of the aquifer was above a low value (0.001 ft^2/s), and his relation (equation 56) for estimating specific storage as a function of the change in water level within a well depends on this result.

Cooper and others (1967) considered the problem of the response of the head in an aquifer and in a well following an instantaneous charge of a known volume of water to the well. Inertial effects related to the movement of water in the well are ignored. Their results are used to relate the time rate of change of the water level in the well to the aquifer properties (transmissivity and storativity), leading to an analytical method for determining these properties from field data acquired in slug testing of the well. The results of Cooper and others (1967) were used as an element of at least one solution (Furbish, 1991) to the problem of determining aquifer parameters from periodic or tidal data.

The well-aquifer scenario was used by Weeks (1979) in an analysis of the effect of atmospheric-pressure fluctuations on the water levels in open wells screened below the water table in deep unconfined aquifers. Because the unsaturated zone resists air movement, a temporary imbalance occurs between pressure below the water table and that at the water surface in the well. The theory of Weeks (1979) provides for the estimation of pneumatic diffusivity of the unsaturated zone, knowledge of which enables well water levels to be corrected for the effects of atmospheric-pressure fluctuations. According to E. P. Weeks (U.S. Geological Survey, written commun., 2003), this approach may not be applicable in southern Florida because of the shallow depth to the water table.

The response to earth tides of an open well screened in a confined aquifer was studied by Narasimhan and others (1984), who recognized the importance of wellbore storage effects, the period of the tidal pulses, and the aquifer properties (permeability and specific storage). They applied a numerical model of saturated flow to demonstrate the qualitative importance of these factors. These relations were presented analytically by Hsieh and others (1987). Ignoring inertial effects of water in the wellbore, Hsieh and others (1987) determined the time-varying drawdown in the open well as a function of periodic pressure-head oscillations in the aquifer (considered to be a simple harmonic function). Expressions were derived for the amplitude response (A) and the phase shift (η):

$$A = \left|\frac{x_0}{h_0}\right| = (E^2 + F^2)^{-1/2} \text{ and} \qquad (64)$$

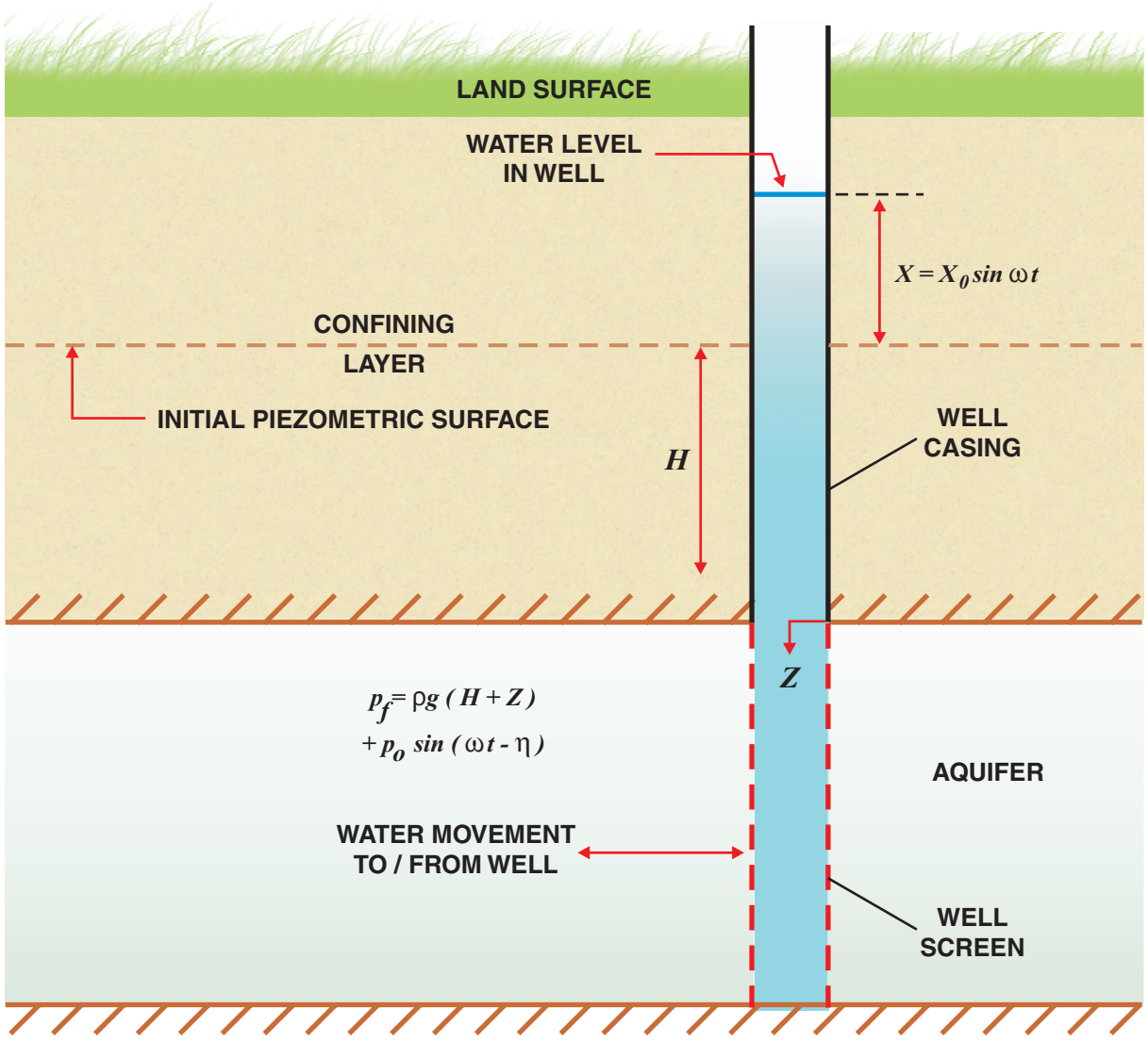

EXPLANATION

x is displacement of water in well (L)
x_o is amplitude of water-level fluctuation (L)
ω is angular frequency of tidal disturbance ($radians / T$)
t is time (T)
H is height of water column in well casing (L)
p_f is fluctuating pressure in aquifer (M / Lt^2)
p is pressure (M / LT^2)
g is gravitational acceleration (L / T^2)
Z is depth below bottom of casing (L)
p_o is amplitude of pressure fluctuation ($M / L T^2$)
ρ is density of water (M / L^3)
η is phase angle *(radians)*
M is mass unit
L is length unit
T is time unit

Figure 41. Idealized representation of an open well in which water-level oscillations are caused by oscillation of artesian pressure (modified from Cooper and others, 1965).

$$\eta = -\text{atan}(F/E)\text{ , where} \quad (65)$$

$$E \approx 1 - \frac{\omega r_c^2}{2T} Kei(\alpha_w)\text{ , and} \quad (66)$$

$$F \approx \frac{\omega r_c^2}{2T} Ker(\alpha_w)\text{, and} \quad (67)$$

$$\alpha_w = \left(\frac{\omega S}{T}\right)^{1/2} r_w\text{,} \quad (68)$$

where

x_0 is the complex amplitude of the water-level oscillation in the well;
h_0 is the fluctuating pressure head in the aquifer;
r_w is the radius of the screened or open portion of the well;
r_c is the radius of the well casing;
ω is the frequency of the oscillations;
T is the aquifer transmissivity;
S is the storage coefficient; and
Ker and *Kei* are Kelvin functions of order zero.

The expressions for E and F are simplified expressions for values of $\alpha_w < 0.1$, which is generally the case for realistic values of r_w, T, and S in earth-tide analysis (Hsieh and others, 1987). The theory was developed for "a single, laterally extensive confined aquifer that is homogeneous and isotropic."

The required data analysis is similar to that done in the ocean-tide application or for the computation of specific storage using the method of Bredehoeft. For the earth-tide analysis, two sets of data are needed to determine the amplitude ratio or the phase shift: (1) water-level oscillation in the well and (2) pressure-head measurements of the tidally generated oscillations in the aquifer. Pressure-head measurements can be obtained from a pressure transducer installed in a shut-in or packed-off well. Dilatometer instruments have been used in a few cases. If measurements of pressure heads or the dilatation of the aquifer are not available, the theoretical tidal potential (W_2) may be used to derive dilatation estimates, subject to reservations concerning departure from theoretical values owing to local conditions.

The well water-level and aquifer pressure-head data are detrended; then, the regression analysis is applied to determine the amplitude and phase of the five major tidal components of each data set. The analysis proceeds with a comparison of the lunar (O_1 and M_2) components of the two data sets, known to not be affected by atmospheric-pressure oscillations. The comparison can be done iteratively on a trial-and-error basis using equations 64-68, by introducing various estimates of T and S. Hsieh and others (1987), however, applied a different approach. Converting from the variables α_w and $\omega r_c^2/T$ to an alternative set of dimensionless parameters, $T\tau/r_c^2$ and Sr_w^2/r_c^2, where τ is the period ($\tau = 2\pi/\omega$), they prepared graphs of the amplitude ratio and phase shift computed from equations 64-68 as a function of $T\tau/r_c^2$ for selected values of Sr_w^2/r_c^2. These illustrations have been expanded and replicated (figs. 42-43) for inclusion in this report. While these are not referred to as type curves by Hsieh and others (1987), they could serve a similar purpose. It is clear that, given estimates of the amplitude ratio and phase lag based on field data and an estimate of the storage coefficient, values of the dimensionless transmissivity can be obtained from the graphs in figures 42-43 and translated into common transmissivity units (ft^2/d) by using the period of the harmonic cycle (τ) and the casing radius (r_c). Use of the phase lag graph (fig. 43) can lead to two interpretations; some pre-knowledge of the likely range of transmissivity of the aquifer could be useful in this case.

Because of the closeness of the graphs for the various values of storage coefficient in figures 42-43, it is noted that the amplitude ratio and phase lag are each weak functions of storage coefficient, as noted by Hsieh and others (1987). If a reasonable estimate of the storage coefficient is available from the literature or previous aquifer testing, then the relations shown in these figures can be used to provide reasonably precise estimates of the transmissivity.

The graphs (figs. 42-43) also indicate a substantial limitation to the applicability of these methods to data from some hydrologic environments. It is noted that, for values of the dimensionless transmissivity approaching 1×10^3, the amplitude ratio curves flatten and converge as they approach the value of 1.0 (no reduction in amplitude) and the phase lag curves flatten and converge as they approach the value of 0.0 (no phase lag). The physical interpretation is that, for sufficiently high values of aquifer transmissivity, the amplitude of earth-tide oscillations is not reduced in the well water levels, nor do the water-level oscillations in the well exhibit a phase lag.

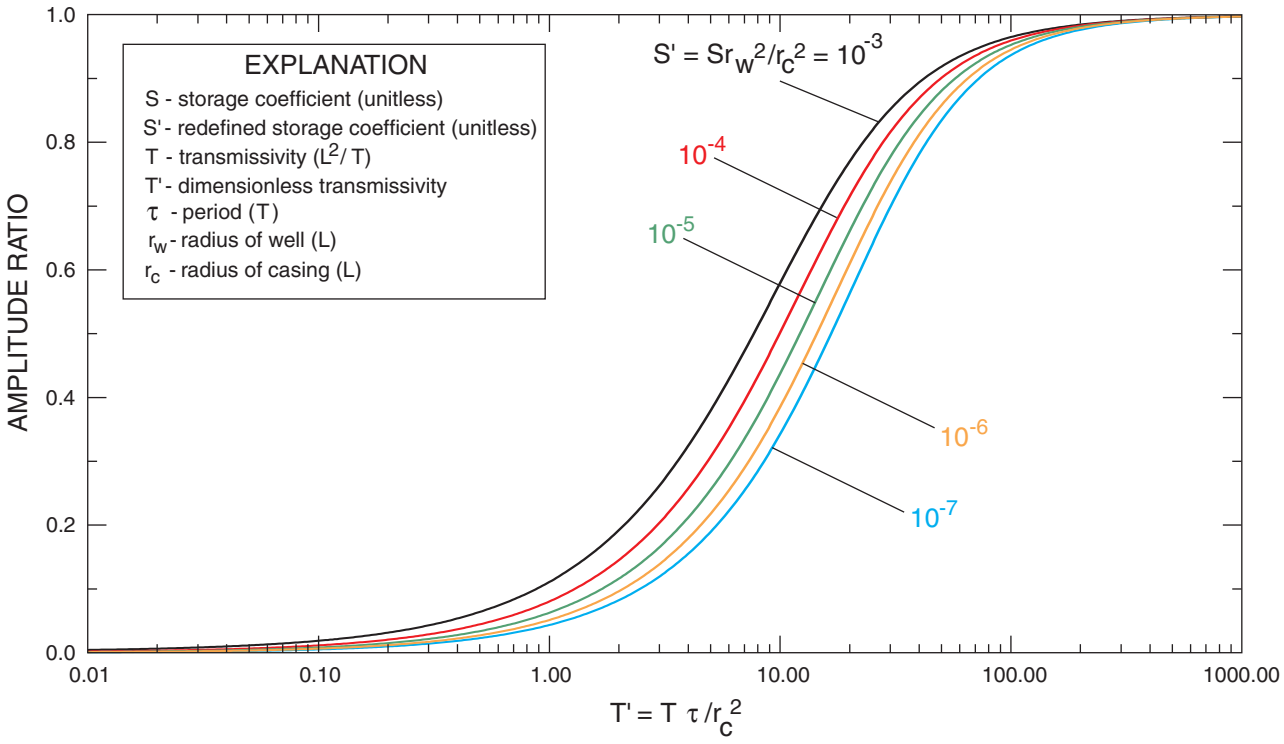

Figure 42. The ratio of the amplitudes of the well water-level and aquifer pressure-head oscillations as a function of dimensionless transmissivity, for various values of redefined storage coefficient.

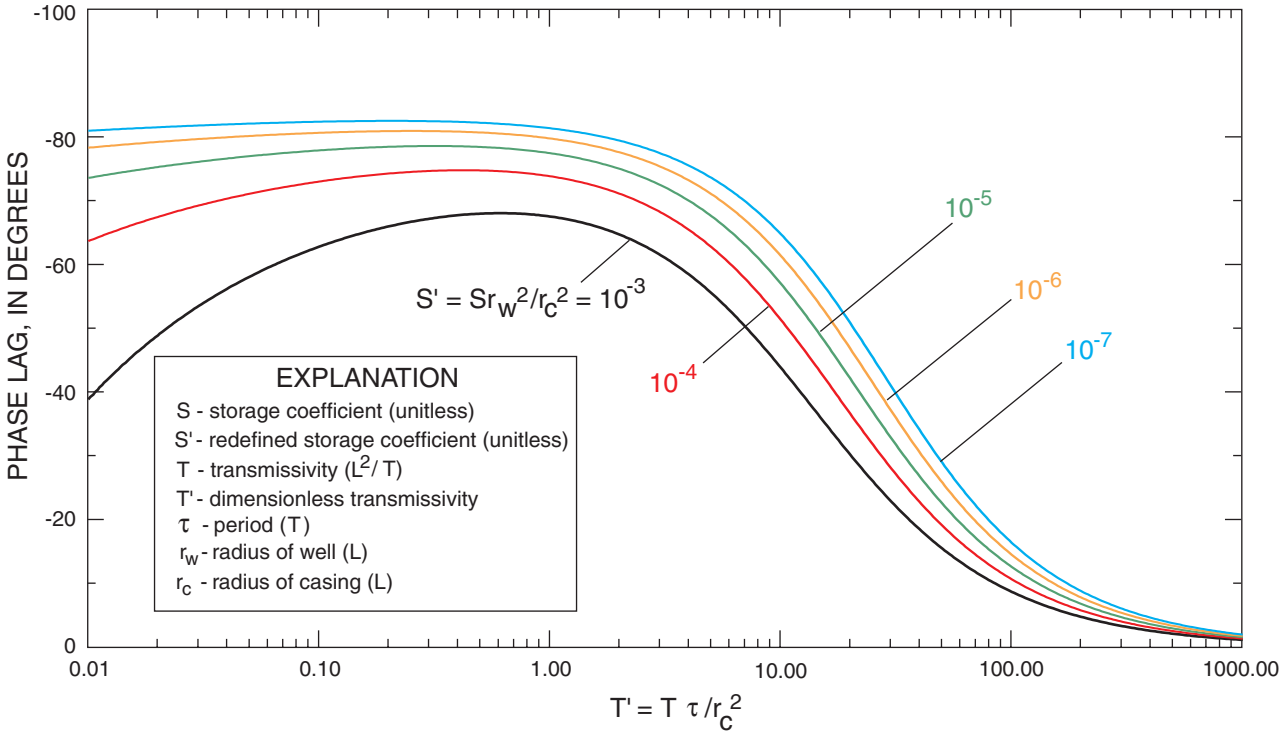

Figure 43. The phase lag between the well water-level and aquifer pressure-head oscillations as a function of dimensionless transmissivity, for various values of redefined storage coefficient.

If 0.95 is accepted as the limit at which the amplitude ratio can be defined by field data, then the highest transmissivity that can be estimated by the amplitude ratio method, given a well casing radius of 0.5 ft and a tidal harmonic period of 0.5 day, is 37 ft^2/d for a dimensionless storage coefficient of 10^{-3} and 59 ft^2/d for a dimensionless storage coefficient of 10^{-7}. If the period is assumed to be 1 day, these estimates are halved. If 5 degrees is accepted as the limit for which the phase lag can be defined by field data, then the highest transmissivity that can be estimated by the phase lag method, given a well casing radius of 0.5 ft and a tidal harmonic period of 0.5 day, is 93 ft^2/d for a dimensionless storage coefficient of 10^{-3} and 182 ft^2/d for a dimensionless storage coefficient of 10^{-7}. Again, if the period is assumed to be 1 day, these estimates are halved.

The conclusion is that the method of Hsieh and others (1987) probably is applicable only to aquifers having transmissivities less than 500 ft^2/d. In fact, the funding for development of similar methods has come from sources interested in testing the degree of confinement of formations vertically adjacent to hazardous waste repositories (P. A. Hsieh, U.S. Geological Survey, oral commun., 2002), where normal aquifer testing procedures are considered hazardous. Estimates of transmissivity of the upper Floridan aquifer developed as part of the present study, and the earlier estimates by SFWMD based on aquifer testing, range above 7,000 ft^2/d. Upper Floridan transmissivity estimates less than 500 ft^2/d are not known to have been reported; thus, the usefulness of the method described here in the upper Floridan aquifer is quite limited. It also is noted that no open wells are constructed into the upper Floridan aquifer in the study area. Such wells would need standpipes several tens of feet above land surface because of the appreciable artesian head in the upper Floridan aquifer. Shut-in wells might not produce useful information regardless of the type of pressure transducer used, because the water level may not exhibit a response to the storage properties of the well. Shut-in wells could, however, provide useful comparison data if open-well data were available from another location.

Solutions to the response of the well-aquifer system to periodic pressure oscillations that take into account additional aspects of the hydrologic system include the work of Rojstaczer (1988). Rojstaczer considers the effect of periodic atmospheric-pressure oscillations on an aquifer system that includes a partially confined aquifer separated from a surficial aquifer by a partially confining layer. The solution takes into account "groundwater flow between the borehole and the aquifer, groundwater flow between the aquifer and the water table, and air flow between the land surface and the water table through the unsaturated zone." The water-level response in the well may show a phase lag because of some of these processes. For convenience, it is assumed that no pressure differential occurs between the aquifer and partially confining layer. Measured data are used for an estimate of barometric efficiency. Parameters that can be estimated include the pneumatic diffusivity of the unsaturated zone, the vertical hydraulic diffusivity of the partially confining layer, and the lateral hydraulic diffusivity of the partially confined aquifer. Rojstaczer identifies three frequency bands (of the perturbing atmospheric pressure), in each of which a distinct set of parameters determines the response.

The analysis of wells in an unconfined aquifer was continued by Rojstaczer and Riley (1990), who considered the response to earth tides and atmospheric loading and reported methods of determining both the pneumatic diffusivity of the unsaturated zone and the vertical hydraulic conductivity of the aquifer. A vertical diffusion equation was stated and solved for the variable pressure within the wellbore. Lateral permeability was assumed to be high enough that wellbore storage effects could be ignored.

Another solution to the well-aquifer problem was documented by Furbish (1991), who suggested that it could "be used to filter raw loading and water-level records" to remove atmospheric-pressure influences. The solution assumes that "the aquifer transmissivity is large relative to the permeability of the confining layer, the confining layer is thick, and oscillations in atmospheric load are of moderately high dimensionless frequency." The solution is a convolution approach. A change in atmospheric pressure, converted to its equivalent in feet of water, is considered to be equivalent to a slug or bail test of the well (the immediate injection or withdrawal of a volume of water in the wellbore), and the solution sums the responses to a discrete series of atmospheric-pressure changes, treated formally as a series of slug or bail tests.

Two alternatives are suggested for the response function. One is precise but computationally intensive, based on the solution of Cooper and others (1967) for the aquifer response to a slug test. The other, due to

Hvorslev (1951) is computationally simple but applicable only to aquifers with small storativity. Application of the solution requires making prior estimates of aquifer parameters and then trying to replicate observed water-level oscillations. Like Hsieh and others (1987), Furbish (1991) notes that "for large transmissivities . . . little attenuation or lag of the signal occurs," and the method is of little use in these cases because any large value of transmissivity will replicate the observed well data.

Using Heads or Water Levels to Estimate Vertical Hydraulic Conductivity

This category of research is the newest discussed in this report. Theoretical developments are still tentative and few field applications have been made; however, the distinctiveness and promise of the approach warrant its being highlighted.

Earth tides and atmospheric-pressure fluctuations can cause vertical flow in the subsurface in certain cases, and measurements that reveal the degree or rate of flow in response to a known degree of forcing can, in theory, be used to deduce the values of hydraulic properties related to vertical flow. The theory of Weeks (1979) leads to a diffusion equation for head fluctuations as a function of pneumatic diffusivity of the unsaturated zone.

Van der Kamp and Gale (1983) note that, under tidal strain or atmospheric loading, "vertical flow may occur in a formation if the overlying and underlying formations have different elastic or hydraulic properties," or under water-table conditions. These authors present a diffusion equation that represents their concept of the process. Rojstaczer and Agnew (1989) present a vertical diffusion equation that incorporates assumptions that the solid fraction is compressible and the deformation caused by surface loading is lateral as well as vertical. Rojstaczer and Riley (1990) implement this equation in an analysis of the response of water levels in an unconfined aquifer to earth tides. An attempt was made by Seo and others (2000) to apply vertical diffusion theory to data from an unconfined aquifer, ignoring effects of air flow in the unsaturated zone. Pressure-head data were acquired from buried transducers, eliminating the need for any consideration of well-aquifer interaction.

CONCLUSIONS

Various methods for using well water-level fluctuations caused by tidal or aperiodic natural forces to estimate aquifer properties are described and evaluated in the preceding pages. Table 9 is a summary of the results of the evaluation. Fifteen methods are described, of which four (nos. 2-5 in table 9) were used in the course of this study. The other methods were not used either because they were not suitable for the hydrologic environment from which the data sets provided for the study were obtained or because they required independent estimates of petrophysical properties that were not available. Only limited statements can be made about the usefulness or validity of the solutions not applied in the present study. A brief discussion of these methods is provided as a guide to readers who desire to investigate them further.

The analyses for transmissivity (based on a prior estimate of storage coefficient) that used data from near-ocean monitor zones using methods 2 and 3 provided answers generally in agreement with results of aquifer performance tests performed by the SFWMD. More precise estimates, however, were difficult to obtain because of the imprecision of estimates of the storage coefficients of the individual monitor zones. In addition, independent estimates of loading efficiency were too low to be consistent with tidal amplitudes measured in the monitor zones, so that amplitude ratio calculations that required loading efficiency estimates could not be completed. Additional research and field work to determine loading efficiencies and the pattern of variation of tidal amplitudes in heads would be useful in providing additional insight into this problem. The phase lag estimates obtained based on separate tidal components using method 2 showed a difference of somewhat less than 100 percent.

Although estimates using method 2 were imprecise, transmissivity estimates based on aquifer testing in carbonate aquifers can show even greater differences. Phase lag estimates using method 3 (assuming some leakance to or from adjacent formations) were in better agreement, and both phase lag and amplitude ratio estimates were lower and in better agreement with the SFWMD estimates. A technique of correcting the near-ocean data for the effects of earth tides is needed and might substantially improve estimates.

Table 9. Summary of methods evaluated, properties determined by each method, and applicability in southern Florida

	Method	Properties determined	Applied in present study	Applicability in southern Florida
1	Analysis of water-level oscillations caused by ocean tide in surficial or fully confined aquifers (confinement ends at the coast). Jacob (1940;1950), Ferris (1951).	Lateral hydraulic diffusivity	No	Only to data from wells very near coast in surficial aquifers, or near the coast of Palm Beach, Broward, or northern Dade Counties in Floridan aquifer system.
2	Analysis of water-level oscillations caused by ocean tide in fully confined aquifers. Confinement is of infinite extent beneath ocean. Van der Kamp (1972).	Lateral hydraulic diffusivity	Yes	Useful for data from wells in confined aquifers near any part of the coast of southern Florida except in Palm Beach, Broward, or northern Dade Counties.
3	Analysis of water-level oscillations caused by ocean tide in fully confined aquifers or semiconfined aquifers separated from the water table by a leaky semiconfining layer. Confinement under ocean is of either finite or infinite extent. Li and Jiao (2001a).	Lateral hydraulic diffusivity	Yes	Useful for data from wells near coast in southern Florida in any aquifer. In surficial aquifers, or (possibly) in the Floridan aquifer system in Palm Beach, Broward, and northern Dade Counties, reduces to Jacob/Ferris method. In fully confined aquifers extensive under ocean, reduces to Van der Kamp method.
4	Analysis of water-level oscillations caused by earth tide in fully confined aquifers. Assumes incompressible solid fraction. Bredehoeft (1967), Hsieh and others (1988).	Specific storage	Yes	Useful for data from wells in confined aquifers at any location. However, data must be free of ocean-tide effects, either by location or by filtering.
5	Computation of porosity of a fully confined aquifer. Jacob (1940).	Porosity	Yes	Anywhere that locally valid estimates of specific storage and barometric efficiency are available.
6	Analysis of water-level oscillations caused by earth tide, ocean tide, and diurnal atmospheric-pressure oscillations in fully confined aquifers. Robinson and Bell (1971), Rhoads and Robinson (1979).	Specific storage	No	Designed for use at inland locations free of ocean-tide influence where barometric efficiency, amplitude, and phase of atmospheric-pressure oscillations are known, or near ocean where tidal efficiency, amplitude, and phase of ocean tides are also known.
7	Analysis of water-level oscillations caused by earth tide in fully confined aquifers with a compressible solid fraction. Van der Kamp and Gale (1983).	Specific storage	No	Potentially useful for data from wells in confined aquifers where an estimate of the compressibility of the solid fraction is available. Data must be free of ocean-tide effects, either by location or by filtering.
8	Analysis of water-level oscillations in an open well penetrating a confined aquifer. Assumes solid portion compressible, also makes other new theoretical assumptions. Rojstaczer and Agnew (1989).	Matrix compressibility, porosity, and specific storage	No	Potentially useful for data from open wells penetrating confined aquifers affected by earth tide and atmospheric-pressure fluctuations. Assumes the availability of an estimate of the compressibility of the solid fraction.
9	Analysis of water-level oscillations caused by atmospheric-pressure fluctuations in an aquifer characterized by dual porosity. Desbarats and others (1999).	Specific storage	No	No apparent geographical restriction. However, assumes availability of independent estimates of barometric efficiency, porosities of the fractured and porous fractions, and other rock properties.

Table 9. Summary of methods evaluated, properties determined by each method, and applicability in southern Florida (Continued)

	Method	Properties determined	Applied in present study	Applicability in southern Florida
10	Analysis of water-level fluctuations caused by atmospheric-pressure fluctuations in open wells screened below the water table in unconfined aquifers. Leads to method of correcting water levels for effects of fluctuations in atmospheric pressure. Weeks (1979).	Pneumatic diffusivity of the unsaturated zone	No	Potentially useful for data from open wells in unconfined aquifers overlain by a thick unsaturated zone.
11	Analysis of water-level oscillations caused by earth tide in an open well penetrating a confined aquifer. Hsieh and others (1987).	Transmissivity and storage coefficient	No	Potentially useful for data from open wells in confined aquifers having a transmissivity less than 500 square feet per day. Minimal opportunity for use in southern Florida.
12	Analysis of water-level fluctuations caused by atmospheric-pressure fluctuations in a partially confined aquifer separated from a surficial aquifer by a leaky semiconfining layer. Rojstaczer (1988).	Barometric efficiency, pneumatic diffusivity of the unsaturated zone, vertical hydraulic diffusivity of the semiconfining layer, and lateral hydraulic diffusivity of the partially confined aquifer	No	Potentially useful for water-level data from an open well penetrating a partially confined aquifer of low transmissivity. Minimal opportunity for use in southern Florida.
13	Analysis of the response of the water level in a well in an unconfined aquifer to earth tide and atmospheric loading. The lateral permeability is high enough that wellbore storage effects can be ignored. A vertical diffusion equation is solved for variable pressure in the water column. Rojstaczer and Riley (1990).	Pneumatic diffusivity of the unsaturated zone and vertical hydraulic conductivity of the aquifer	No	Potentially useful for data from open wells in unconfined aquifers.
14	Analysis of water-level fluctuations caused by atmospheric-pressure fluctuations in a well open to a confined aquifer. A convolution method is used to replicate the water-level response. Furbish (1991).	Transmissivity and storage coefficient	No	Potentially useful for data from an open well penetrating a confined aquifer of low transmissivity. Minimal opportunity for use in southern Florida.
15	Analysis of pore-pressure fluctuations caused by atmospheric-pressure fluctuations in an unconfined aquifer. A vertical diffusion equation is used to determine the vertical hydraulic diffusivity by a trial-and-error process. Seo and Choe (2000).	Vertical hydraulic diffusivity	No	Potentially useful for pore-pressure data from unconfined aquifers. Data must be free of effects on water-table altitude caused by recharge and drying.

The well-aquifer methods (nos. 11-13) for determining transmissivity based on data from inland wells are not suitable for use in the study area because these methods are based on physical processes that are measurable only in formations of low transmissivity. Permeable zones in the Floridan aquifer system commonly have transmissivities much higher than those considered sufficiently low for these methods. The inland head data, however, was used successfully in method 4 to estimate specific storage. Independent estimates based on separate harmonic components in each monitor zone showed a high degree of consistency, and were of reasonable magnitude. Estimates of porosity using method 5 were entirely consistent with results from petrophysical analyses performed by the SFWMD.

Using naturally forced data to obtain estimates of aquifer properties has been found to provide generally useful transmissivity estimates and realistic estimates of specific storage and porosity. However, the methods used have not provided a completely satisfactory answer to the problem of determining properties that describe flow and storage in the subsurface. This field of research has concentrated on theoretical development supported by "theoretical applications" or application to synthetic data sets. While the research is useful in providing techniques that have the potential to be used by hydrologists, few attempts have been made to apply the theory to real-world data sets. Although field studies are costly, the most productive approach in future efforts might be to combine theoretical development with a fully committed field application with a view to resolving apparent inconsistencies between them. A fully developed and tested field technique consistent with theory would be highly useful in future studies.

SUMMARY

Aquifers are subjected to mechanical stresses from natural, non-anthropogenic, processes. These include pressure loading or mechanical forcing of the aquifer by ocean tides, earth tides, and pressure fluctuations in the atmosphere. The resulting head fluctuations are evident in deep confined aquifers that maintain a substantial head difference from surface formations across tight confining layers. The present study: (1) reviews the research that has been done on the use of tidally influenced and other naturally forced head fluctuations for estimating the values of aquifer properties, (2) determines which of these methods would be useful in the hydrologic environment of southern Florida, and (3) applies selected algorithms to a data set of heads from wells in Collier and Hendry Counties.

The Upper Floridan aquifer in southwestern Florida consists of several thin water-bearing zones of relatively high permeability interlayered with thick zones of much lower permeability. Water in the upper Floridan producing zones is under artesian pressure and flows from wells open at land surface. Tidally influenced head data for this study were acquired from monitor zones in three wells drilled by the South Florida Water Management District (SFWMD) as part of a program to investigate the Floridan aquifer system in southwestern Florida as a possible future source of water for public supply. Monitor-zone depth intervals extend from 690 feet (ft) in the basal Hawthorn unit to 2,350 ft in the dolomite-evaporite unit.

Barometric efficiency is the ratio of the change in water level in a well to the atmospheric- pressure change at the surface. Barometric efficiency is needed in some analytic methods to determine aquifer diffusivity and porosity. Clark (1967) devised a method to determine the barometric efficiency based on aperiodic, long-term pressure variations arising from the movement of air masses and corresponding head changes in the well. Using Clark's method, estimates that appeared valid based on data from certain monitor zones ranged from 63 to 86 percent. It was concluded that the Clark method can be an effective tool for determining barometric efficiency when the head data are of good quality. It seems essential that a process of correcting head data sets for atmospheric-pressure effects be applied to determine whether barometric efficiency values determined by the Clark method are correct. Where they are not or where results of the method are ambiguous, barometric efficiency must be determined by a trial-and-error approach.

A modified version of Clark's method was applied to total-head data from the same monitor zones. Resulting estimates of loading efficiency that appeared valid ranged from 15 to 37 percent, and are subject to the same reservations as those for barometric efficiency estimates. Barometric and tidal efficiencies theoretically sum to 1.0, as did estimates made in this study, so that an estimate of one is equivalent to an estimate of the other.

Being of solar and lunar origin, ocean and earth tides have a periodicity that can be described as a combination of "harmonic" components, sinusoidal functions of given amplitude and frequency and phase relation to some common time reference. Of all the harmonic components, only five are of importance geophysically, together accounting for approximately 95 percent of the tidal potential. Analysis of time-series data collected for this study using the discrete Fourier transform technique for spectral analysis demonstrated the presence of these five principal harmonics.

The analysis of tidally influenced data sets for estimates of aquifer parameters depends largely on being able to resolve the amplitude and phase of the various harmonic components of those data sets. In particular, the amplitude and phase of the five principal harmonic components must be determined. A means for doing this is by regression analysis. A computer program to perform this analysis was applied to ocean tide data at Naples and to the tidally influenced head data in each monitor zone in wells C-1111, C-1112, and HE-1087. Before tidally influenced data could be analyzed, it was necessary to detrend the data so that fluctuations would be strictly tidal in origin. The detrending procedure was generally done in two steps: (1) estimating a trend line by using a low-pass filter, and (2) computing the detrended data set by subtracting the trend line from the raw data.

Research into the analytical use of tidally influenced and other naturally forced head fluctuations to estimate values of aquifer properties can be segregated into four principal categories: (1) use of heads influenced by ocean tides to estimate aquifer diffusivity (transmissivity divided by storage coefficient); (2) use of heads influenced by earth tides or atmospheric-pressure fluctuations for estimating specific storage and porosity; (3) use of water levels from open wells penetrating a confined aquifer and influenced by earth tides or atmospheric-pressure fluctuations to estimate aquifer transmissivity and storage coefficient; and (4) use of water levels or pressure heads to determine vertical hydraulic conductivity.

The analytical solution of Van der Kamp (1972) to the problem of calculating aquifer diffusivity from aquifer-head oscillations at a location near enough to the ocean to be influenced by ocean tides, and which assumes a non-leaky confining unit of infinite extent, was applied to data from the three monitor zones in well C-1111. In applying this method, only the lunar diurnal (O_1) and lunar semidiurnal (M_2) data were used, because the solar components (K_1 and S_2) were influenced by atmospheric pressure. It was observed that T values computed based on the M_2 phase lags are about half those computed based on the O_1 phase lags. Furthermore, loading efficiency estimates were not consistent with results of the amplitude ratio analysis, as they indicated that tidal oscillations in monitor zones should have been much smaller than observed.

Depending mainly on results of the phase lag analysis and assuming a storage coefficient value of 1×10^{-5}, results can be interpreted to suggest estimates of T for the three monitor zones to range between 20,000 and 38,000 feet squared per day (ft^2/d) (MZ-1), between 15,000 and 27,000 ft^2/d (MZ-2), and between 75,000 and 140,000 ft^2/d (MZ-3). These values are higher, but in general agreement with the results of aquifer performance tests in MZ-1 and MZ-2 performed by the SFWMD in 1996-1997 (Bennett, 2001b). Transmissivity values estimated from these tests were 15,560 and 7,018 ft^2/d, respectively, for MZ-1 and MZ-2.

Li and Jiao (2001a) derived a more general solution in which the coastal aquifer system consists of a leaky semiconfining layer separating an unconfined aquifer from an underlying semiconfined aquifer. Assuming that the aquifer and semiconfining layer extend for an infinite distance beneath the ocean, and assuming a leakance value large enough to permit a small degree of leakage into the aquifer, application of this method yielded estimates based on the phase lag analysis that are mutually consistent, appreciably lower than those from the non-leaky Van der Kamp method, and closer to the SFWMD estimates. When the leakance is 2×10^{-5} d^{-1}, and loading efficiency (L_e) equals 50 percent, the amplitude ratio estimates for MZ-1 are in a narrow range of 26,500-28,000 ft^2/d and the phase lag estimates are almost identical at 14,000 ft^2/d. Using the leakance value of 2×10^{-5} d^{-1} to analyze the data from MZ-2, and assuming L_e is 50 percent, the amplitude ratio analysis provides T estimates of 23,000-24,000 ft^2/d, and the phase lag analysis provides estimates of 11,000 ft^2/d for both O_1 and M_2 components.

A numerical model was applied to: (1) use an alternative means to illustrate the response of a coastal aquifer to ocean-tide loading; (2) investigate additional aspects of the effects of tidal forces on pressure heads in the monitor zones; and (3) demonstrate an application of a numerical model to the problem of aquifer

response to ocean-tide loading. The model code applied was MODFLOW (1996 version). A cross-sectional grid design was devised in which ocean-tide oscillations were represented by specified-head boundary conditions on the left-hand side of the grid. A single value of horizontal and vertical hydraulic conductivity was assigned to confining zones associated with the Floridan aquifer system. With increasing specified values for this parameter, the tidal response lessens. Tidal oscillations in head are negligible in vertically adjacent layers because of their low transmissivity. If the adjacent layers are slightly permeable vertically, then pressure oscillations in the aquifers dissipate vertically into them. This result highlights the importance of aquifer confinement in the theory of Ferris (1952) and Van der Kamp (1972), and the potential usefulness of a solution that accounts for vertical leakage (Li and Jiao, 2001a).

The second cited category of research was the use of inland head oscillations caused by earth-tide and periodic atmospheric-pressure oscillations to derive estimates of the elastic storage capability of the aquifer. By considering the dilatation of the aquifer material and relating it mathematically to the specific storage of the aquifer and to the tide-generating potential, Bredehoeft (1967) derived a relation between specific storage and the head oscillation observed in a well. Applying this relation, estimates of specific storage range from 0.49×10^{-6} to 0.76×10^{-6} ft^{-1} and average 0.60×10^{-6} ft^{-1}. The relation between porosity, barometric efficiency, and specific storage reported by Jacob (1940) and based on the work by Theis (1938) was used for estimates of porosity in the monitor zones of the inland wells. Estimated values range from 19 to 39 percent.

The third cited category of research is based on a theoretical consideration of the well-aquifer system. In most theoretical developments, the well is assumed to be open to the atmosphere, and the well is assumed to be either screened or open throughout the thickness of a confined aquifer, and cased to the top of the aquifer. When oscillations of pressure-head in the aquifer occur, water moves into or out of the screened or open part of the well. This causes an oscillation of the water surface in the open well, which, depending on aquifer and well characteristics, might be damped or lagged in time relative to the pressure-head oscillations, although the frequency will be the same. The response to earth tides of an open well screened in a confined aquifer was studied by Hsieh and others (1987). The limitation to the applicability of their methods in some hydrologic environments is that, for sufficiently high values of aquifer transmissivity (more than 500 ft^2/d), the amplitude of earth tide oscillations is not reduced in the well, nor is there a phase lag of oscillations in the well. Thus, the applicability of these methods might be limited in studies of the upper Floridan aquifer.

REFERENCES CITED

Bear, J., 1972, Dynamics of fluids in porous media: Elsevier, New York, American Elsevier Co., Inc., 764 p.

Beaumont, C., and Berger, J., 1975, An analysis of tidal strain observations from the United States of America, (1) The laterally homogeneous tide: Siesmological Society of America Bulletin, v. 65, no. 6, p. 1,613-1,629.

Bennett, M.W., 2001a, Hydrogeologic investigation of the Floridan aquifer system at L-2 Canal site, Hendry County, Florida: South Florida Water Management District Technical Publication WS-3.

Bennett, M.W., 2001b, Hydrogeologic investigation of the Floridan aquifer system at the I-75 Canal site, Collier County, Florida: South Florida Water Management District Technical Publication WS-7.

Birch, F., 1966, Compressibility, elastic constants *in* Handbook of Physical Constants: Geological Society of America, 97-173.

Bredehoeft, J.D., 1967, Response of well-aquifer systems to earth tides: Journal of Geophysical Research v. 72, no. 12, p. 3,075-3,087.

Chapman, Sydney, and Lindzen, R.S., 1970, Atmospheric tides, thermal and gravitational: Dordrecht, Holland, D. Reidel Publishing Co., 200 p.

Clark, W.E., 1967, Computing the barometric efficiency of a well: Journal of the Hydraulics Division, American Society of Civil Engineers, v. 93, no. HY4, p. 93-98.

Cooper, H.H., Jr., Bredehoeft, J.D., Papadopolous, I.S., and Bennett, R.R., 1965, The response of well-aquifer systems to seismic waves: Journal of Geophysical Research, v. 70, no. 16, p. 3,915-3,926.

Cooper, H.H., Jr., Bredehoeft, J.D., and Papadopolous, I.S., 1967, Response of a finite-diameter well to an instantaneous charge of water: Water Resources Research, v. 3, no. 1, p. 263-269.

Desbarats, A.J., Boyle, D.R., Stapinsky, M., and Robin, M.J.L., 1999, A dual-porosity model for water level response to atmospheric loading in wells tapping fractured rock aquifers: Water Resources Research, v. 35, no. 5, p. 1,495-1,505.

Domenico, P.A., and Schwartz, Frank, 1997, Physical and chemical hydrology, 2nd Edition: New York, John Wiley and Sons, 528 p.

Doodson, A. T., and Warburg, H. D., 1941 (reprinted 1966), Admiralty manual of tides: London, Her Majesty's Stationary Office.

Erskine, A.D., 1991, The effect of tidal fluctuation on a coastal aquifer in the UK: Ground Water, v. 29, no. 4, p. 556-562.

Ferris, J.G., 1951, Cyclic fluctuations of water level as a basis for determining aquifer transmissibility: Internat. Geodesy Geophysics Union, Assoc. Sci. Hydrology Gen. Assembly, Brussels, v. 2, p. 148-155; duplicated 1952 as U. S. Geological survey Ground Water Note 1.

Furbish, D.J., 1991, The response of water level in a well to a time series of atmospheric loading under confined conditions: Water Resources Research, v. 27, no. 4, p. 557-568.

Godin, G., 1972, The analysis of tides: Toronto, University of Toronto Press, 264 p.

Gregg, D.O., 1966, An analysis of ground-water fluctuations caused by ocean tides in Glynn County, Georgia: Ground Water, v. 4, no. 3, p. 24-32.

Hanson, J.M., and Owen, L.B., 1982, Fracture orientation analysis by the solid earth tidal strain method: Presented at the 57th Annual Fall Technical Conference and Exhibition of the Society of Petroleum Engineers of AIME, American Institute of Mechanical Engineers, New Orleans, Louisiana, September 26-29, 1982.

Harbaugh, A.W., and McDonald, M.G., 1996a, User's documentation for MODFLOW-96, an update to the U.S. Geological Survey modular finite-difference ground-water flow model: U. S. Geological Survey Open-File Report 96-485, 56 p.

———1996b, Programmer's guide for MODFLOW-96, an update to the U.S. Geological Survey modular finite-difference ground-water flow model: U. S. Geological Survey Open-File Report 96-486, 220 p.

Hickey, J. J., 1989, An approach to the field study of hydraulic gradients in variable-salinity ground water: Ground Water, v. 27, n. 4, p. 531-539.

Hsieh, P.A., Bredehoeft, J.D., and Farr, J.M., 1987, Determination of aquifer transmissivity from earth tide analysis: Water Resources Research, v. 23, no. 10, p. 1824-1832.

Hsieh, P.A., Bredehoeft, J.D., and Rojstaczer, S.A., 1988, Response of well-aquifer systems to earth tides: Problem revisited: Water Resources Research, v. 24, no. 3, p. 468-472.

Hvorslev, M.J., 1951, Time lag and soil permeability in ground-water observations: U. S. Army Corps of Engineers Waterways Experiment Station Bulletin 36, Vicksburg, Mississippi.

Jacob, C.E., 1940, On the flow of water in an elastic artesian aquifer: American Geophysical Union Transactions, part 2, p. 574-586; duplicated 1953 as U. S. Geological Survey Ground Water Note 8.

———1950, Flow of groundwater *in* Engineering Hydraulics, edited by H. Rouse, New York, John Wiley and Sons.

Jiao, J.J., and Tang, Z., 1999, An analytic solution of groundwater response to tidal fluctuation in a leaky confined aquifer: Water Resources Research, v. 35, no. 3, p. 747-751.

Leake, S.A., and Lilly, M.R., 1997, Documentation of a computer program (FHB1) for assignment of transient specified-flow and specified-head boundaries in applications of the modular finite-difference ground-water flow model (MODFLOW): U. S. Geological Survey Open-File Report 97-571, 50 p.

Li, G., and Chen, C., 1991, Determining the length of confined aquifer roof extending under the sea by the tidal method: Journal of Hydrology, v. 123, no. 1/2, p. 97-104.

Li, H., and Jiao, J.J., 2001a, Tide-induced groundwater fluctuation in a coastal leaky confined aquifer system extending under the sea: Water Resources Research, v. 37, no. 5, p. 1,165-1,171.

———2001b, Analytic studies of groundwater-head fluctuation in a coastal confined aquifer overlain by a semi-permeable layer with storage: Advances in Water Resources, v. 24, p. 565-573.

Lohman, S.W., 1979, Ground-water hydraulics: U. S. Geological Survey Professional Paper 708, 70 p.

Lusczynski, N.S., 1961, Head and flow of ground water of variable density: J. Geophys. Res. 12(66), p. 4247-4256.

Marine, I.W., 1975, Water level fluctuations due to earth tides in a well pumping from slightly fractured rock: Water Resources Research, v. 11, no. 1, p. 165-173.

Mason, J. L., and Kipp, K. L., Jr., 1998, Hydrology of the Bonneville Salt Flats, northwestern Utah, and simulation of ground-water flow and solute transport in the shallow-brine aquifer: U. S. Geological Survey Professional Paper 1585, 108 p.

Melchior, P., 1964, Earth tides *in* Research in Geophysics, v. 2, edited by H. Odishaw, Cambridge, Massachusetts, Massachusetts Institute of Technology Press, p. 183-193.

———1983, The tides of the planet earth, 2nd edition: New York, Pergamon Press, 641 p.

Merritt, M.L., 1997, Computation of the time-varying flow rate from an artesian well in central Dade County, Florida, by analytical and numerical simulation methods: U. S. Geological Survey Water-Supply Paper 2491, 44 p.

Meyer, F.W., 1974, Evaluation of hydraulic characteristics of a deep artesian aquifer from natural water-level fluctuations, Miami, Florida: Florida Bureau of Geology Report of Investigations No. 75, 32 p.

———1989, Hydrogeology, ground-water movement, and subsurface storage in the Floridan aquifer system in southern Florida: U. S. Geological Survey Professional Paper 1403-G, 59 p.

Miller, J.A., 1986, Hydrogeologic framework of the Floridan aquifer system in Florida and in parts of Georgia, Alabama, and South Carolina: U. S. Geological Survey Professional Paper 1403-B, 91 p.

Moench, A.F., 1985, Transient flow to a large-diameter well in an aquifer with storative semiconfining layers: Water Resources Research, v. 21, no. 8, p. 1,121-1,131.

Munk, W.H., and McDonald, G.J.F., 1960, The rotation of the earth: London, Cambridge University Press.

Narasimhan, T.N., Kanehiro, B.Y., and Witherspoon, P.A., 1984, Interpretation of earth tide responses of three deep, confined aquifers: Journal of Geophysical Research, v. 89, no. B3, p. 1,913-1,924.

Nowroozi, A.A., Sutton, G.H., and Auld, B., 1966, Oceanic tides recorded on the sea floor: Annals of Geophysics, v. 22, p. 512-517.

Nowroozi, A.A., Kuo, J., and Erving, M., 1969, Solid-earth and oceanic tides recorded on the ocean floor off the coast of northern California: Journal of Geophysical Research, v. 74, no. 2, p. 605-619.

Reese, R.S., 2000, Hydrogeology and the distribution of salinity in the Floridan aquifer system, southwestern Florida: U. S. Geological Survey Water-Resources Investigation Report 98-4253, 86 p., 10 plates.

Rhoads, G.H., and Robinson, E.S., 1979, Determination of aquifer parameters from well tides: Journal of Geophysical Research, v. 84, no. B11, p. 6,071-6,082.

Ritzi, R.W., Jr., Sorooshian, S., and Hsieh, P.A., 1991, The estimation of fluid flow properties from the response of water levels in wells to the combined atmospheric and earth tide forces: Water Resources Research, v. 27, no. 5, p. 883-893.

Robinson, E.S., and Bell, R.T., 1971, Tides in confined well-aquifer systems: Journal of Geophysical Research, v. 76, no. 8, p. 1,857-1,869.

Rojstaczer, S., 1988, Determination of fluid flow properties from the response of water levels in wells to atmospheric loading: Water Resources Research, v. 24, no. 11, p. 1,927-1,938.

Rojstaczer, S., and Agnew, D.C., 1989, The influence of formation material properties on the response of water levels in wells to earth tides and atmospheric loading: Journal of Geophysical Research, v. 94, no. B9, p. 12,403-12,411

Rojstaczer, S., and Riley, F.S., 1990, Response of the water level in a well to earth tides and atmospheric loading under unconfined conditions: Water Resources Research, v. 26, no. 8, p. 1,803-1,817.

Ryder, P.D., 1985, Hydrology of the Floridan aquifer system in west-central Florida: U. S. Geological Survey Professional Paper 1403-F, 63 p.

Scott, T.M., 1988, The lithostratigraphy of the Hawthorn Group (Miocene) of Florida: Florida Geological survey Bulletin 59, 147 p.

Seo, H.H., Jones, L.C., and Choe, J., 2000, Variation of hydraulic head to changes in barometric pressure measured with buried pressure transducers in a saturated porous formation *in* Proceedings of the 2000 AIH Conference, Raleigh, North Carolina.

Sepúlveda, N., 2002, Simulation of ground-water flow in the intermediate and Floridan aquifer systems in peninsular Florida: U. S. Geological Survey Water-Resources Investigation Report 02-4009, 130 p.

Serfes, M.E., 1991, Determining the mean hydraulic gradient of ground water affected by tidal fluctuations: Ground Water, v. 29, no. 4, p. 549-555.

Shumway, R.H., 1988, Applied statistical time series analysis: Englewood Cliffs, New Jersey, Prentice- Hall, 379 p.

Spane, F.A., 2002, Considering barometric pressure in groundwater flow investigations: Water Resources Research, v. 38, no. 6, 18 p.

Theis, C.V., 1938, The relation between the lowering of the piezometric surface and the rate and duration of discharge of a well using ground-water storage: Trans. Amer. Geophys. Union, 16th Annual Meeting, p. 519-524.

Uchupi, Elezar, 1966, Map showing relation of land and submarine topography, De Soto Canyon to Great Bahama Bank: U. S. Geological Survey Miscellaneous Geologic Investigations Map I-475, 1 sheet.

Van der Kamp, G., 1972, Tidal fluctuations in a confined aquifer extending under the sea: International Geological Congress, v. 24, no. 11, p. 101-106.

Van der Kamp, G., and Gale, J.E., 1983, Theory of earth tide and barometric effects in porous formations with compressible grains: Water Resources Research, v. 19, no. 2, p. 538-544.

Weeks, E.P., 1979, Barometric fluctuations in wells tapping deep unconfined aquifers: Water Resources Research, v. 15, no. 5, p. 1,167-1,176.